






Statens vegvesen

Ferry free E39 -Fjord crossings Bjørnafjorden

304624

Rev.	Publish date	Description	Made by	Checked by	Project appro.	Client appro.
0	15.08.2019	Issued for use	Team	JOS	KH	
Client	 Statens vegvesen					
Contractor	 					
Contract no.:			18/91094			

Document name:

Alternative K12 – Consolidated technical report

Document no.:

SBJ-33-C5-OON-22-RE-001

Rev.:

0

Pages:

123



CONCEPT DEVELOPMENT FLOATING BRIDGE E39 BJØRNAFJORDEN

Alternative K12 - Consolidated technical report

Norconsult 

 DR. TECHN.
OLAV OLSEN

 Prodtex
Production / Technology / Excellence

 IFE

Pure Logic
The science of problem-solving

HEYERDAHL ARKITEKTER AS

 H&BB

 MIKO
MARINE AS

 BUKSÉR OG
BERGING

 FORCE
TECHNOLOGY

 SWERIM

REPORT

Project name:

CONCEPT DEVELOPMENT FLOATING BRIDGE E39
BJØRNAFJORDEN

Document name:

ALTERNATIVE K12 - CONSOLIDATED TECHNICAL REPORT

Project number: 12777
Document number: SBJ-33-C5-OON-22-RE-001
Date: 15.08.2019
Revision: 0
Number of pages: 123
Prepared by: Project team
Controlled by: Jon Solemsli
Approved by: Kolbjørn Høyland

Table of Content

1	INTRODUCTION	6
1.1	Current report	6
1.2	Project context	6
1.3	Project team	6
1.4	Project scope	7
2	CONCEPT DESCRIPTION	9
2.1	Architecture	9
2.2	Key figures	12
2.3	Bridge girder	13
2.4	Cable-stayed bridge	15
2.5	Pontoons and columns	16
2.6	Mooring system	19
2.7	Anchors	21
2.8	Abutments and end-anchoring	24
2.9	Approach bridge Gulholmane and tunnel portals	26
3	LOADS AND LOAD COMBINATIONS	27
3.1	General	27
3.2	Permanent loads (G)	27
3.3	Variable loads (Q)	27
3.4	Accidental loads	28
3.5	Load combinations	29
4	STRUCTURAL RESPONSE ANALYSES	30
4.1	General	30
4.2	Quasi-static loads response	31
4.3	Global dynamic loads response	34
4.4	Ship impact assessment	41
4.5	Fatigue assessment	56
5	STRUCTURAL DESIGN	62
5.1	Design of bridge deck girder	62
5.2	Design of pontoons and columns	67
5.3	Design of cable stayed bridge	72
5.4	Design of abutments	72
5.5	Design of mooring	79

6	ENGINEERING GEOLOGY EVALUATIONS.....	83
6.1	Background	83
6.2	Southern landfall/anchoring and bridge tower foundation	83
6.3	Northern landfall/anchoring.....	88
7	MARINE GEOTECHNICAL DESIGN	91
7.1	Bathymetry and soil conditions.....	91
7.2	Anchor site evaluations with respect to slope stability and holding capacity.....	92
7.3	Anchor holding capacity.....	93
8	CONSTRUCTION AND INSTALLATION.....	95
8.1	General	95
8.2	Floating bridge construction and installation.....	95
8.3	Cable-stayed bridge	109
8.4	Abutments	111
8.5	Completion	112
9	CONCEPT ROBUSTNESS	113
9.1	General Robustness Evaluation.....	113
9.2	Resulting Consequence Components for K12	114
9.3	Resulting Consequence Sensitivities for K12.....	115
9.4	K12 Robustness Evaluation	116
10	COST, SCHEDULE AND SUSTAINABILITY.....	117
10.1	Total cost	117
10.2	Sustainability	118
10.3	Schedule	119
11	REFERENCES	123

1 INTRODUCTION

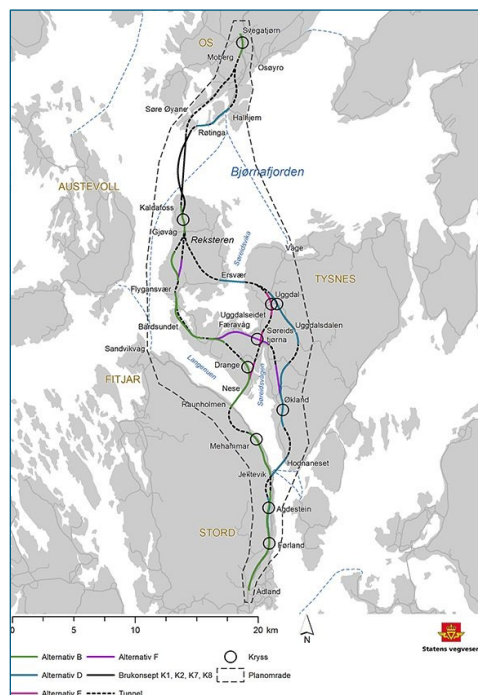
1.1 Current report

This report is a technical description of concept K12, and the work carried out up to assessment and final selection. The development of the concepts and the assessment and selection is described in separate reports.

1.2 Project context

Statens vegvesen (SVV) has been commissioned by the Norwegian Ministry of Transport and Communications to develop plans for a ferry free coastal highway E39 between Kristiansand and Trondheim. The 1100 km long coastal corridor comprise today 8 ferry connections, most of them wide and deep fjord crossings that will require massive investments and longer spanning structures than previously installed in Norway. Based on the choice of concept evaluation (KVU) E39 Aksdal Bergen, the Ministry of Transport and Communications has decided that E39 shall cross Bjørnafjorden between Reksteren and Os.

SVV is finalizing the work on a governmental regional plan with consequence assessment for E39 Stord-Os. This plan recommends a route from Stord to Os, including crossing solution for Bjørnafjorden, and shall be approved by the ministry of Local Government and Modernisation. In this fifth phase of the concept development, only floating bridge alternatives remain under consideration.



1.3 Project team

Norconsult AS and Dr.techn.Olav Olsen AS have a joint work collaboration for execution of this project. Norconsult is the largest multidiscipline consultant in Norway, and is a leading player within engineering for transportation and communication. Dr.techn.Olav Olsen is an independent structural engineering and marine technology consultant firm, who has a specialty in design of large floating structures. The team has been strengthened with selected subcontractors who are all highly qualified within their respective areas of expertise:

- Prodtex AS is a consultancy company specializing in the development of modern production and design processes. Prodtex sits on a highly qualified staff who have experience from design and operation of automated factories, where robots are used to handle materials and to carry out welding processes.
- Pure Logic AS is a consultancy firm specializing in cost- and uncertainty analyses for prediction of design effects to optimize large-scale constructs, ensuring optimal feedback for a multidisciplinary project team.
- Institute for Energy Technology (IFE) is an independent nonprofit foundation with 600 employees dedicated to research on energy technologies. IFE has been working on high-performance computing software based on the Finite-Element-Method for the industry, wind, wind loads and aero-elasticity for more than 40 years.

- Buksér og Berging AS (BB) provides turn-key solutions, quality vessels and maritime personnel for the marine operations market. BB is currently operating 30 vessels for harbour assistance, project work and offshore support from headquarter at Lysaker, Norway.
- Miko Marine AS is a Norwegian registered company, established in 1996. The company specializes in products and services for oil pollution prevention and in-water repair of ship and floating rigs, and is further offering marine operation services for transport, handling and installation of heavy construction elements in the marine environment.
- Heyerdahl Arkitekter AS has in the last 20 years been providing architect services to major national infrastructural projects, both for roads and rails. The company shares has been sold to Norconsult, and the companies will be merged by 2020.
- Haug og Blom-Bakke AS is a structural engineering consultancy firm, who has extensive experience in bridge design.
- FORCE Technology AS is engineering company supplying assistance within many fields, and has in this project phase provided services within corrosion protection by use of coating technology and inspection/maintenance/monitoring.
- Swerim is a newly founded Metals and Mining research institute. It originates from Swerea-KIMAB and Swerea-MEFOS and the metals research institute IM founded in 1921. Core competences are within Manufacturing of and with metals, including application technologies for infrastructure, vehicles / transport, and the manufacturing industry.

In order to strengthen our expertise further on risk and uncertainties management in execution of large construction projects Kåre Dybwad has been seconded to the team as a consultant.

1.4 Project scope

The objective of the current project phase is to develop 4 nominated floating bridge concepts, document all 4 concepts sufficiently for ranking, and recommend the best suited alternative. The characteristics of the 4 concepts are as follows:

- K11: End-anchored floating bridge. In previous phase named K7.
- K12: End-anchored floating bridge with mooring system for increase robustness and redundancy.
- K13: Straight side-anchored bridge with expansion joint. In previous phase named K8.
- K14: Side-anchored bridge without expansion joint.

In order to make the correct recommendation all available documentation from previous phases have been thoroughly examined. Design and construction premises as well as selection criteria have been carefully considered and discussed with the Client. This form basis for the documentation of work performed and the conclusions presented. Key tasks are:

- Global analyses including sensitivity studies and validation of results
- Prediction of aerodynamic loads
- Prediction of hydrodynamic loads
- Ship impact analyses, investigation of local and global effects
- Fatigue analyses
- Design of structural elements
- Marine geotechnical evaluations
- Steel fabrication

- Bridge assembly and installation
- Architectural design
- Risk assessment

2 CONCEPT DESCRIPTION

2.1 Architecture

2.1.1 General

The differences between the concepts are limited to assessments of the landing and the aesthetic experience of the bridge. The aesthetic assessment must be seen against the landscape, the actual construction and against the visual experience one gets by driving over the bridges.

The other architectural bridge elements, such as vertical curvature, bridge box, pillars, pontoons and pylon, will essentially be equal in all cases and therefore do not affect the evaluation between the 4 concepts.

2.1.2 The bridge and the landscape

The 4 bridge concepts will mainly appear to be equivalent in the large landscape picture. We have the same cable-stayed use structure over the shipping route. They will approximately have the same vertical curvature. The design of pylon, columns and pontoons will also generally be the same. The cable-stayed part of the bridge will, for all concepts, be located close to the shore in the south end of the crossing. The perception of the horizontal curvature is less obvious from a distance, and will best be experienced from the road, from the sides of the bridge or at a bird's eye view.



> *Figure 2-1: K12 bird eye view*

Traditionally, a bridge is perceived as the shortest possible straight line across waters. This is logically architectural, economical and constructive, and characterizes our expectations of a bridge. In our case, we are facing a floating bridge construction that challenges our beliefs about bridges. Wind and current conditions in the sea are now crucial parameters for the

design. Architecturally, a curved horizontal line will express the forces to which the bridge is exposed, while the straight line must be physically forced into place,- against the forces of the sea. This is a classic architectural issue. Should it emphasize the current and inherent performances of the task, or should the architecture reflect the task's physical and functional challenges. One can say to some extent that the 4 concepts relate differently to this classic issue.

K12 is a variant of K11, where one introduces some side anchoring. This makes the arc impact somewhat smaller and the construction perhaps more economical. This does not change the visual expression of the concepts and can be considered equal to K11

2.1.3 The perception of driving over the bridge.

The length of the bridge is about 5 kilometers. With the maximum permitted speed you have driven over the bridge within about 3 minutes. During these minutes you will experience the fjord landscape, the pylon and the bridge's alignment over the fjord. The perception is about how to enter the bridge, what are your perceptions along the way and finally how to leave the bridge. However, the experience of the pylon is central. If you drive straight ahead towards the pylon, you will not experience any remote effect of the cable bridge or its span. If you drive in an arc towards the pylon, you will also be able to experience the bridge from the side. This would clearly enrich the driving events and give you an experience of the bridge construction in the fjord landscape.

The curved line provides a varied driving experience because perspectives will change as you drive over the bridge. The cable-stayed bridge will be seen in perspective from sideward to frontal.



> *Figure 2-2: Driving along K12*

2.1.4 Bridge heads and landscaping adjustments

11

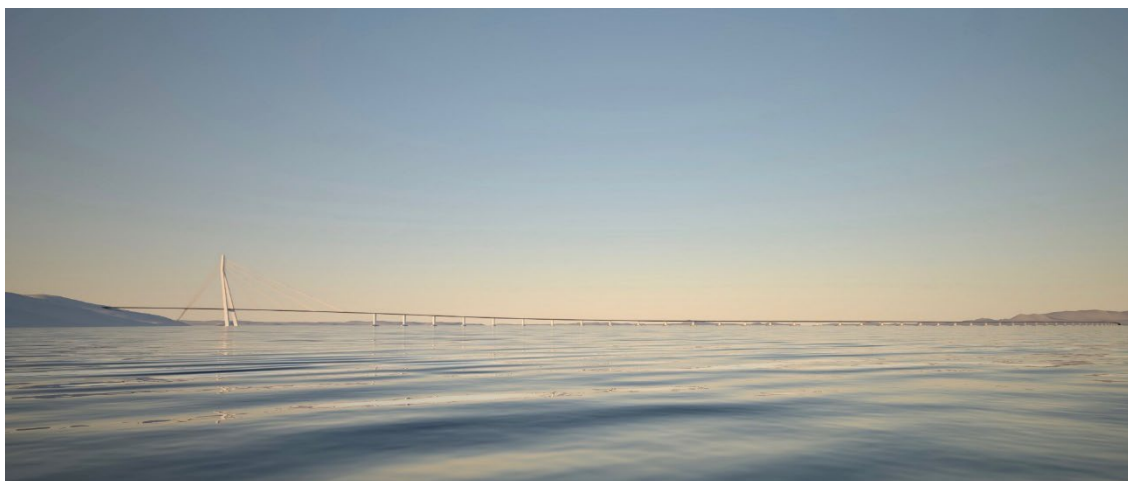


> *Figure 2-3 Vertical curvature K12*

The bridge concepts clearly have different landings. In the north, the differences between the concepts are of minor importance. In the south, however, the impacts are large and partly very unfortunate seen from the fjord and as a part of the large landscape. For all the concepts, it is assumed a high level of alignment for the road in order to avoid tunnels. It is also assumed, for all concepts, that the pylon is to be situated at Svarvhelleholmen. In the south, the impact of K11 / K12 and K13 will be directly negative. K14 has a greater potential and will be better adapted to the terrain.

K12 has a routing that gives a powerful cut in the ridge cam towards Langenuen and outer Bjørnafjord. The ridge Vestre Klovsteinen is being touched. The cuts will be about 30 to 15 meters high and will be strongly marked in the fjord landscape.

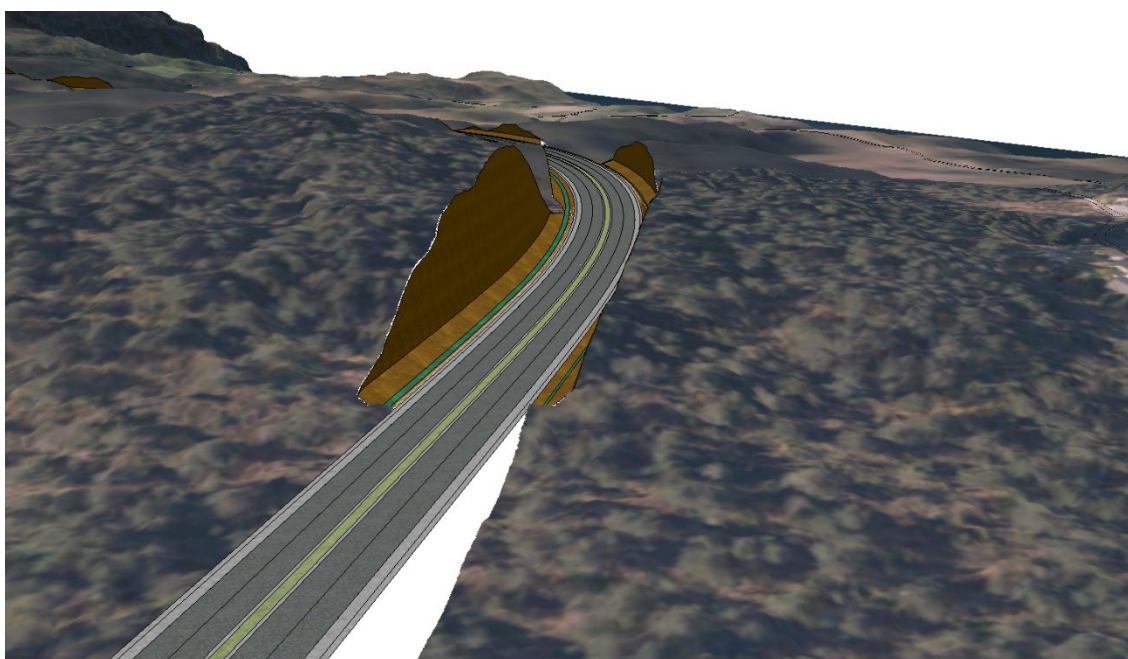


> *Figure 2-4 Landscape, cutting in Klovsteinen K12*

2.2 Key figures

> Table 2-1: Key conceptual figures

Geometry - arch	R = 5 000 m
Length	5 518 m
Cable stayed bridge main span – pylon to first pontoon	510 m
No of pontoons	46
Pontoon spacing	100 m
No of expansion joints	0
No of bearings	0
First 5 horizontal eigenperiods	67, 50, 31, 22, 16 s
Mooring no.	2
Mooring position Approx.	0,33L 0,67L
Horizontal mooring stiffness – anchor group	800 kN/m
Bridge girder steel	74 969 ton
Pontoon steel	35 159 ton
Column steel	5 293 ton
Asphalt, ballast etc.	25 216 ton
Total displacement	140 637 ton
Girder cross section - typical	1,47 m ²
Girder I _z - typical	114,9 m ⁴
Girder I _y - typical	2,71 m ⁴

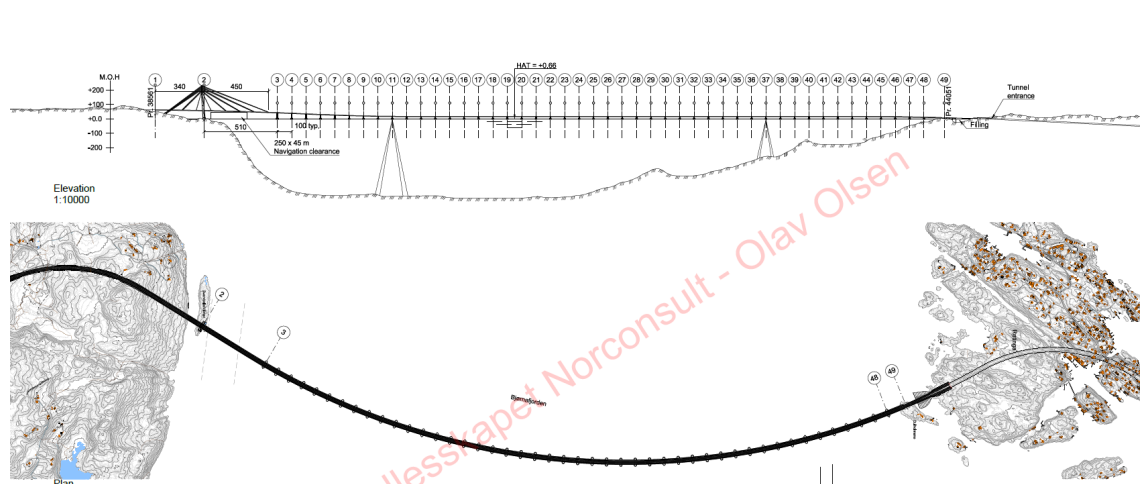


> Figure 2-5 General elevation and plan view

2.3 Bridge girder

The bridge girder is constructed as a conventional steel box girder welded together from steel plates stiffened by trapezoidal stiffeners. Such cross sections have a high strength to weight ratio and are commonly used for long span bridges. The outer shape of the girder is designed to reduce aerodynamic drag forces and the shape is inspired by the box girders of typical Norwegian suspension and cable-stayed bridges.

In the horizontal plane the girder has an arc shape with a radius of 5000 m. The girder is vertically supported by the abutments at both ends of the bridge, by the columns resting on the pontoons and by the cables of the cable-stayed part of the bridge. Span lengths between vertical supports are typically 100 m. Horizontally the girder is fixed at the abutments and supported by two groups of mooring lines approximately in one third and two thirds of the total bridge length.

The shape and main dimensions of the bridge girder is shown in the figure below. Internal transverse girders are placed with a typical center distance of 4,0 m. Typical plate thicknesses is 14 mm for the top deck plates, 12 mm for the bottom plates and 40 mm for left and right vertical web plates.

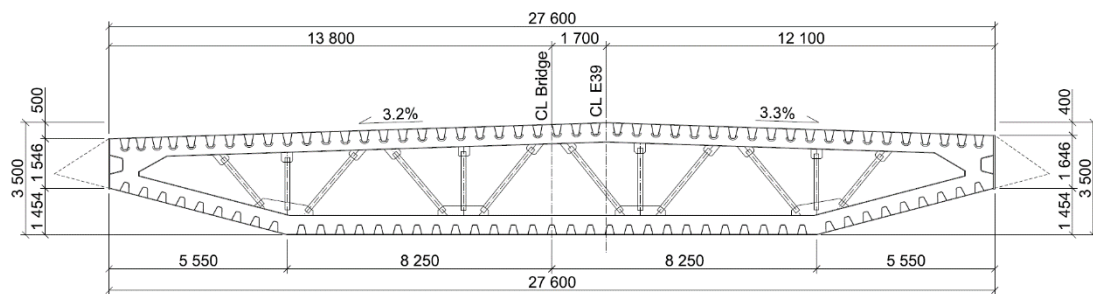


> Figure 2-1 Bridge girder shape and main dimensions

The trapezoidal stiffeners are continuous in the length of the bridge. This means that it is made cut outs for the stiffeners in the transverse girders. The main objective of stiffeners is to provide sufficient stiffness to the plate members of the cross section in compression to avoid buckling. They also provide more strength to cross section due to additional cross section area. The stiffeners of the top deck plates are in addition a part of the orthotropic bridge deck subjected to local traffic loads (wheel pressures). The orthotropic bridge deck spans between the transverse girders. Typical geometry of the stiffeners is shown in the figure below.

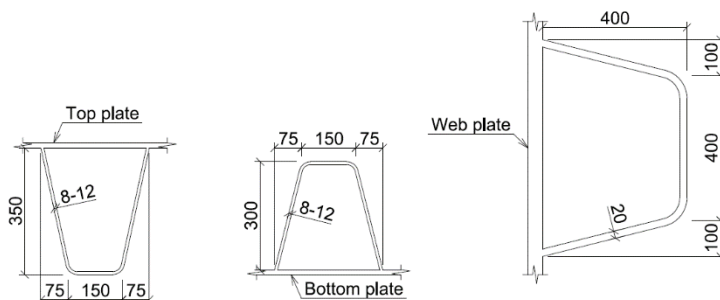


> Figure 2-2 Typical geometry of trapezoidal stiffeners

In the high part of the floating bridge, at the end of the cable-stayed bridge, the cross section is reinforced due to increased sectional forces in this part of the bridge. The reinforcing is done by increasing the thickness of the stiffeners in the top and bottom plate from 8 to 12 mm.

The girder is also reinforced against the abutments at both ends of the bridge. The outer shape of the box girder is also changed against the bridge ends to coincide with the geometry of the concrete construction at the abutments. The shape and main dimensions of the bridge girder at the abutments are shown in the figure below.

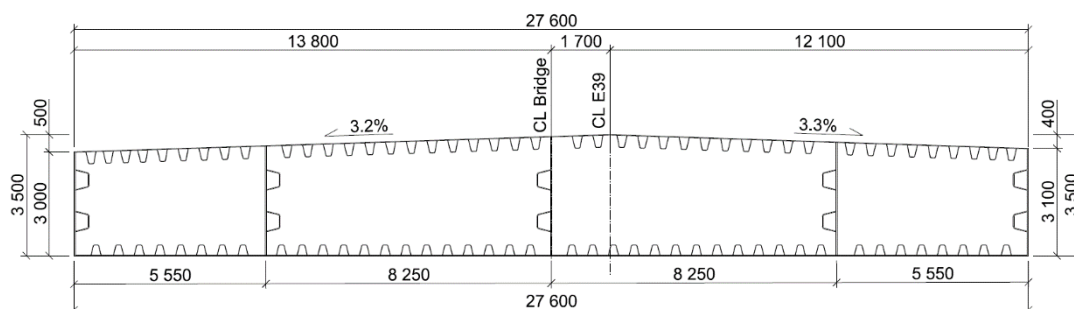


> Figure 2-3 Bridge girder shape and dimensions at the abutments

Internal transverse girders are placed with a typical center distance of 4,0 m. The transverse girders are constructed as a T-profile (T 600x200x12x15 mm) welded to the plates and stiffeners of the box girder. Bracings of rectangular hollow sections are provided to support the T-profile. This results in an effective and light weight transverse frame. The transverse girders have two main tasks. The first one is to carry the traffic loads on the bridge deck to the webs of the box girder. The second one is to restrain the outer shape of the box girder to avoid distortions due to torsional shear stress. Typical geometry of the transverse girders is shown in the figure below.

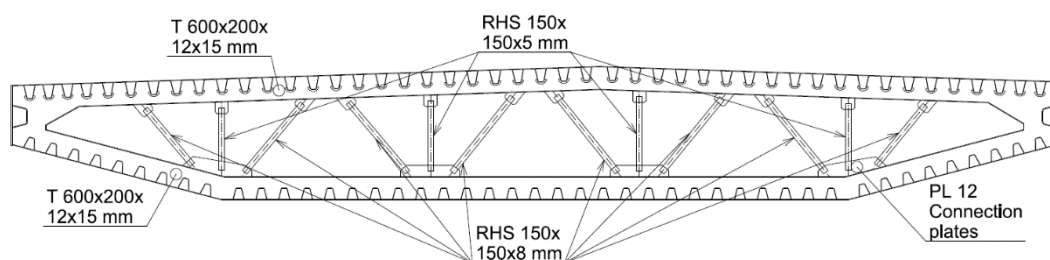


> Figure 2-4 Geometry of internal transverse girders

At the connections between the girder and pontoon columns the girder needs to be reinforced to handle especially accidental loads from ship impact. The detailing of this connection is still on going, but it will be the same for all the concepts (K11, K12, K13 and K14). The internal transverse girders will be replaced by internal diaphragms and internal longitudinal web plates will be added over the columns. The principal is shown in the illustration below.

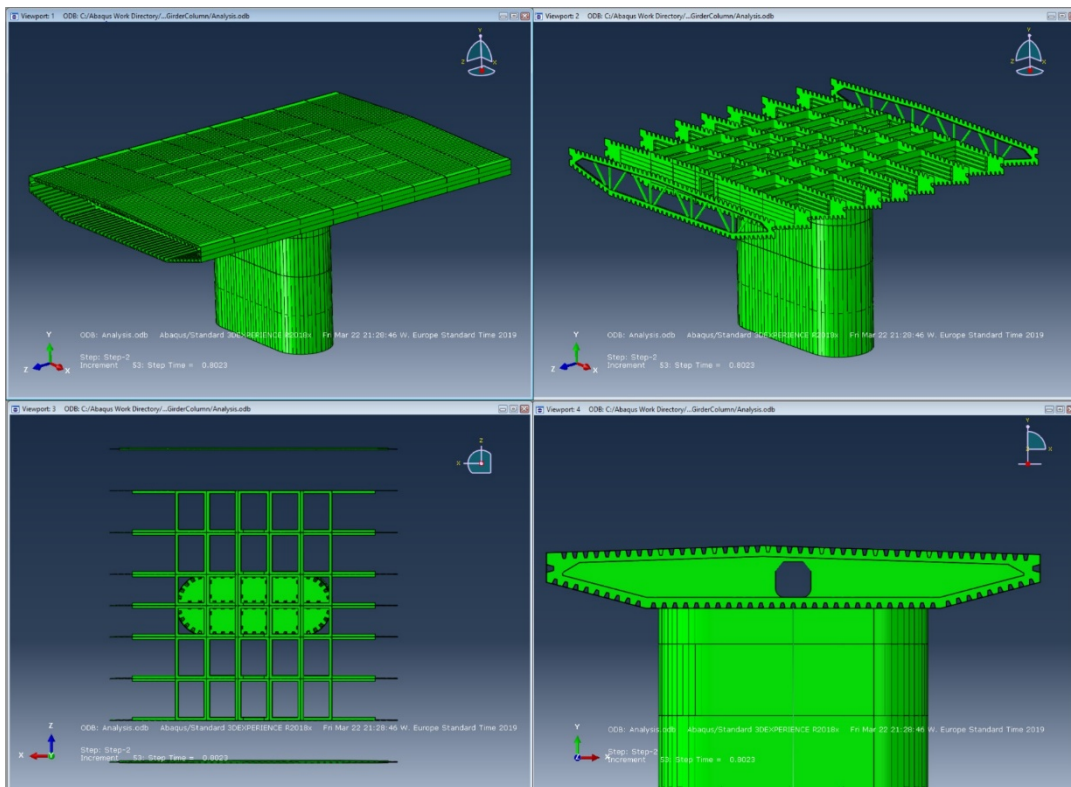


> Figure 2-5 Internal diaphragms and longitudinal web plates over column connections

2.4 Cable-stayed bridge

In the previous phase the cable stayed bridge was planned with one single pylon located on Svarvhelleholmen, a side span of 310 meters on the shore side and a main span of 510 meters connected to the floating bridge to ensure the required ship channel with a navigation clearance of 400 meters.

So far in this phase, this part of the bridge is approximately unchanged from the former phase. The main span and the side span are the same, the box girder is the same, but some changes have been made, mainly for architecturally and esthetically reasons. The main span could have been reduced, because the navigation clearance in this phase has been reduced from 400 to 250 meters. However, in connection with the coupling of the floating part to the cable stayed part of the bridge, it has been important to make the cable stayed bridge as flexible as possible to allow the vertical movements of the floating bridge without exceeding the bending capacity of the box girder. This has turned out to be quite challenging, and a shorter main span would have increased these difficulties.

Furthermore, a reduction of the main span would give an almost confusing look of the cable stayed bridge with two equal spans. An important mission for this bridge is to point out the navigation channel for the ships in a way that give no doubt about where to sail. This is obtained with a significant difference between the side span and the main span.

The size and strength of the steel box are mainly dictated from the floating bridge, so it is bigger and stronger than necessary for the cable stayed bridge. The distance between the stays along the girder could therefore have been increased to about 100 meters to

communicate with the span of the floating part. The number of stays could correspondingly have been reduced from 22 to about 5 in the main span and from 14 to 3 in the side span, which would give a harmonic interaction with the rest of the bridge. This reduction of stays would also increase the flexibility of the bridge which is helpful.

However, the consequence would be some very heavy and unmanageable cables which would be difficult to fabricate, assemble and replace. In order to obtain the same effect, the number of cables is retained, but gathered in 5 groups in the main span and in 3 groups in the side span.

Furthermore, the pylon is undergoing some changes. Most prominently is a about 7 degrees backward inclination which together with a bigger main span emphasize the location of the ship channel.

2.5 pontoons and columns

The pontoons and columns are designed as conventional plated steel ship type structures. The design service life is 100 years. The conventional design makes production possible worldwide including Norwegian shipyards. DNV GL materials and fabrication standards will be used. Super duplex steel in the splash zone from previous phase is no longer applied.

The top of the columns is connected to the bridge girder, and the bottom of the columns is connected to the top of the pontoons.

There is one central column at each pontoon supporting the bridge girder. The column design is rectangular with rounded corners. Inside the column there are internal walls in both beam co-ordinate directions.

The sizing of the pontoons is still ongoing and outer dimensions are kept constant from former phase. The pontoons are subdivided into compartments so that an accidental flooding of 2 compartments will not jeopardize the floating bridge integrity and post-accident behavior.

Both the pontoon and the column are designed to withstand ship impact. Permanent damage is allowed, but sufficient residual load carrying ALS capacity must be assured for both the pontoon and the column. The pontoon is exposed to direct ship hit and will have the highest permanent damage.

> *Table 2-2: Pontoon dimensions and weights, typical*

Pontoon types	L (m)	B (m)	H (m)	Weight (ton)	Nos.
1. Low bridge - Axis 13 through 48	58	10	9	750	36
2. Ramp - Axis 7 through 12	58	12	9	900	6
3. High bridge – Axis 4 through 6	58	14	9	1 040	3
4. Ship navigation channel – Axis 3	58	16	9	1 180	1
Total				36 700	46

> *Table 2-3: Column dimensions and weights, typical*

Pontoon types	L (m)	B (m)	H (m)	Weight (ton)	Nos.
1. Low bridge - Axis 13 through 48	15	6	10.0	188	36
2. Ramp - Axis 7 through 12	15	6	14.8 (avg.)	279 (avg.)	6
3. High bridge – Axis 4 through 6	15	7	27.9 (avg.)	558 (avg.)	3
4. Ship navigation channel – Axis 3	15	7	36.2	725	1
Total				~ 10841	46

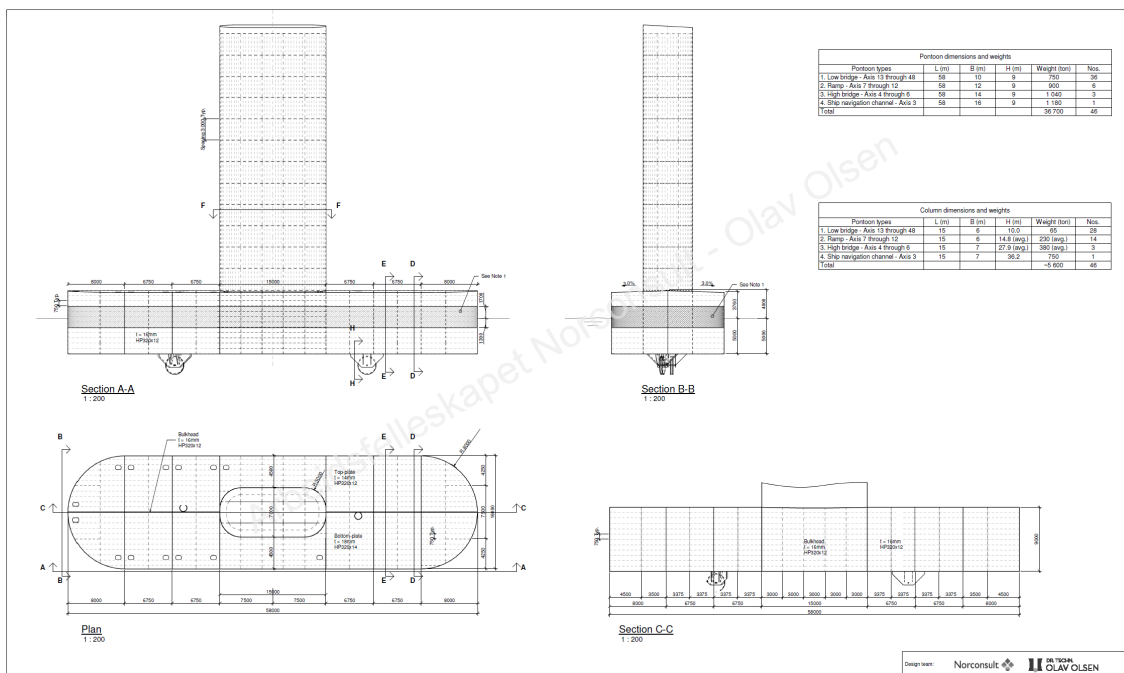


> Figure 2-6: Structural arrangement, pontoons and columns, type 4

If installed, there will be two anchor lines connected to a pontoon. The anchor lines will go via a chain cable from the underside of the pontoon and all the way to the top of the pontoon through a square steel cylinder with approximate dimensions 800mm by 800mm.

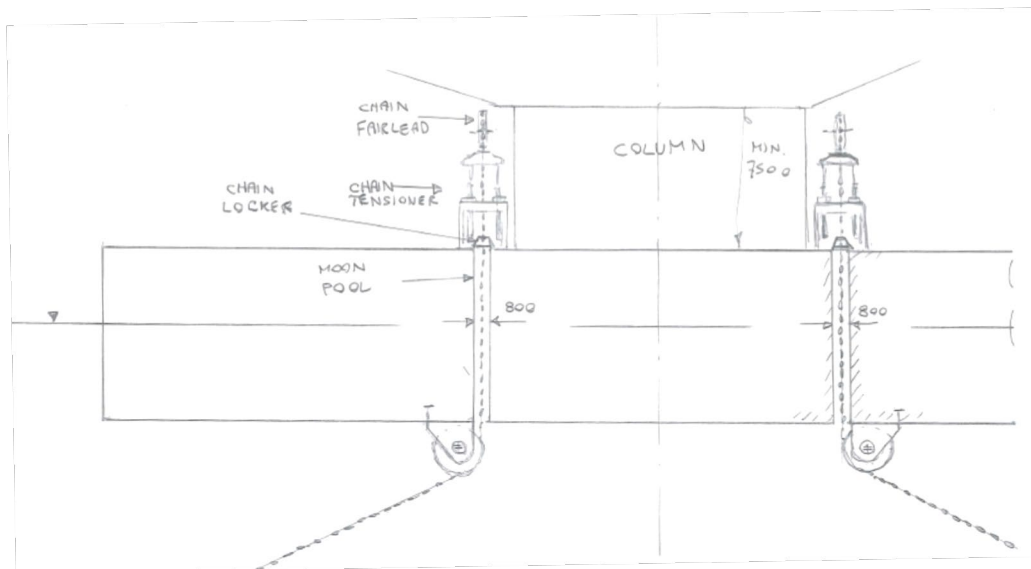


> Figure 2-7: Sketch of anchor lines connection

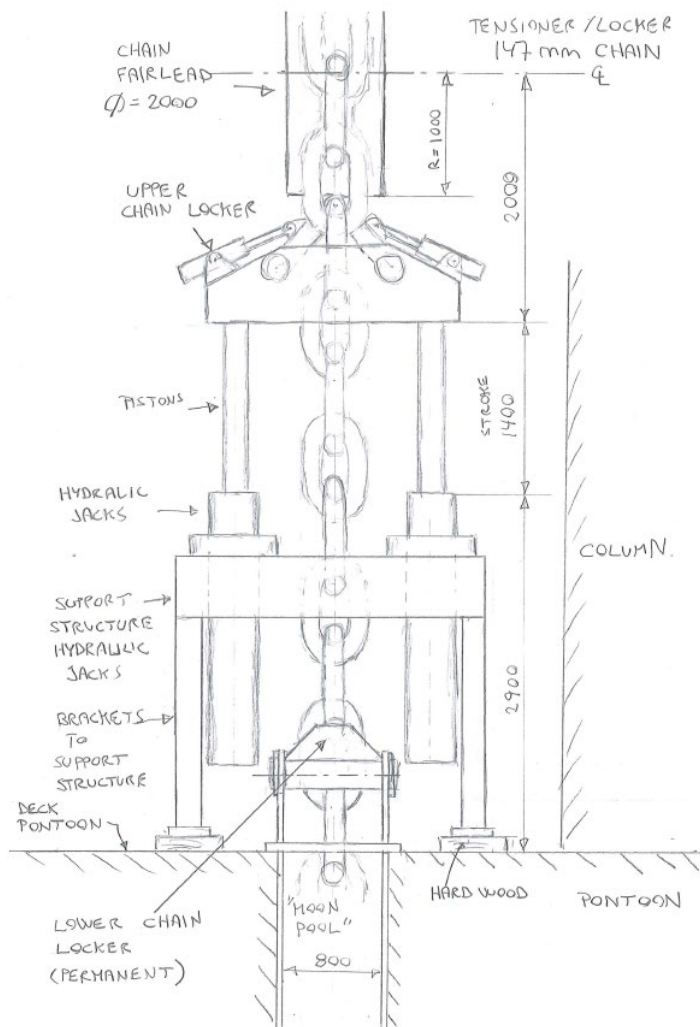


> Figure 2-8: Chain tensioning and chain locking

2.6 Mooring system

The mooring system for K12 consists of two groups of mooring lines, each group consisting of eight mooring lines. The lines are connected to four pontoons, with one line to each side. The groups are equally spaced along the bridge length (Approximately at 1/3 and 2/3 of the length). The main functional requirement for the mooring line groups is to have sufficient horizontal stiffness as estimated based on the global analyses. The global analysis indicated that a minimum required stiffness per group would be in the range of 0.6 MN/m, and a minimum mooring group stiffness of 0.8 MN/m is thus set as a requirement for the mooring system design to account for uncertainty.

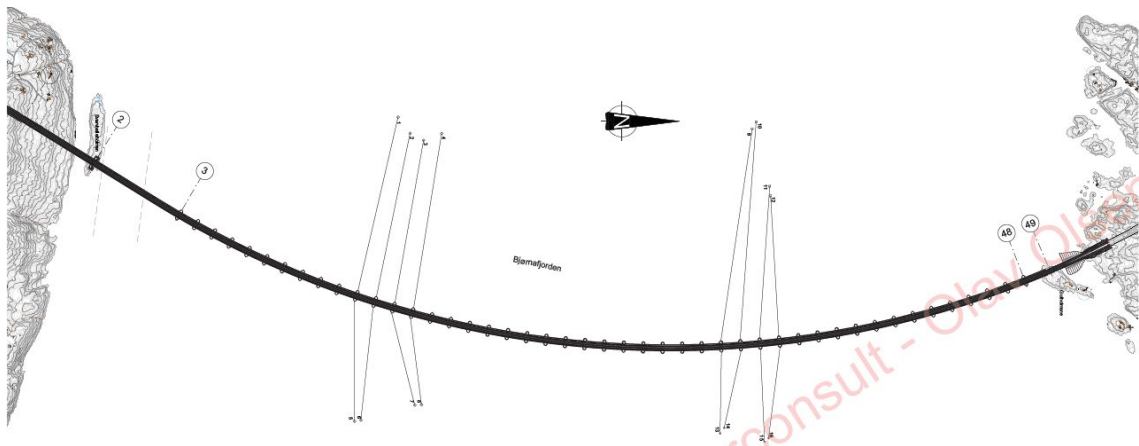


> Figure 2-9: Top view of mooring line configuration.

A taut line mooring system is proposed, consisting of polyester fibre rope as main component, with mooring chain towards the anchor and pontoon terminations. A taut system based on polyester mooring will give a robust and reliable system with a practically linear resorting stiffness. The lines will generally also have additional capacity with respect to extreme offset beyond the expected ULS offset. The lines are prestressed to avoid “slack” during the ULS range of pontoon motions. Slack in this context does not mean that the rope goes into compression, but that it loses its pretension and hence stiffness. The fibre rope itself will always experience tension due to heavy top and bottom chain. The actual behaviour when approaching slack will be studied with more refined analysis in the next phase giving a possibility for further optimization.

The level of prestressing in each line is chosen to avoid slack during ULS. A safety margin of 0.85 for favorable loads are used for the determination of the pretension level. The lines have different configuration on each side of the pontoon, with different angles and depths due to limitations in feasible anchor locations. This results in different prestressing loads and dimensions for the lines. The prestressing levels is tuned to be in equilibrium in the direction normal to the bridge for each pair of lines.

A brief description of each main component is further given.

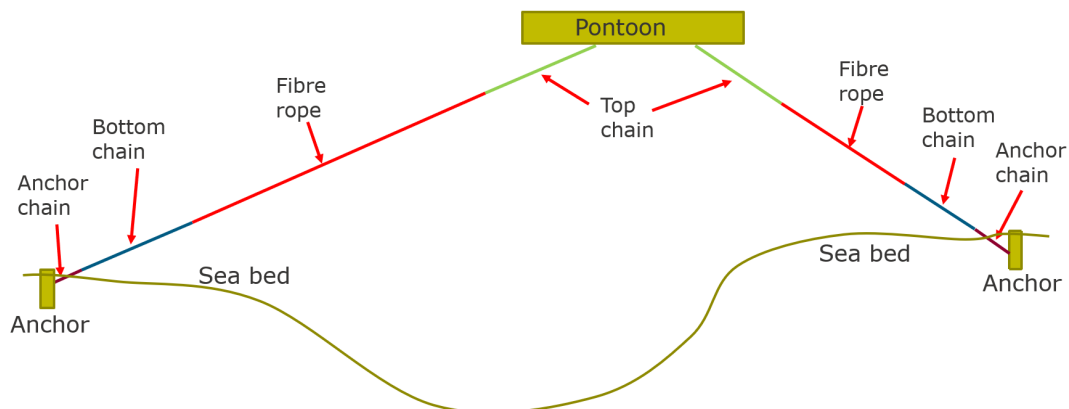


> Figure 2-10 Principle drawing (side view) of one pair of mooring lines.

Anchor chain (for anchors with connection to chain in soil)

- Installed together with anchor
- Connected to the anchor and the bottom chain
- Not inspectable, and hence more complicated to replace.
- Must be robust wrt. fatigue and corrosion

Bottom chain

- Sufficient length to prevent contact between fibre rope and seabed.
- Easy connection to preinstalled anchor by ROV.
- Design lifetime may be an issue due to corrosion and fatigue.
- Proven for long term mooring in the oil and gas industry.

Fibre rope

- Good elongation characteristics – gives nearly linear force-deformation curve.
- Easy to handle due to low weight
- Fatigue is not expected to be an issue (fibre rope designed to have a maximum utilization below 0.7 in intact ULS)
- Proven for offshore applications (i.e Aasta Hansteen spar platform and Goliat FPSO)

Top chain

- Robust during installation and tensioning (wear and tear)
- Gives termination of fibre rope at reasonable depth, reducing risk of damage by ship propeller and degradation by marine growth and UV light.
- Gives tolerances for determining pre-constructed rope lengths and
- Easy to replace
- Corrosion and fatigue (tension-tension and OPB) may be an issue.
- Proven for long term mooring in the oil and gas industry

It is expected, based on experience from oil and gas, that a design life of 25-50 years should be possible for the mooring system when accounting for corrosion and fatigue. Inspection and monitoring during the operational phase of the project might elongate the actual life of the system.

2.7 Anchors

Each mooring line is connected to its own anchor. The anchor type is dependent on the soil conditions and the surrounding topography. For anchor locations near bedrock a gravity anchor will be used. Meanwhile for sites with adequate soil thickness, suction anchors will be utilized. Global anchor dimensions are estimated from the current ULS line loads and it's expected that the geometry can be optimized. Furthermore, for the holding capacity calculations it is assumed undrained conditions, i.e. short load duration, is governing for the design of suction anchors. The design line loads are summarized in the Table 5-4.

For gravity anchors, steel plates are welded to a supporting steel frame which is placed on a bedding of crushed rock close to the bedrock. The purpose of the bedding is to even out the surface, thereby allowing for greater surface area and higher friction capacity. The outer dimensions for the current ULS loads is estimated to be 15m x 15m x 5m (LxBxH) with an

average steel weight of 220 tonne. To achieve sufficient capacity the box is filled with olivine with an average mass of 2200 tonne per anchor.

Most of the anchors will consist of suction anchors with varying geometry depending on the soil thickness and seabed inclination. For anchor sites with more than 20m of soil thickness it's estimated a 10m diameter and 15m skirt length is needed to withhold the mooring loads. The weight (non-submerged) is assumed to be approximately 210 tonnes. In areas with scarce soil thickness, suction anchors with 15m diameter and 10m skirt length is deemed at this stage to be adequate to withhold the line forces. The weight for these anchors is assumed to be 310 tonnes due to extra stiffeners.

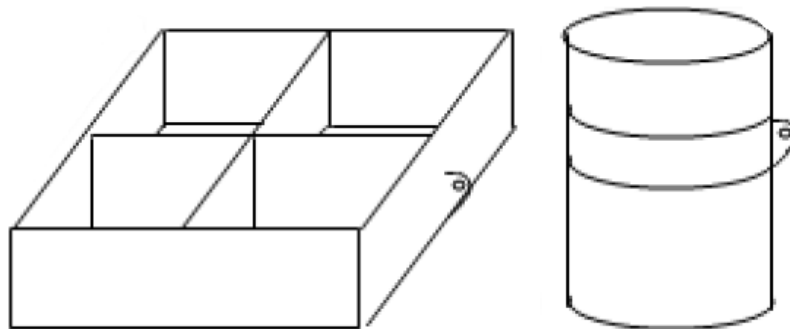


> *Figure 2-11 Principal sketch of a gravity anchor [1]*

A summary of the different anchor types, dimensions and soil conditions are given in table below. Further work involves calculating needed consolidation time, effect of creep and earthquake loading on foundation.

> Table 2-4 Summary of anchor size, type and local soil conditions.

Anchor group	Anchor ID	Soil thickness [m]	Seabed inclination [°]	Anchor type	D [m]	L _{skirt} [m]	B=L [m]
1	1	69.8	1.0	Suction	10	15	-
	2	54.0	0.5	Suction	10	15	-
	3	47.8	1.0	Suction	10	15	-
	4	60.7	1.0	Suction	10	15	-
2	5	21.2	7.6	Suction	10	15	-
	6 *	23.3	6.7	Suction	10	15	-
	7	22.1	7.6	Suction	10	15	-
	8	22.6	5.3	Suction	10	15	-
3	9	0.8	2.0	Gravity	-	-	15
	10	1.0	3.0	Gravity	-	-	15
	11	2.0	3.0	Gravity	-	-	15
	12	2.5	3.0	Gravity	-	-	15
4	13	11.4	3.2	Suction	15	10	-
	14 *	9.5	5.5	Suction	15	10	-
	15	14.6	2.0	Suction	15	10	-
	16	13.0	2.5	Suction	15	10	-

* The anchor positions can be slightly adjusted to achieve better holding capacity with negligible changes in the global response.

2.8 Abutments and end-anchoring

2.8.1 Abutment and bridge girder connection concepts

The restraint of the superstructure is resolved by concrete gravity base structures with a box-shaped, cellular configuration founded on prepared bedrock base. Solid ballast and post-tensioned rock anchors are used to enhance the abutments overturning and sliding resistance. The main alternative is a bridge box girder connection that is monolithically connected to the abutment. For the north end there is also investigated an alternative concept with a plate hinge solution that releases the weak axis moment in the connection. Section 2.8.2 and 2.8.3 points out the characteristics of the different concepts.

For both concepts, to enhance overload performance of the interface, unbonded tendons are used due to their ability to redistribute strains over their full length. Compared to bonded post-tensioning cables, unbonded tendons yields at a larger overall joint rotation. The result is a connection that can undergo large non-linear bridge end deformation without yielding the post-tensioning steel and without a significant loss in self-centering capability. The unbonded tendons will be installed in rigid steel sheathing, stressed from the rear end of the abutment and filled with grease for corrosion protection.

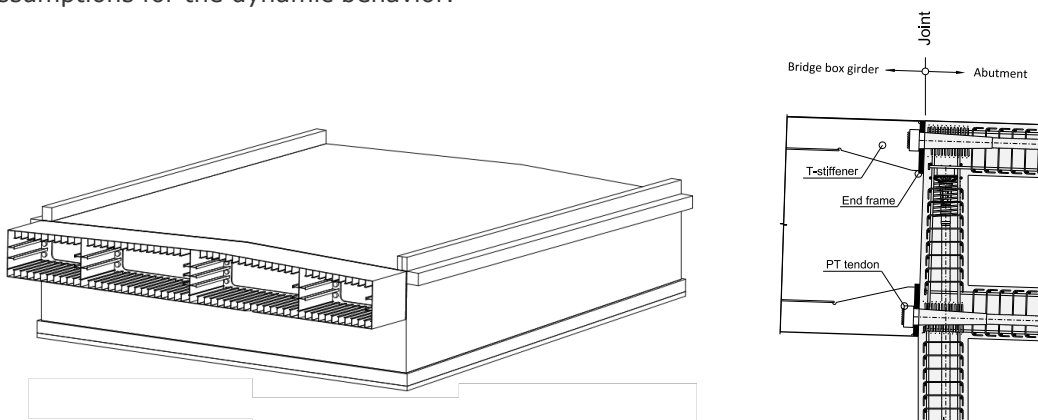
The caisson is designed as a box composed of slabs and walls which are predominantly subjected to membrane action. Slab and wall thicknesses are mainly governed by geometric requirements for fitting orthogonal post-tensioning tendons. The post-tensioning tendons are anchored at the rear end of the abutment to obtain a favorable transfer of the bridge end reactions through the longitudinal walls to the base.

The abutments are founded directly on the bed rock. To assure a predictable transfer of base shear and normal pressure, only the outer and the longitudinal walls are cast directly onto rock whereas the base slab is cast onto a sand/gravel layer. The sliding capacity is determined from base friction only.

The contribution from post-tensioned rock anchors to the base friction capacity and to the overturning resistance is well within the limits prescribed by N400 11.6.2.2 [2].

2.8.2 Monolithic connection to abutment

The fixed end restraint of the bridge is obtained by means of post-tensioned tendons closely arranged along the periphery of the box girder and anchored directly into the girder end frame (Figure 2-12). The post-tensioning demand is given by the criterion that the joint shall remain in compression at ultimate state condition in order not to interfere with the assumptions for the dynamic behavior.



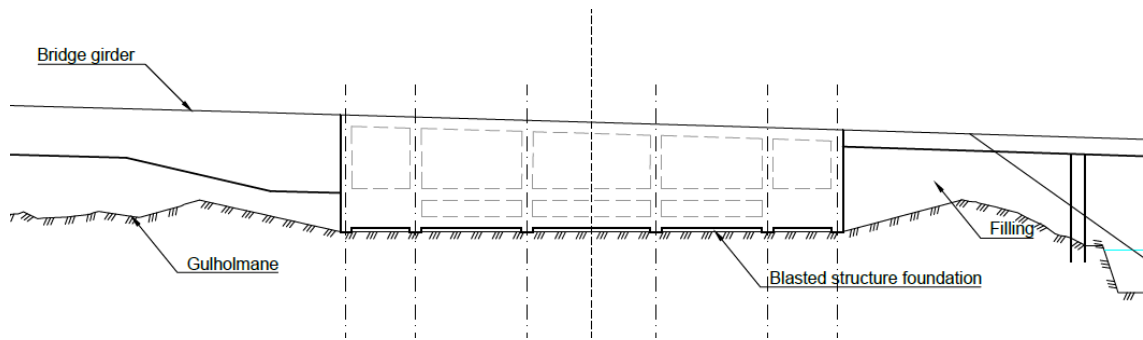


> Figure 2-12 Isometric view of bridge end connection (upper left), detail of post-tensioned joint (upper right) and side view (below).

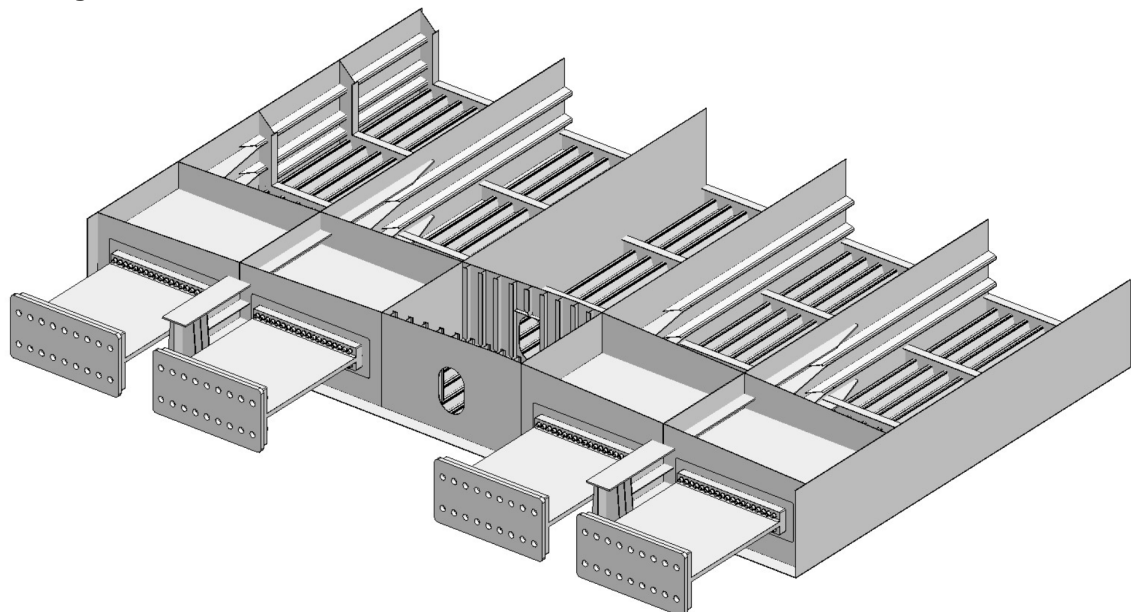
A high level of prestress is required to fully compress the joint. The assumption of a rigid end frame yields a PT intensity of 6-37 tendons @ 0.5 m for abutment north. For abutment south, using the same tendons, the center distance can be somewhat increased. The PT anchors will be spread out both (PT in walls and in slabs) in the rear end of the abutment, to achieve necessary space for the stressing jacks.

The end frame plate of the bridge girder is matching the thickness of the adjoining concrete slabs and walls. A high strength concrete with a concrete grade of B85 is required in the areas near the anchors, to resist the bearing stresses in the joint in ULS. The general concrete grade can be much lower.

To provide the necessary moment capacity and to achieve enough space for the post-tensioning arrangement, the height and width of the bridge box girder cross-section must be increased at the connection.

2.8.3 Plate hinge connection to abutment

The alternative optional concept with a plate hinge, releases the weak axis moment in the connection. The release is provided by an arrangement of flexural cast steel plates that are connected into the abutment by post-tensioning cables and bolted into the bridge box girder, see Figure 2-13.



- > *Figure 2-13 Flexural steel plates releases the weak axis moment in the connection to the abutment.*

The post-tensioning demand is given by the same criterion as for the monolithic connection, i.e. that the joint shall remain in compression at ultimate state condition in order not to interfere with the assumptions for the dynamic behavior.

The connection consists of 4 plates arranged in pairs at each side, with a vertical load bearing cantilever in between each pair. Hence, the axial force, the strong axis moment and the horizontal shear force is taken by the plates while the vertical shear and torsional moment is handled by the bearing cantilevers.

A high strength concrete with a concrete grade of B75 is required in the areas behind the plates, to resist the bearing stresses in the joint in ULS. The general concrete grade in the abutment can be much lower.

2.8.4 Concept comparison

The monolithic connection is the primary choice of abutment concept. It represents a robust solution without any potential interchangeable parts. No bearings are needed. However, the bridge girder terminal end must be increased both in height and width and the amount of post-tensioning is significantly higher than for the hinged connection.

The hinged connection requires no significant cross-section increase and enables a significantly lower post-tensioning intensity. However, the hinge rotation introduces a break in the vertical line routing of the road that must be further investigated since it is inconsistent with N400 chapter 13.12.1.1 (for speed limits above 70 km/h). This solution will most likely require some degree of maintenance during its lifetime.

2.9 Approach bridge Gulholmane and tunnel portals

It is important for the aesthetics and recreational use, to keep open a channel for small boats inside Gulholmen. This is easily solved with a separate ordinary concrete slab bridge with two or more spans. The bridge, precast and portals for the tunnel, will be further detailed and illustrated in the next stage of this project.

3 LOADS AND LOAD COMBINATIONS

3.1 General

The loads are divided into categories based on their nature and the likelihood of their occurrence:

- Permanent loads (G)
- Variable loads (Q)
- Accidental loads (A)

3.2 Permanent loads (G)

The permanent loads include the self-weight of the girder and the columns, buoyancy of the pontoons, pretension loads of the cable stays and the mooring lines. A summary of the self-weight and additional permanent weights are given in the Analysis method report [3].

The mooring system is described in chapter 2.6. Loss of two mooring lines is considered a permanent load for a period of two years of operation.

Marine fouling is calculated in accordance with N400 [2].

A summary of the self-weights used is presented in Table 3-1.

> *Table 3-1 Self-weight summary*

Element	Value	Unit
Structural steel	77	kN/m ³
Reinforced concrete	26	kN/m ³
Asphalt, driving lanes	2.0	kN/m ²
Asphalt, pedestrian lanes	1.5	kN/m ²
Permanent equipment	500	kg/m
Asphalt, driving lanes	2.0	kN/m ²

3.3 Variable loads (Q)

All variable loads are described in the Analysis method report [3] and consist of the following:

- Traffic loads
- Temperature variations
- Environmental loads
 - Water level variations
 - Wave loads
 - Wind loads
 - Current loads

Load specifications are based on Design basis [4]. Wind and wave loads are in general dominating and are therefore presented in brief here.

Mean wind speeds applied for different return periods are shown in Table 3-2.

> *Table 3-2 1h and 10min mean wind speeds for given return periods at z=10m*

Return period (years)	Wind speed 1h mean (m/s)	Wind speed 10min mean (m/s)
1	21.4	22.9
10	25.8	27.6
50	28.5	30.5
100	29.6	31.7
10000	35.9	38.4

The most severe 100-year wave condition considered is shown in Table 3-3.

> *Table 3-3 100-year wave condition*

	Hs [m]	Tp [s]	Gamma	Spread, s
LC04	2.2	5.5	2.30	11

The wind generated waves are represented by spatially inhomogeneous sea-conditions where both Tp and Hs vary along the bridge.

For a more thorough description of the wave scaling along bridge, sea state directions with respect to bridge, and load cases considered, see the Analysis method report [3].

3.4 Accidental loads

The most relevant accidental loads with regards to concept selection are based on Design basis [4] and include:

- Ship impact loads
- Failure in mooring system
 - Loss of two mooring lines
- Underwater landslides
 - Loss of two anchors
- Abnormal environmental loads
 - 10.000-year environmental conditions

3.5 Load combinations

All load combinations applied are described in the Analysis method report [3], and include:

- Ultimate Limit State
 - EQU
 - STR
 - FAT (according to procedure established by DNVGL as described in Design basis [4])
- Accidental Limit State
 - Stage A
 - Stage B
- Serviceability Limit State
 - Characteristic
 - In-frequent
 - Quasi-permanent
- Geotechnical load factors
 - ULS
 - ALS

The load combinations and factors are based on Design basis [4].

The governing load combination with respect to extreme loads is the combination including 100-year environmental conditions, also shown in Table 3-4.

> *Table 3-4 ULS-STR load combination factors, $\gamma \times \psi_0$*

Load		Dominating load E
Self-weight	G	1.2/1.0
Temperature	T	0.84
Environmental, 100 year, without traffic	E	1.6
Other loads	C	1.05

4 STRUCTURAL RESPONSE ANALYSES

4.1 General

An overview of the stress points in the main girder is seen in Figure 4-1 for the main cross sections (HF4, HF5 and HF6) applied in the bridge. The local coordinate systems of the elements are also given in this figure.

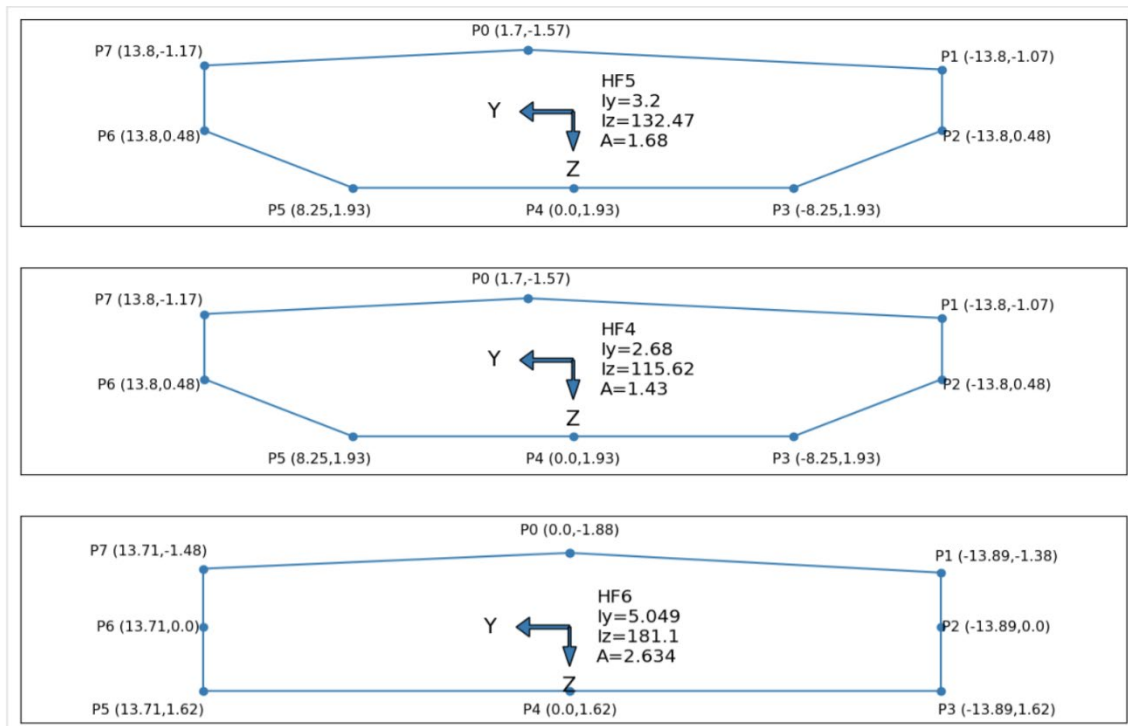


> Figure 4-1 Overview of stress points and local element directions

The mooring lines seen in Figure 4-2 are numbered 1 to 16.

- 1 to 4 is on the *left top* of the figure.
- 5 to 8 is on the *left bottom* of the figure.
- 9 to 12 is on the *right top* of the figure.
- 13 to 16 is on the *right bottom* of the figure.

Within these superior arrangements the mooring lines are numbered from left to right.

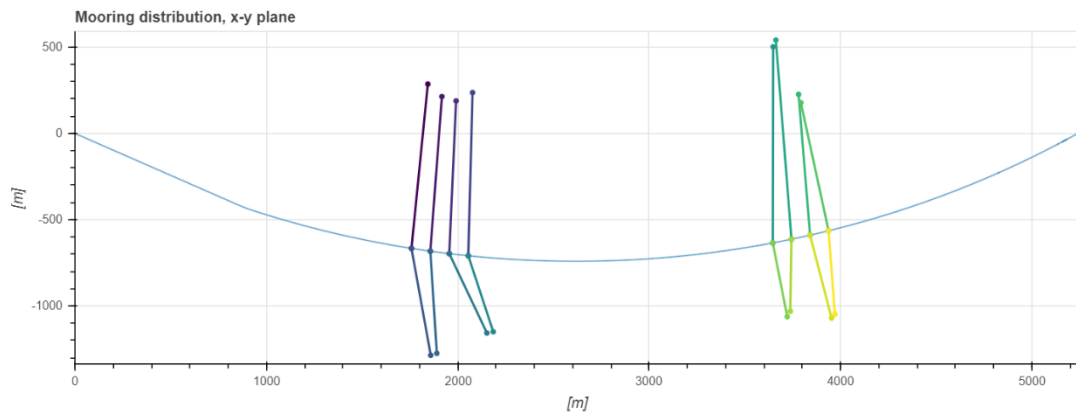


> Figure 4-2 Overview of mooring lines

4.2 Quasi-static loads response

The response presented in this chapter is the characteristic response from the applied static or quasi-static loads presented in Chapter 3. The response is given in terms of envelope curves. Only the most relevant response variables are presented for each load type.

For more detailed response, go to the interactive result webpage [5]. The applied GreenBox model is K12 – model 7.

4.2.1 Permanent loads

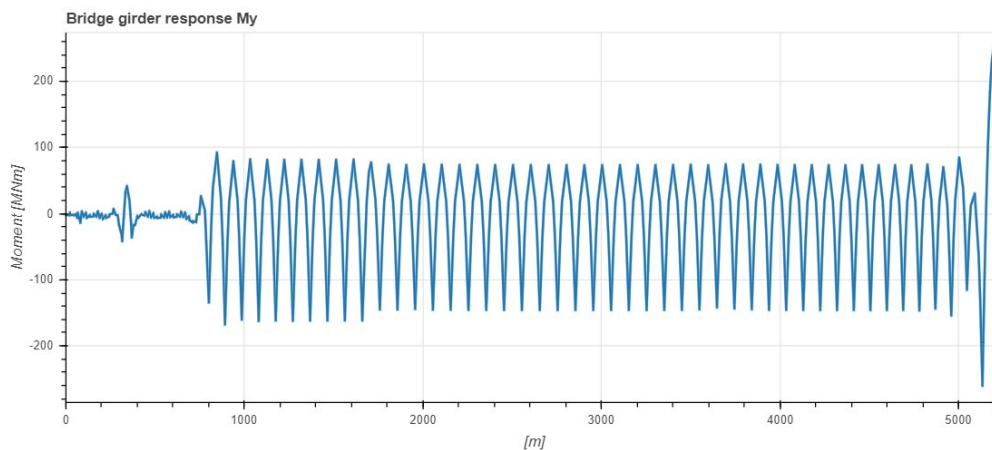


> Figure 4-3 Permanent loads – Weak axis moment in bridge girder

4.2.2 Tidal force

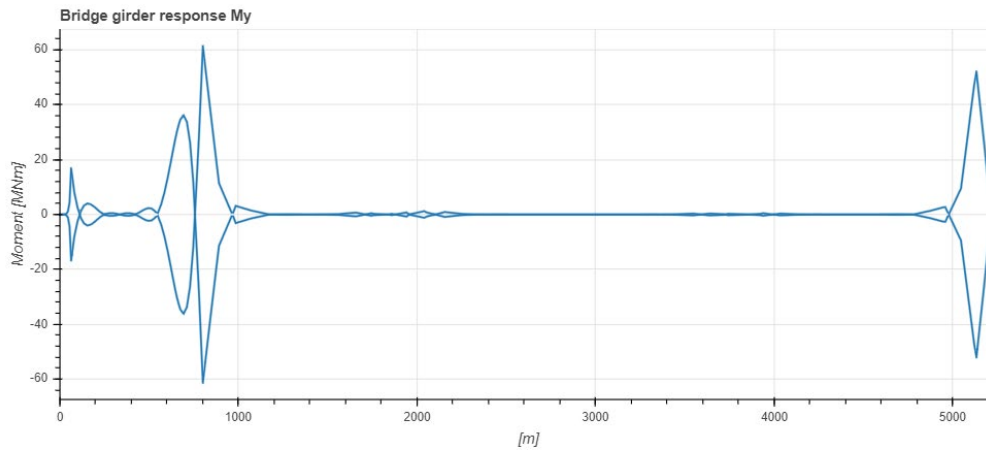


> Figure 4-4 Tidal force – Weak axis moment in bridge girder

4.2.3 Current

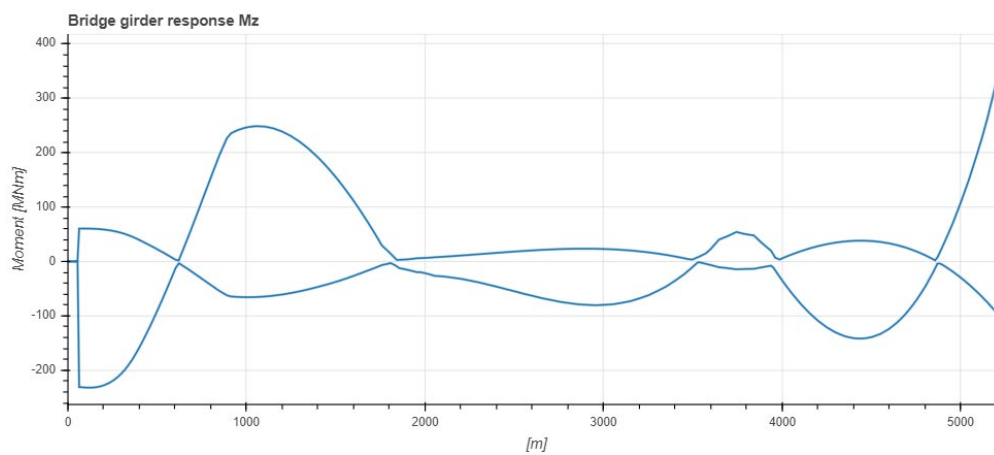


> Figure 4-5 Current - Strong axis moment in bridge girder

4.2.4 Traffic

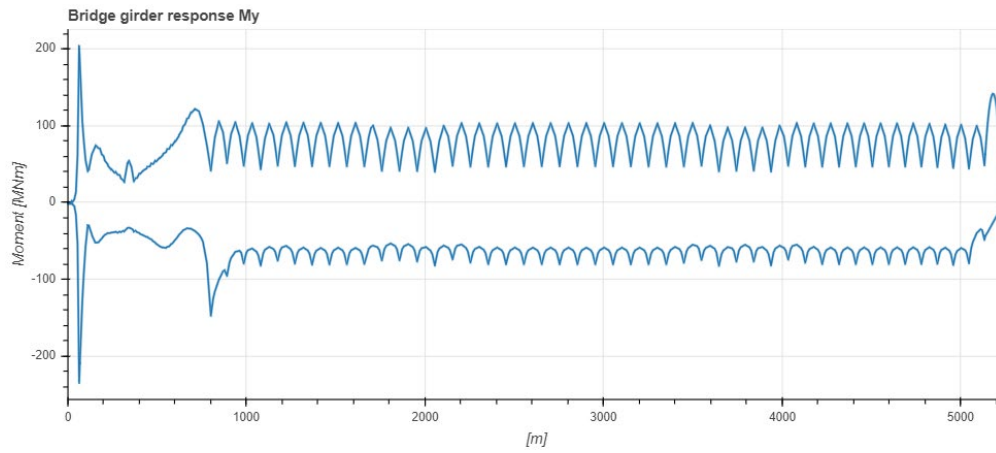


> Figure 4-6 Traffic - Weak axis moment in bridge girder

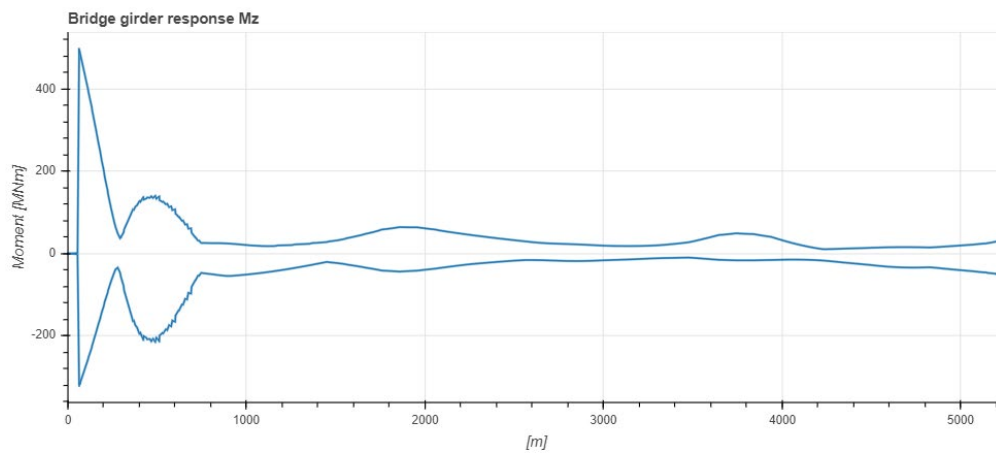


> Figure 4-7 Traffic - Strong axis moment in bridge girder

4.2.5 Static wind

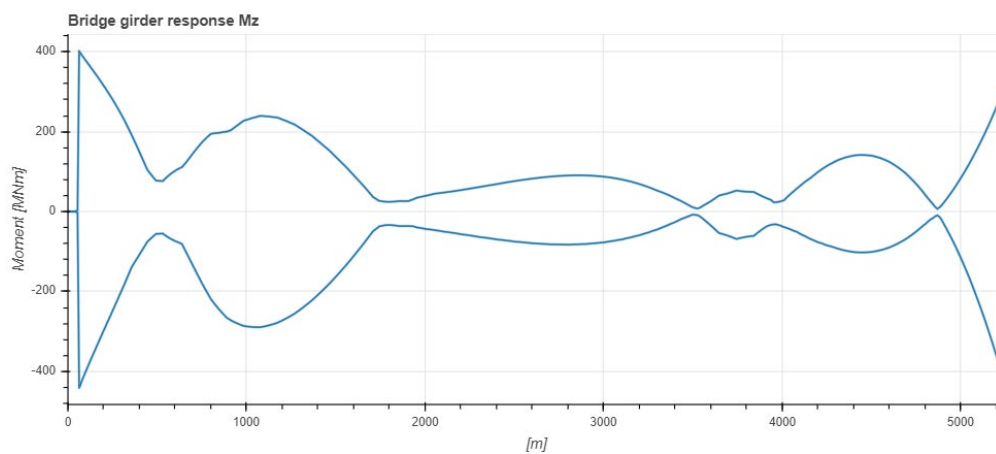
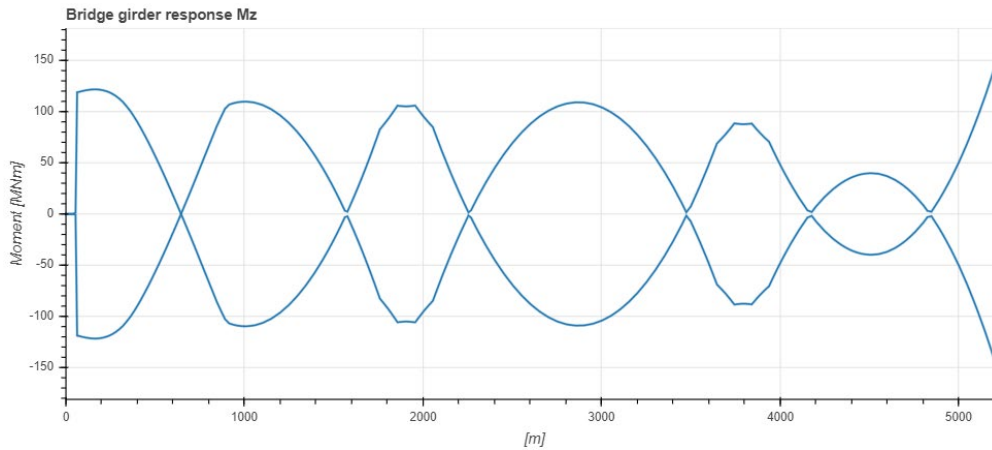


> Figure 4-8 Static wind 100y - Strong axis moment in bridge girder

4.2.6 Temperature



➤ Figure 4-9 Temperature - Strong axis moment in bridge girder

4.3 Global dynamic loads response

The response in this chapter is presented as envelope curves of the coupled load cases described in Chapter 3.

A short summary of the Eigen modes and Eigen periods that trigger the response is given in Chapter 4.3.1, while a short summary of the actual behavior is given in Chapter 4.3.2 to 4.3.4.

The most relevant response of the global dynamic analyses are presented in Chapter 4.3.5 and 4.3.8 for the bridge girder and mooring lines respectively. This response concerns;

- Axial force in the bridge girder
- Weak and strong axis moment in the bridge girder
- Displacement of bridge girder in all global directions
- Stress in three points of the bridge girder
- Axial force in the mooring lines

For more detailed response, go to the interactive result webpage [5]. The applied GreenBox model is K12 – model 7.

4.3.1 Eigen modes and Eigen periods

Horizontal Eigen periods:

The first 14 Eigen modes are mainly horizontal eigen periods. These vary from a period of 68.9s (Figure 4-10) to 6.57s.

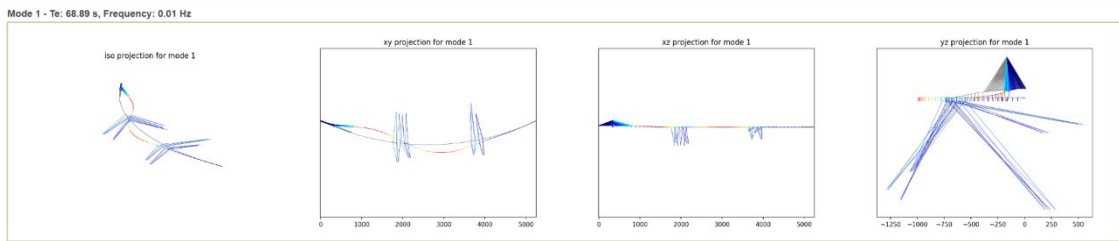


> Figure 4-10 Mode 1 - Period=68.9s

Torsional Eigen periods:

Some torsional contributions are seen in most Eigen modes, but some modes like number 9 (Figure 4-11) and 11 have larger contributions.

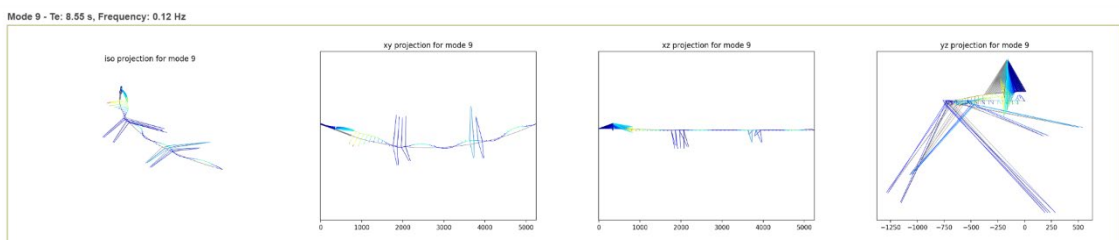


> Figure 4-11 Mode 9 - Period=8.55 s

Vertical Eigen periods:

The first vertical Eigen mode is located in the high bridge and has an Eigen period of 6.42s (Figure 4-12). The first Eigen modes in the low bridge starts around 6.1s

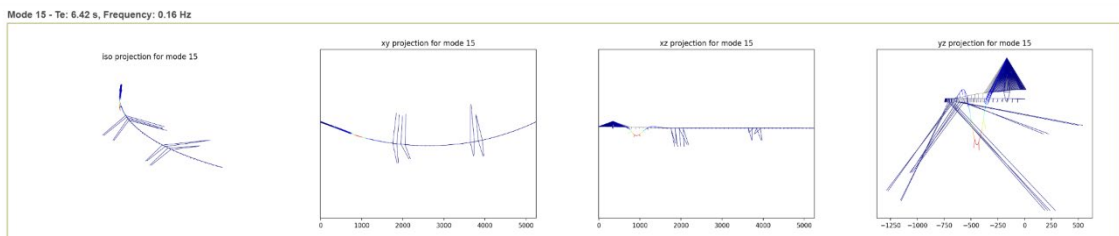


> Figure 4-12 Mode 15 - Period=6.42s

4.3.2 Horizontal response in the bridge girder

The main contributor to the horizontal response in the coupled analyses are the static and turbulent wind contributions. The static behavior from mean wind and mean wave drift are as seen in Figure 4-13, and are shaped by the placement of the anchor system.

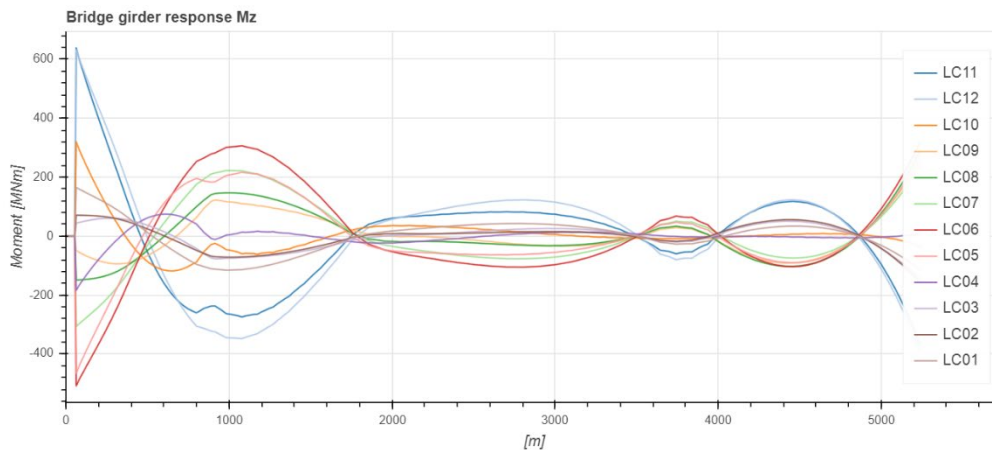


> Figure 4-13 Horizontal static behavior - Strong axis moment (LCs are described in Chapter 3)

The turbulence energy increases for rising periods. The main contributors to the horizontal response from wind comes from the excitation of the first horizontal eigen modes.

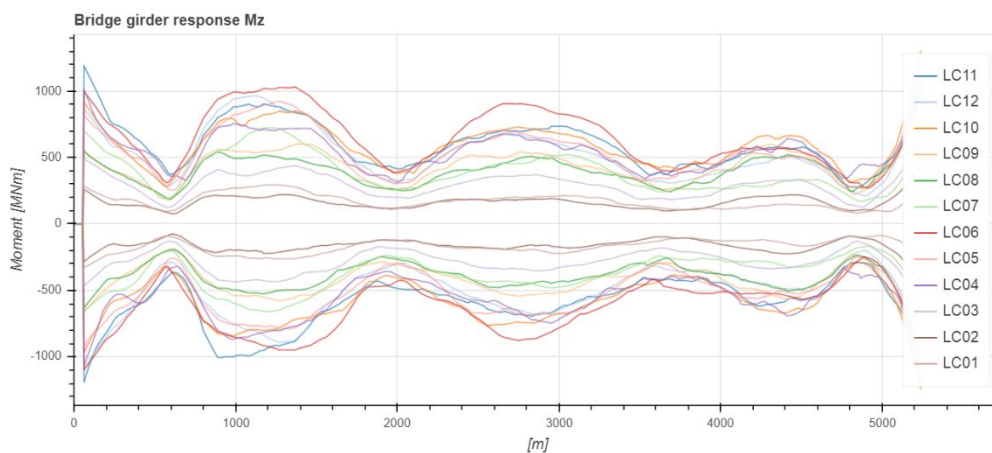


> Figure 4-14 Horizontal dynamic behavior- Strong axis moment (LCs are described in Chapter 3)

The response from swell waves are not included in these analyses. However, they are investigated in the Sensitivity study report [6] and found considerably smaller than the response from turbulent wind. When combining the two contributions, the swell contribution "drowns" in the larger wind contribution due to lack of correlation between the two contributions.

4.3.3 Vertical response in the bridge girder

The vertical response is mostly dominated by the contributions from wind generated sea. Waves propagating parallel to the bridge (normal to the longer side of the pontoons) trigger a pendulum effect in the pontoon connection to the bridge girder and leads to a significant weak axis moment in the bridge girder. Waves coming in normal to the bridge are somewhat larger than those coming in parallel, and trigger the vertical response in the pontoon which also have a significant impact on the weak axis moment in the bridge girder. The weak axis

moment is as seen in Figure 4-15 larger for the higher part of the bridge (left) and towards the landside in north than in the middle part of the bridge. This has to do with both the changing wave conditions along the bridge, and the different elevations of the bridge girder along the span.

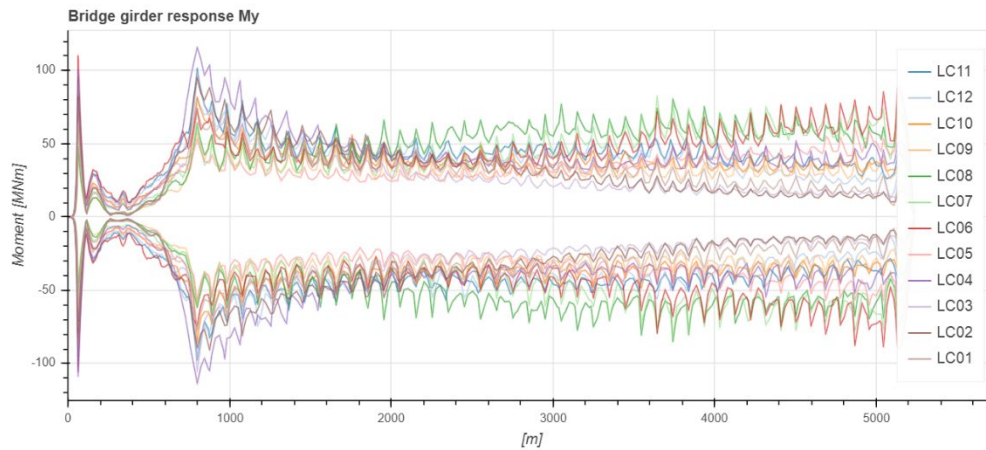


> Figure 4-15 Vertical dynamic behavior - Weak axis moment (LCs are described in Chapter 3)

4.3.4 Behavior of mooring system

The forces in the mooring system are mainly given by the horizontal translations of the bridge. This dynamic contribution of this behavior is mainly driven by higher eigen periods excited by turbulent wind. Thus, the dynamic forces in the mooring systems are dominated by low frequent behavior.

4.3.5 Bridge girder - Forces and moments

Forces and moments are given in local coordinate system, see Figure 4-1.

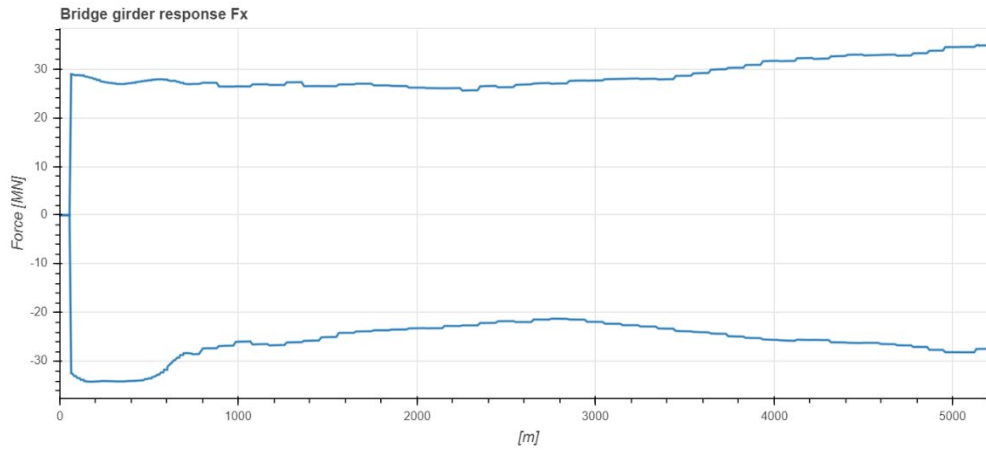


> Figure 4-16 Axial force in bridge girder

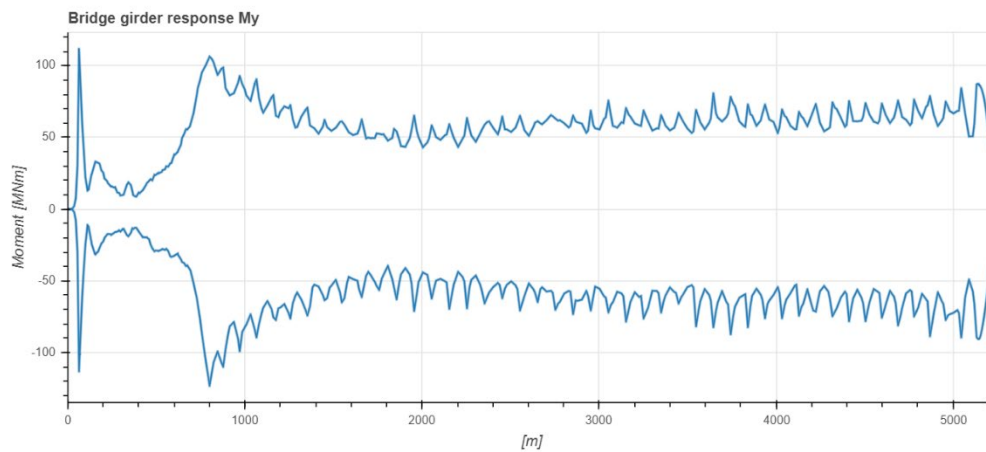


> Figure 4-17 Weak axis moment in bridge girder

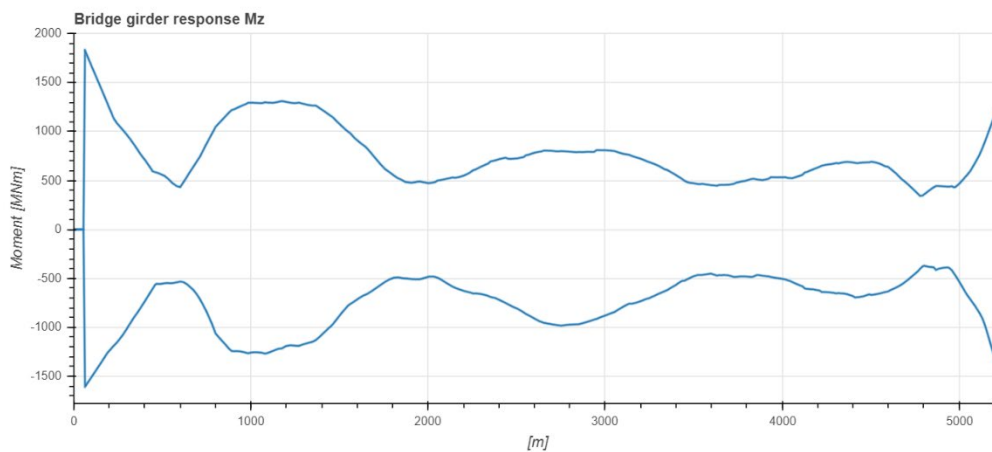


> Figure 4-18 Strong axis moment in bridge girder

4.3.6 Bridge girder displacements

Displacements are given in global coordinate system.

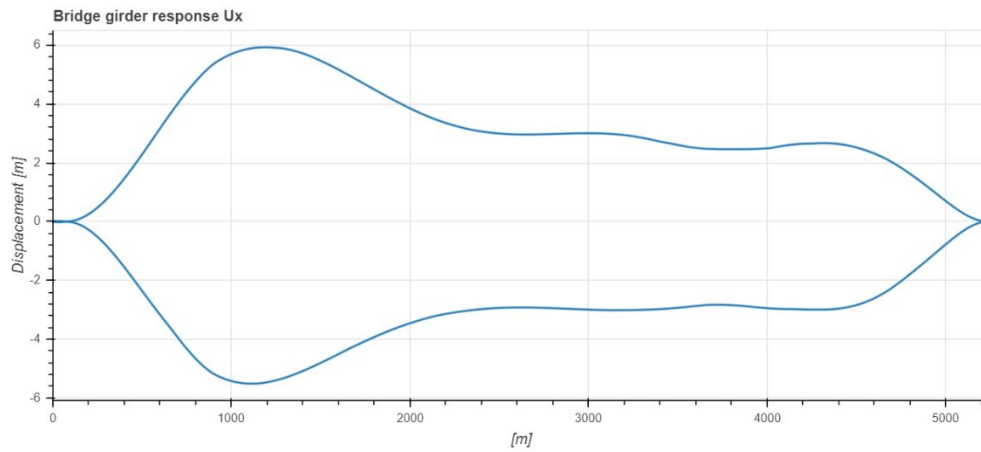


> Figure 4-19 Displacement in global X-direction

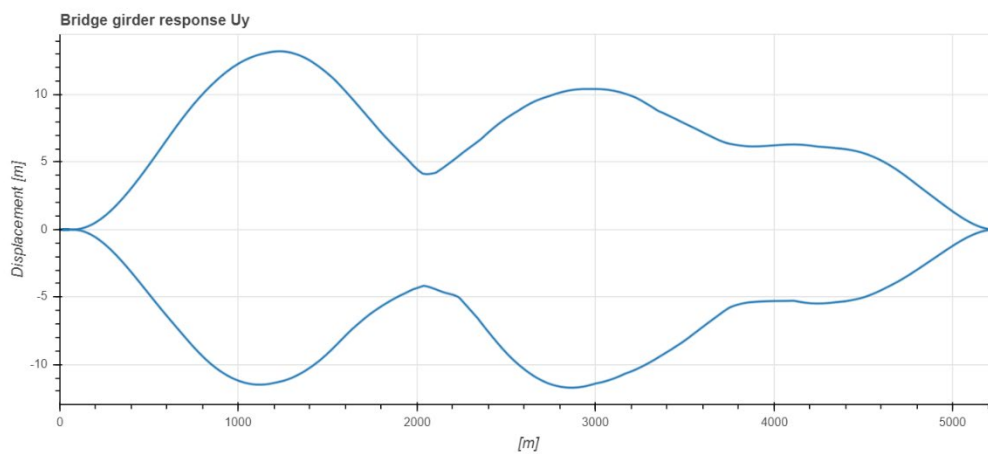


> Figure 4-20 Displacement in global Y-direction

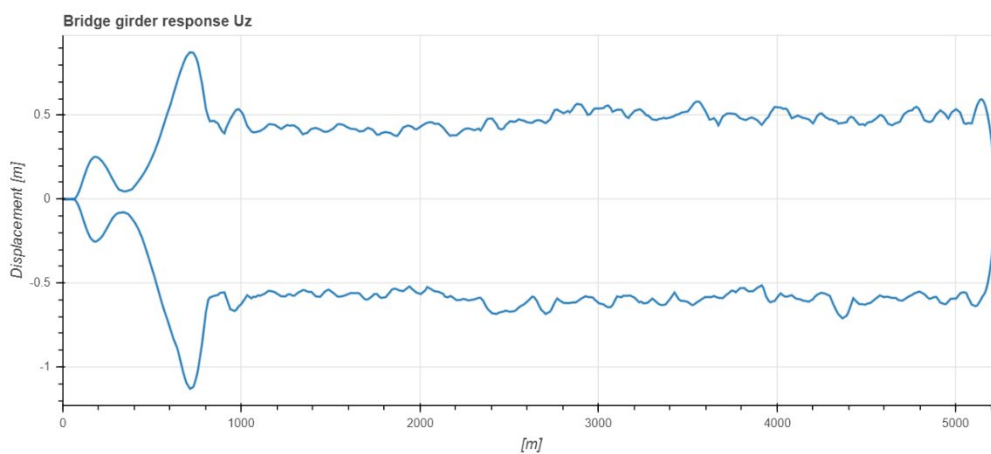


> Figure 4-21 Displacement in global Z-direction

4.3.7 Bridge girder axial stress

The axial stress is based on contributions from axial force, weak axis moment and strong axis moment.

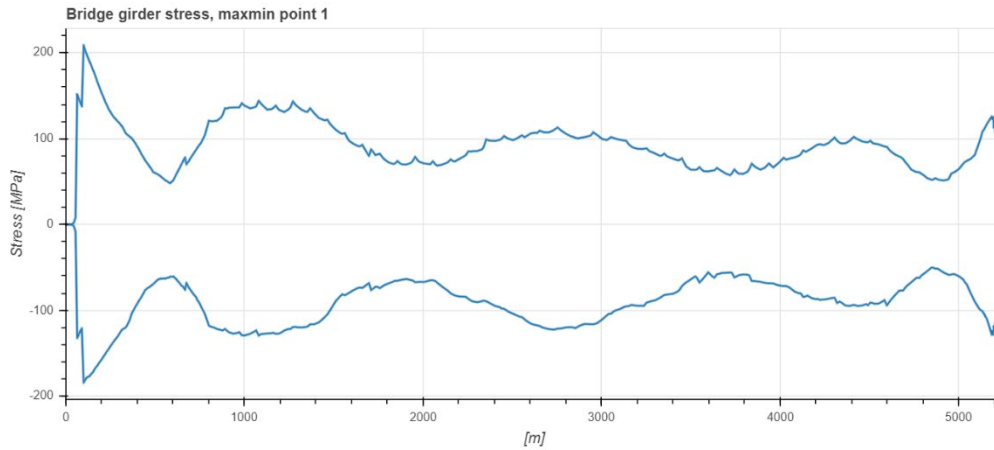


> Figure 4-22 Axial stress in point 1

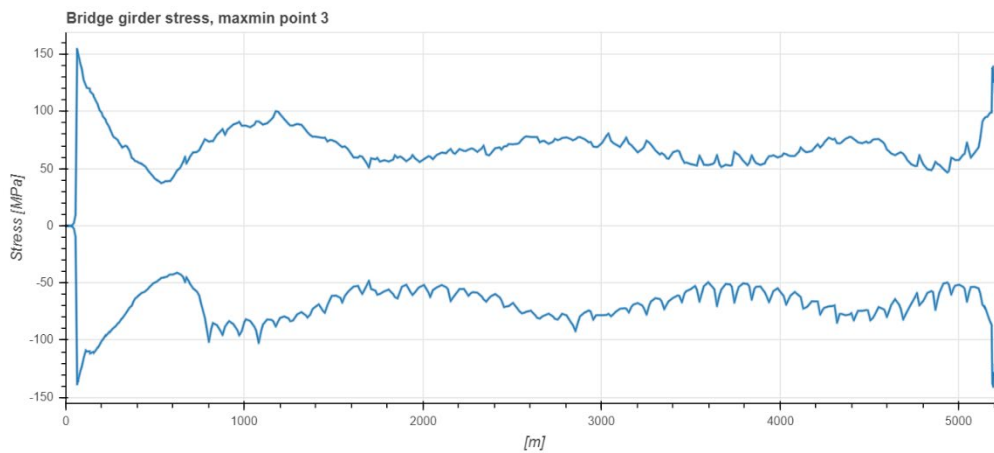


> Figure 4-23 Axial stress in point 3

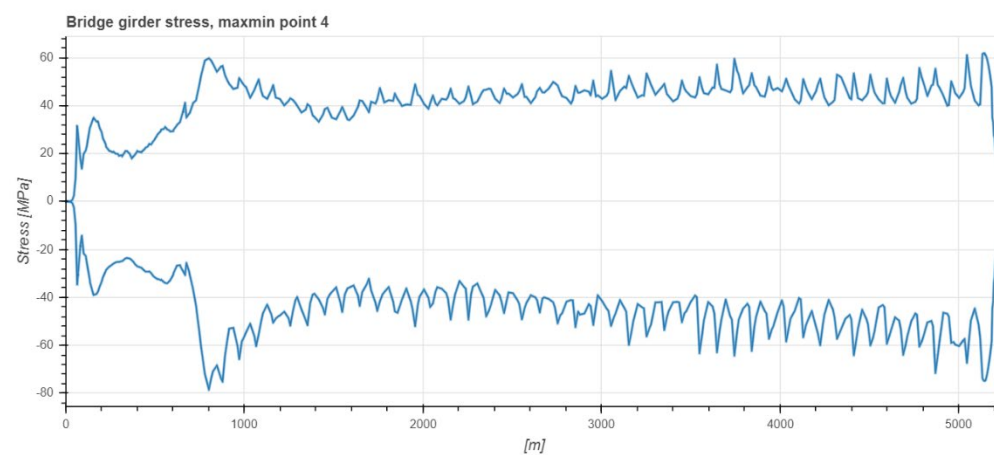


> Figure 4-24 Axial stress in point 4

4.3.8 Mooring system

The mooring line forces are given in terms of local axial direction. The reference between the mooring line number given in Figure 4-25 and the physical layout is presented in Chapter 4.1. In the current analyses the mooring system is modelled simplified by use of a single cable element. This is the reason why we have both positive and negative axial forces in the mooring lines. This must be, and is, compensated for in design.

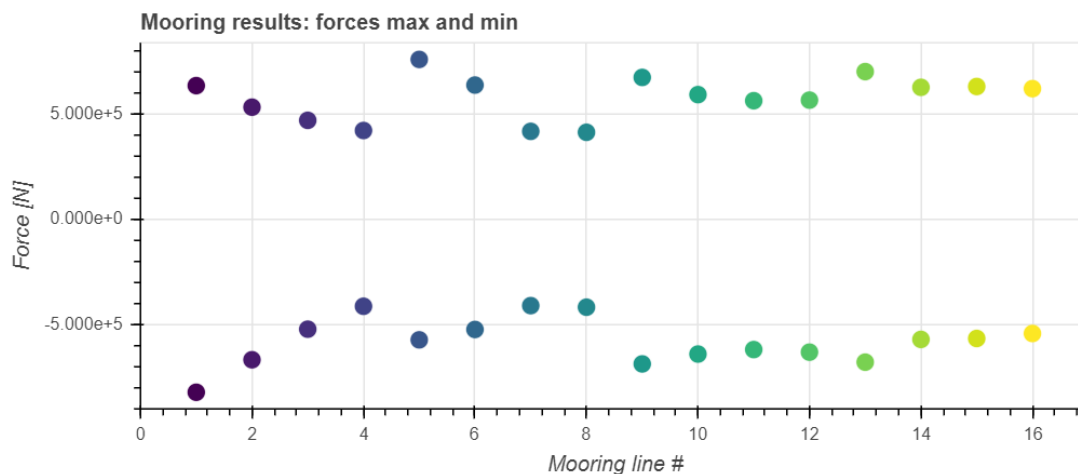


> Figure 4-25 Axial force in the different mooring lines

4.4 Ship impact assessment

4.4.1 Overview

The ship impact workflow investigates dynamic response for each concept subject to ship impact in a variety of points on the bridge girder and pontoons in directions normal to and parallel to the bridge axis.

The ship impact workflow is split in two:

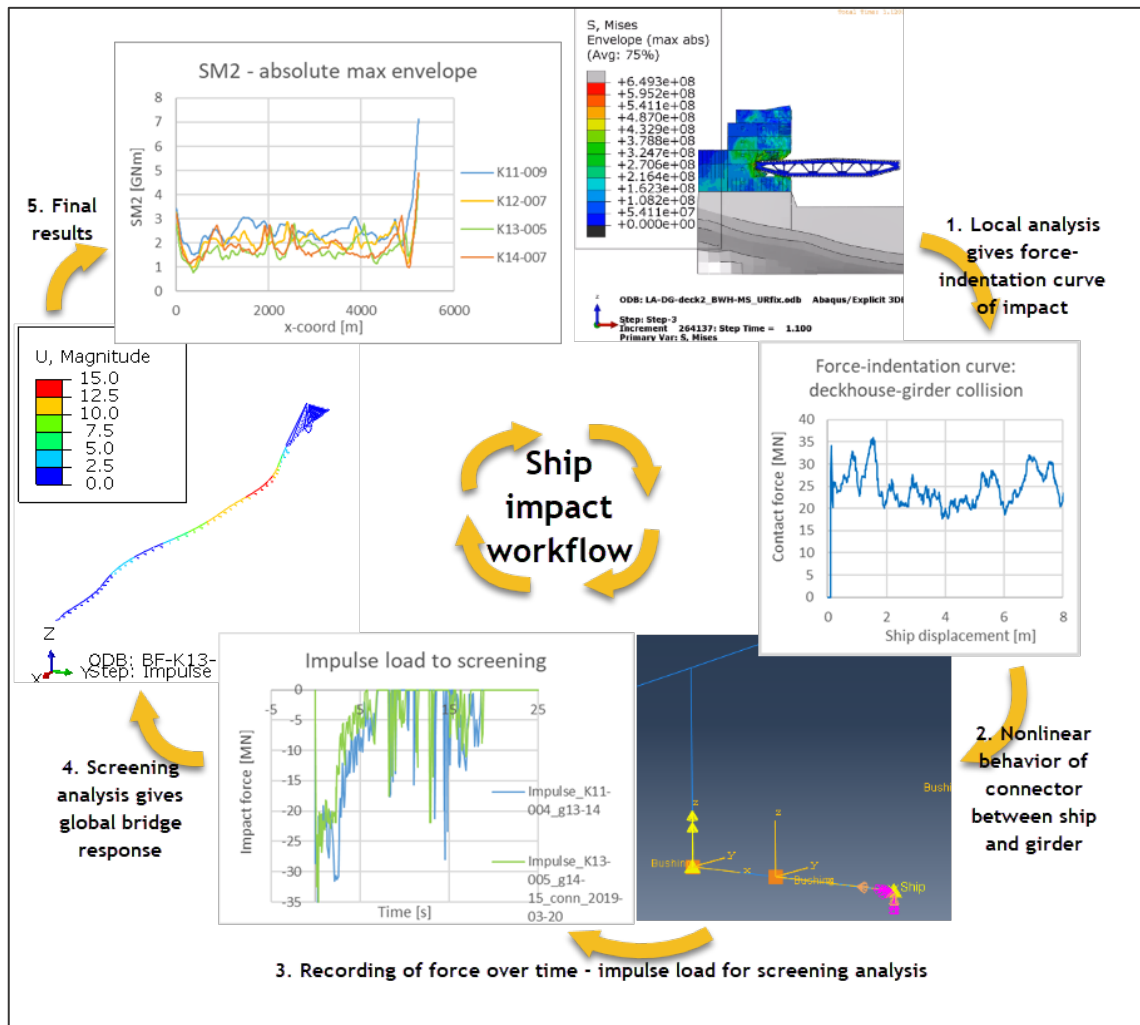
1. Local analysis: given accurate geometry and material modeling for ship, pontoons and bridge girder, determine response between the ship and its impact with force, displacement and energy.
2. Global analysis: given a global model of beam elements and a ship modelled as a mass point in motion, determine the global motion of the bridge.

Differences in local analysis are negligible across concepts, and the same local analysis results can thus be used for different global concepts. Central to local analysis results is a force-displacement diagram across the boundary between the ship and its impact surface.

A nonlinear spring is used to model local deformation and damage for the ship and its impact. This nonlinear spring is taken directly from the force-displacement curve found in the local model.

We consider strong axis bending moment (SM2 in figures) in the bridge girder to be characteristic for the global model response. Hence there has been performed a screening analysis with girder impacts in a variety of points, as the girder impact has the most energy.

The workflow for the results presented in this report is shown on Figure 4-26 below.



- > Figure 4-26 Ship impact workflow. Local analysis: step 1. Global analysis and post processing step 2-5.

This report focuses on what differentiates the bridge concepts K11-K14, which is the global response due to girder impacts. The local effects from pontoon impacts will be similar on all concepts, as the global response in the bridge is quite slow. This will be presented in later reports.

The software Abaqus/Explicit [7] is utilized for local analyses, and Abaqus/Standard [7] for global analyses.

4.4.2 Local response – Pontoons

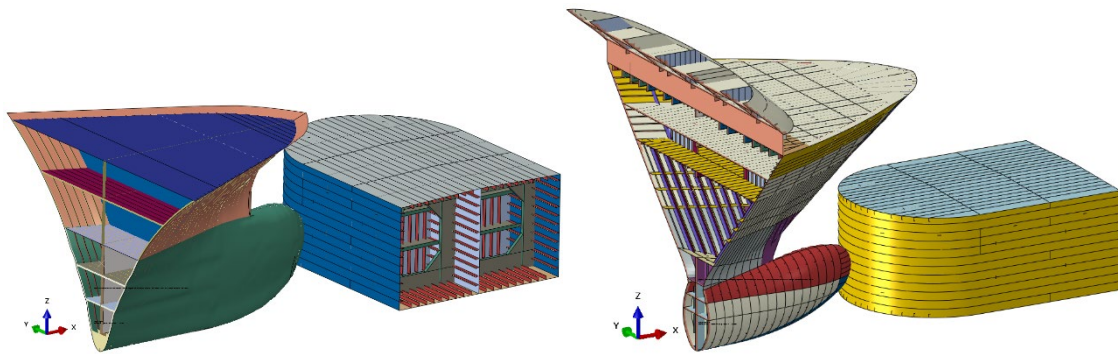


> Figure 4-27 Pontoon finite element model with container bow 90-degree impact (left) and ice-strengthened bow head-on impact (right)

Local response of bow-pontoon collision is studied for the pontoon in axis 3, which is subjected to the largest impact energy according to the design basis [4]. The geometry of the pontoon is taken from the K7 end-anchored floating bridge of phase 3, drawings K7-057 [8] and K7-063 [9]. The pontoon width is 17 m in concept K12 of phase 5 instead of 16 m; this is not considered as governing.

Pontoon finite element model data overview:

- Length modelled: 21.5 m (6 compartments), pontoon fixed at boundary cut-off
- Plate thicknesses: 14 mm (top), 16 mm (walls and bulkheads), 18 mm (bottom)
- Frames: 1500x300x12x15 and 1250x300x12x15
- Stiffeners: HP320x12 for all plates
- Elements: Mainly S4R (linear shell elements with reduced integration) and characteristic size 100 mm at impact area

Two ship bow models are provided by the client and described in the design basis [4]. A container bow with a conventional bulb and an ice-strengthened bow with a stiffer and smaller bulb. Characteristic element size of both ship models is 100-150 mm, while the size of stiffeners is 70-210 mm.

> Table 4-1 Material parameters

	Steel quality	Yield stress ¹	$\epsilon_{\text{plateau}}$	K	n
Ship bows	S275	331.8 MPa	0.017	764 MPa	0.185
Pontoon stiffeners	S355	357 MPa	0.015	796 MPa	0.178
Pontoon plates	S420	422.5 MPa	0.012	827 MPa	0.155
Pontoon splash zone ²	superduplex	530 MPa	0.01	1260 MPa	0.215

¹ For thicknesses 16 mm and below

² Only for sensitivity analyses. The splash zone is from 1.3 m below to 1.7 m above water level.

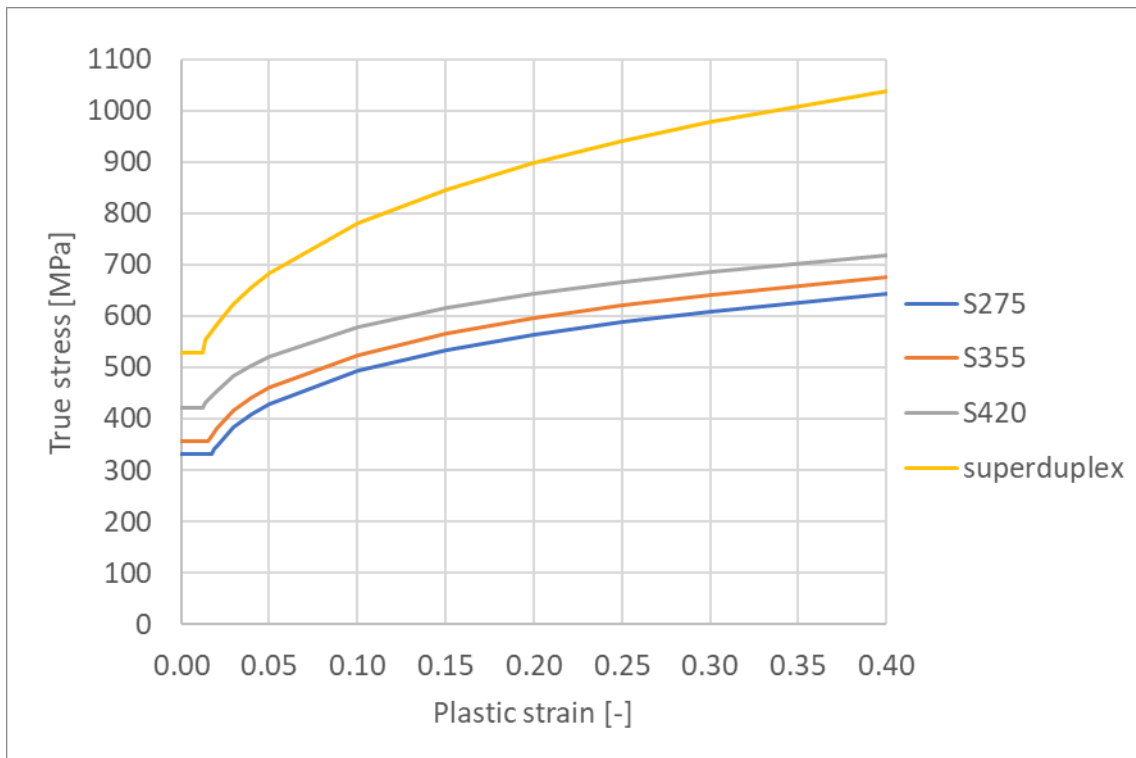


> Figure 4-28 True stress-strain curves of the steel materials

Material modelling:

- Bressan-Williams-Hill (BWH) instability criterium, with mesh scaling. Provided by NTNU and described in [10] [11]
- For reference comparison with a standard strain-based FLD (forming limit diagram)-material described in the Abaqus documentation [7]

Impact scenarios:

- Impact velocity on pontoon in axis 3: 5.6 m/s [4] (increase to 5.7 m/s gives negligible differences)
- Head-on or 90-degree impact + 90-degree impact between bulkheads and frames
- Container bow: Impact height at assumed design draught 1 m above scantling draught (8.6 m) (scantling draught (9.6 m) is non-conservative)
- Ice-strengthened bow: Impact height at design draught (6.8 m)

The resulting contact force for bow-pontoon collision is given in Figure 4-29. The maximum and mean contact force is for comparison given for the period up to 4 m ship displacement.

Load case	Max. contact force [MN] 0-4 m	Mean contact force [MN] 0-4 m
Container, head-on	34	27
Container, 90-degree	27	21
Ice-strengthened, head-on	19	11
Ice-strengthened, 90-degree	22	13
Ice-strengthened, 90-degree between bulkheads/frames	23	7

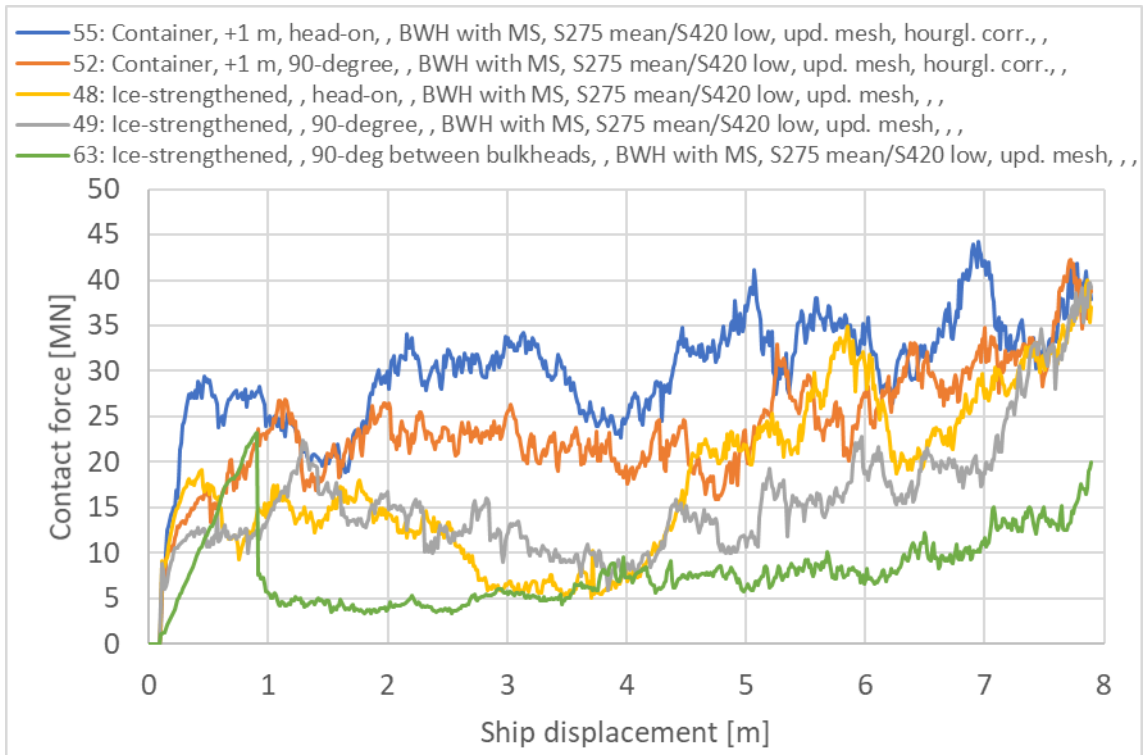


> Figure 4-29 Contact force [MN] impact bow-pontoon

Figure 4-30 shows the internal energy dissipated in the bow and the pontoon. Here, the internal energy is the sum of strain energy, plastic dissipation and artificial energy. It is seen that the pontoon dissipates most of the energy. The impact energy to be dissipated in axis 3 is 248 MJ (locally and globally, 5 % added mass included).

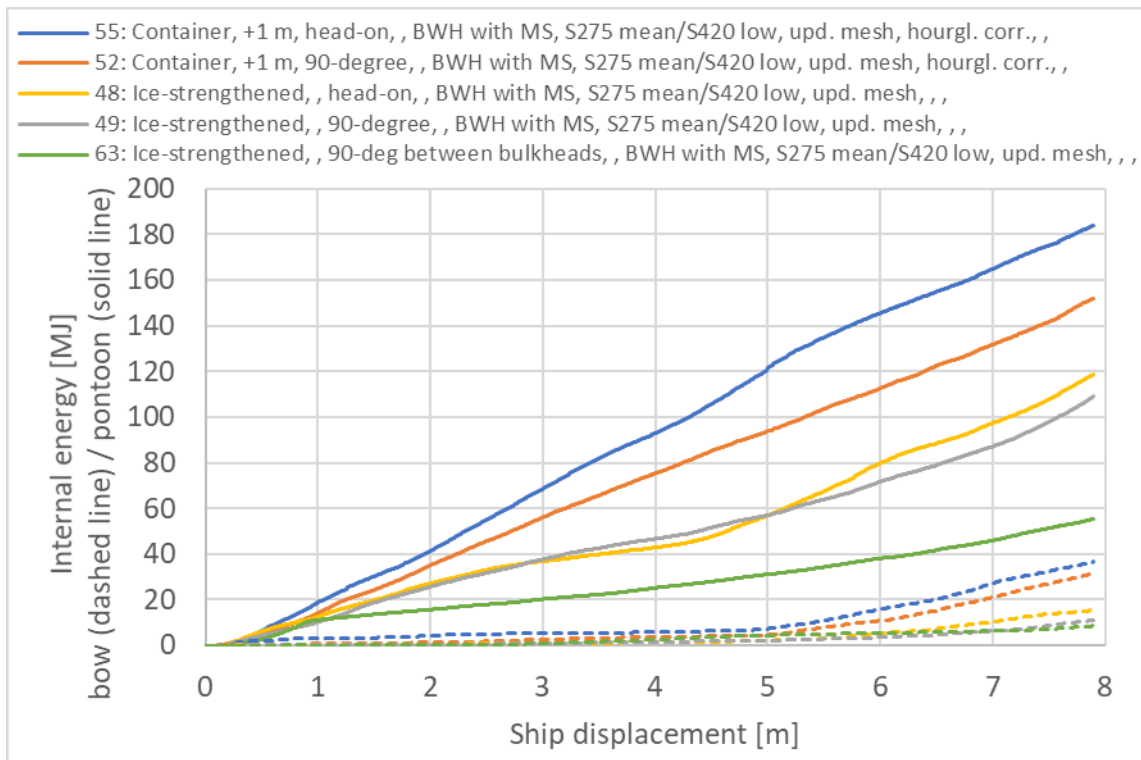


> Figure 4-30 Internal energy [MJ] impact bow-pontoon

Different impact force reduction options have been tested. This included reduced plate thicknesses with 2 mm, reduced stiffeners to HP240x12 and corrugated bulkheads in the front of the pontoon. The damage of the pontoon is regardless severe for a slender design, which is preferred for other load cases and limit states. However, a reduced force level for pontoon collision is beneficial for the bridge girder.

The reduction of the force level is limited for the modifications investigated. The type of ship that hits the pontoon and the direction of the impact is of greater importance but cannot be controlled.

Sensitivity of the finite element models for local response of pontoon collision is studied for material parameters, material damage model, mesh size, element type, impact height and ship velocity.

The choice of material parameters defining the isotropic hardening affects the collision response. Generally, a higher material curve also represents a higher force and energy level. Since the pontoon is more damaged than the ship bow, the pontoon is also more sensitive for the choice of material parameters. Consciousness should be addressed when choosing the hardening parameters.

The models with superduplex steel affect the impact results to both lower and higher force and energy level, but the differences are not prominent. The BWH model with mesh scaling (MS) is considered as the most reliable material damage model tested. The finite element model behaves more independently of the mesh size when mesh scaling is applied.

The element size is sufficiently fine as the modelled size is equal to the orphan mesh of the ship models. Smaller elements result in lower contact force. The proportion of artificial to

internal energy is 8-12 %, which is a bit high. The artificial energy reduces to 4-5 % when utilizing elements with full integration but is time demanding. The model with reduced integration behaves in the same manner as the model with full integration. However, the latter model displays lower energy dissipation in the pontoon and higher energy dissipation in the bow. Employing reduced integration is on the safe side with regards to local damage evaluation of the pontoon.

4.4.3 Local response – Bridge girder

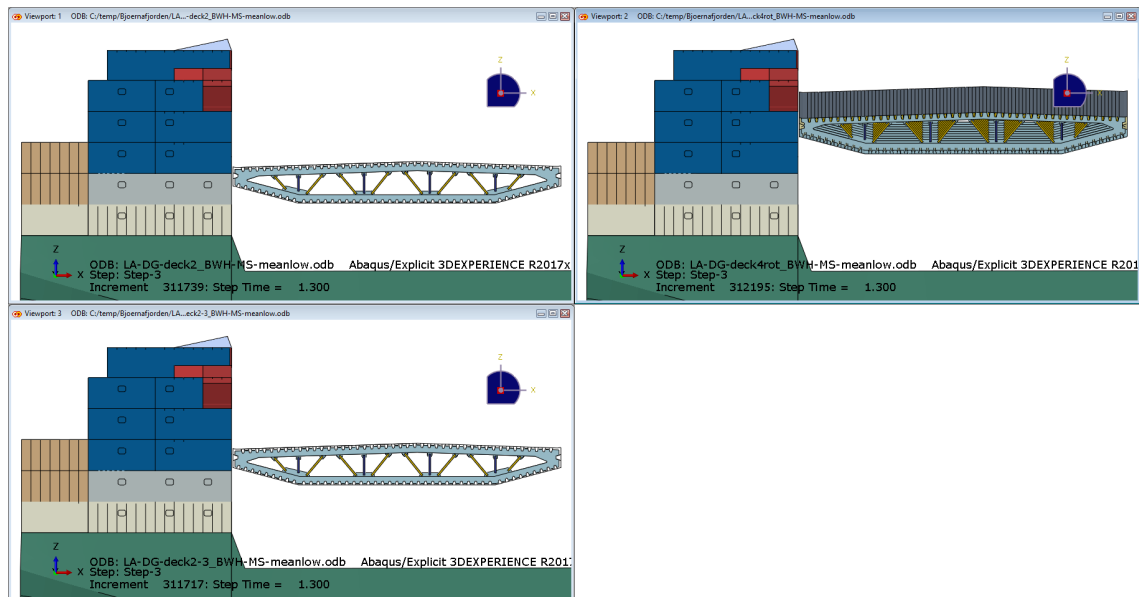


> *Figure 4-31 Deckhouse finite element model with bridge girder at deck 2, inclined at deck 4 and between deck 2 and 3*

Local response of deckhouse-girder collision is studied according to the design basis [4]. The geometry of the bridge girder is taken from the K7 bridge of phase 3, drawing K7-031 [12]. A reinforced bridge girder cross section with equal plate and stiffener thicknesses as the cross section in drawing no. SBJ-33-C5-OON-22-DR-006-A [13] is controlled.

Bridge girder finite element model data overview:

- Length modelled: 44 m (11 sections between bulkheads), bridge girder fixed at boundary cut-offs
- Plate thicknesses: 14 mm (top), 35 mm (side walls), 12 mm (bottom)
- Bulkheads: 600x200x12x15
- Stiffeners: 8 mm (top), 16 mm (side walls), 7 mm (bottom)
- Elements: Mainly S4R and characteristic size 100 mm at impact area

The ship deckhouse model is provided by the client and described in the design basis [4]. The characteristic element size of the deckhouse is 100 mm, while the size of stiffeners is 80-140 mm.

Material modelling is equal to local response of pontoons in section 4.4.2. The ship deckhouse is modelled as S275, and the bridge girder as S420.

Impact scenarios:

- Impact velocity: 6.2 m/s [4]
- Bridge girder at deck 2 (11.5 m clearance to water level), inclined at deck 4 (high bridge) or between deck 2 and 3

The resulting contact force for deckhouse-girder collision is given in Figure 4-32. The maximum and mean contact force is for comparison given for the period up to 8 m ship displacement.

Location	Max. contact force [MN] 0-8 m	Mean contact force [MN] 0-8 m
At deck 2	44	30
At deck 4 inclined	38	27
Between deck 2 and 3	35	20

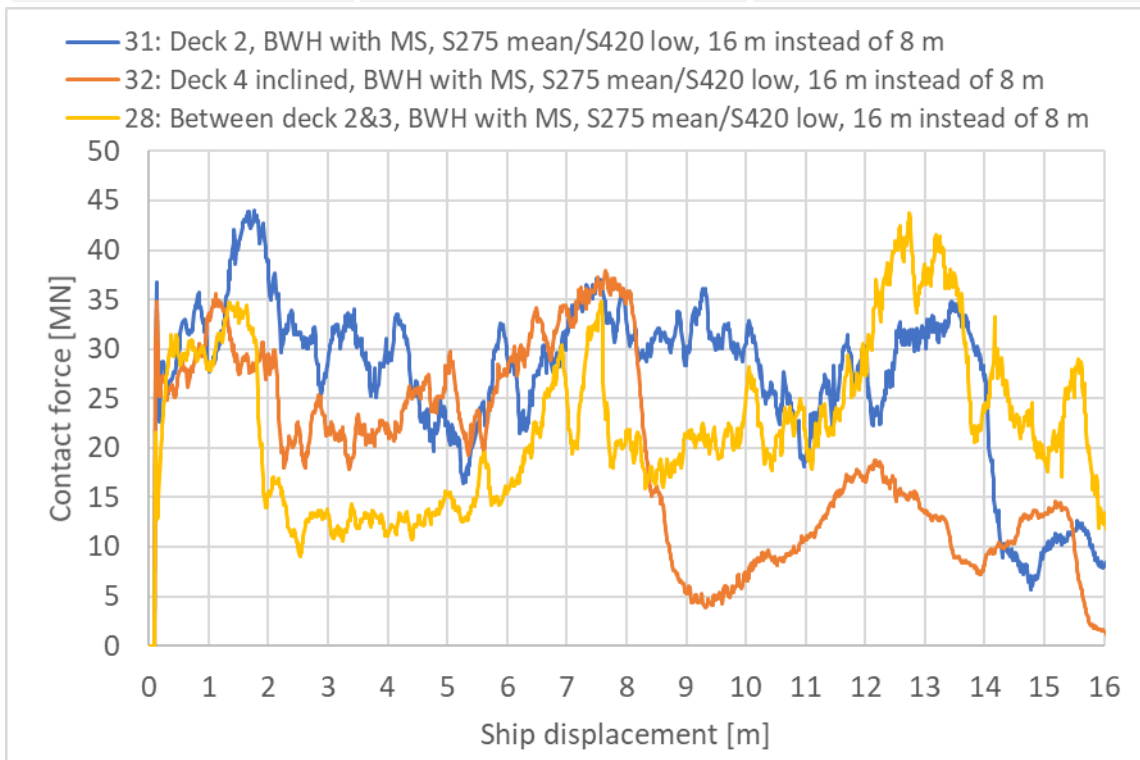


> Figure 4-32 Contact force [MN] impact deckhouse-girder

Figure 4-33 shows the internal energy dissipated in the deckhouse and the girder. It is seen that the deckhouse dissipates most of the energy, while the dissipated energy in the bridge girder stabilizes. The impact energy to be dissipated at the bridge girder is 385 MJ (locally and globally, 5 % added mass included).

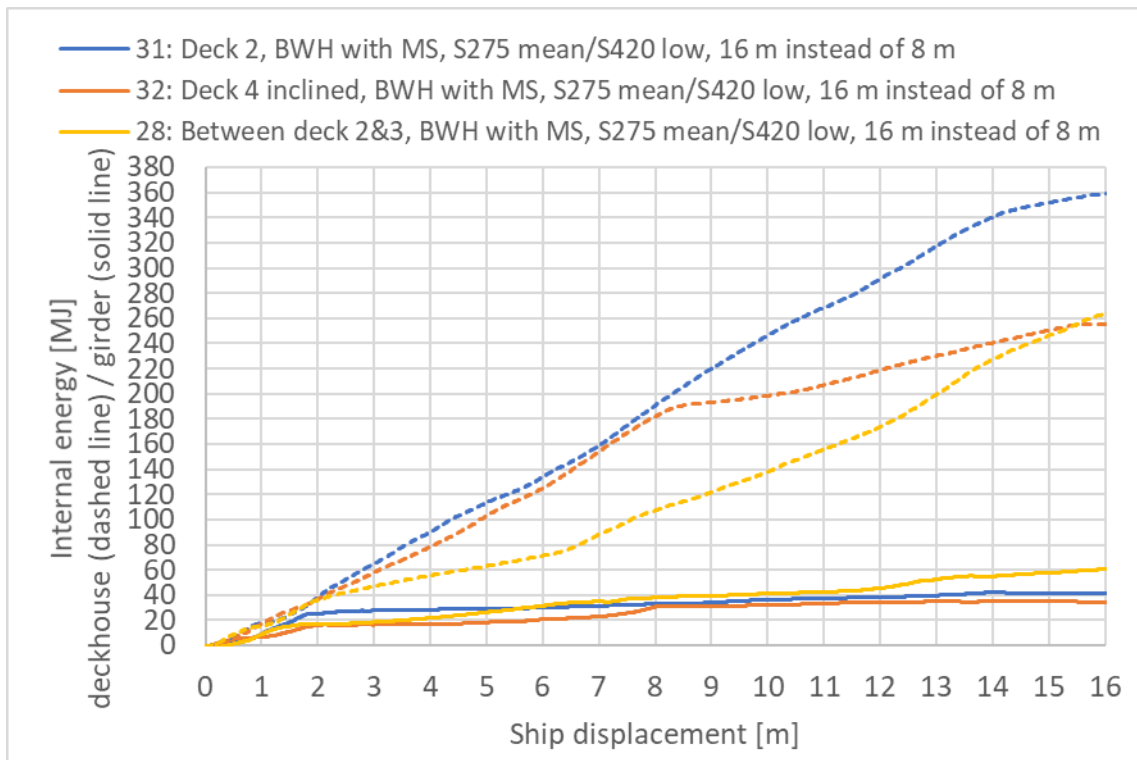


> Figure 4-33 Internal energy [MJ] impact deckhouse-girder

The reinforced bridge girder cross section results in a bit higher force level and higher dissipated energy in the deckhouse. The dissipated energy in the reinforced bridge girder is equal as the non-reinforced bridge girder from the K7 bridge of phase 3. It is concluded that the reinforced bridge girder is equally damaged as the non-reinforced bridge girder. Utilizing the non-reinforced bridge girder in the simulations is conservative.

Sensitivity of the finite element models for local response of bridge girder collision is studied for material parameters, material damage models, element type and mass scaling.

As for the bow-pontoon collision models, the choice of material parameters affects the collision response. However, since the bridge girder is less damaged than the deckhouse, the bridge girder is also less sensitive for the choice of material parameters.

The proportion of artificial to internal energy is also 8-12 % in the FE-models for local response of bridge girder. The artificial energy reduces to 3 % when utilizing elements with full integration but is time demanding. The model with reduced integration behaves in the same manner as the model with full integration. The latter model displays lower energy dissipation both the bridge girder and the deckhouse. Employing reduced integration is on the safe side with regards to local damage evaluation of the bridge girder.

Some elements in the deckhouse model are very small. An automatic mass scaling which limits the minimum time increment is therefore applied to the deckhouse, scaling about 20 % of the total mass. A model without mass scaling gives negligible differences, and the applied mass scaling is satisfactory.

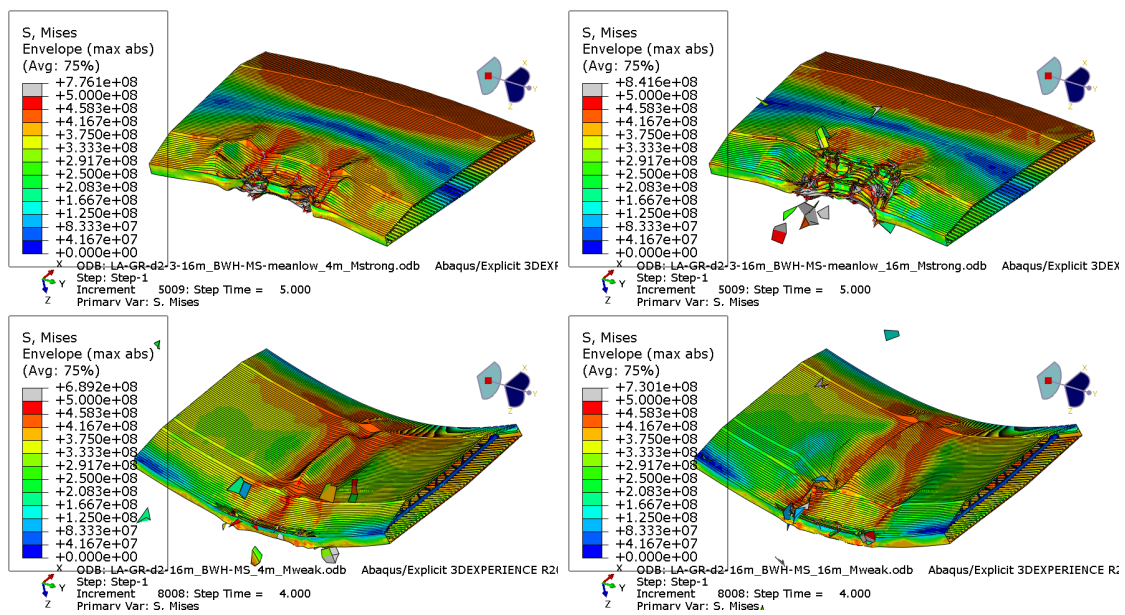


> Figure 4-34 Damaged bridge girder after 4 m (left) and 16 m ship displacement (right) applied with moment about strong axis (upper) and weak axis (lower). Deformations are scaled with factor 10 (and cause enlargement of damaged elements).

It is desired to study the strength of the bridge girder after a ship impact. The residual capacity is evaluated by applying rotations at the cut-off boundaries of the bridge girder. This is performed for the intact bridge girder and for the damaged bridge girder after corresponding 4 m, 8 m, 12 m and 16 m ship displacement.

The damaged girder from collision between deck 2 and 3 is the basis for the residual capacity evaluation of moment about strong axis, while the damaged girder from collision at deck 2 is the basis for the residual capacity evaluation of moment about weak axis. The reason for the different bases is because these locations resulted in the lowest capacities for the respective unit moments. Stresses and deformations from the ship impact analysis are preserved for the residual evaluation.

The material is equal to local response of bridge girder, S420 with BWH instability criterium, likewise the mesh of the girder. Imperfections are not included; this is not necessary as the goal is to compare the capacity of the damaged girders.

The resulting load-rotation curves are given in Figure 4-35 and Figure 4-36. The hand calculated values (without material factors) based on first yield of the girder edges are included for comparison. Table 4-2 evaluates the residual capacity as the apex of the load-rotation curves. It is seen that the reduction of capacity does not drastically fall even up to 16 m ship displacement. The reason is because the deckhouse dissipates most of the energy, while the dissipated energy in the girder almost stabilizes, see Figure 4-33. More than 16 m ship displacement is not very relevant as the deckhouse depth is 17.6 m.

The non-smooth curves and instant "jumps" seen especially in Figure 4-35 are due to explicit evaluation of the capacity. This has been verified by comparing the explicit evaluation with implicit evaluation. The explicit analysis gives higher capacity than the implicit analysis. However, for relative residual capacity evaluation the explicit solver is satisfactorily to utilize. Control of energy balance has been performed for the explicit models. The error is satisfactorily low.

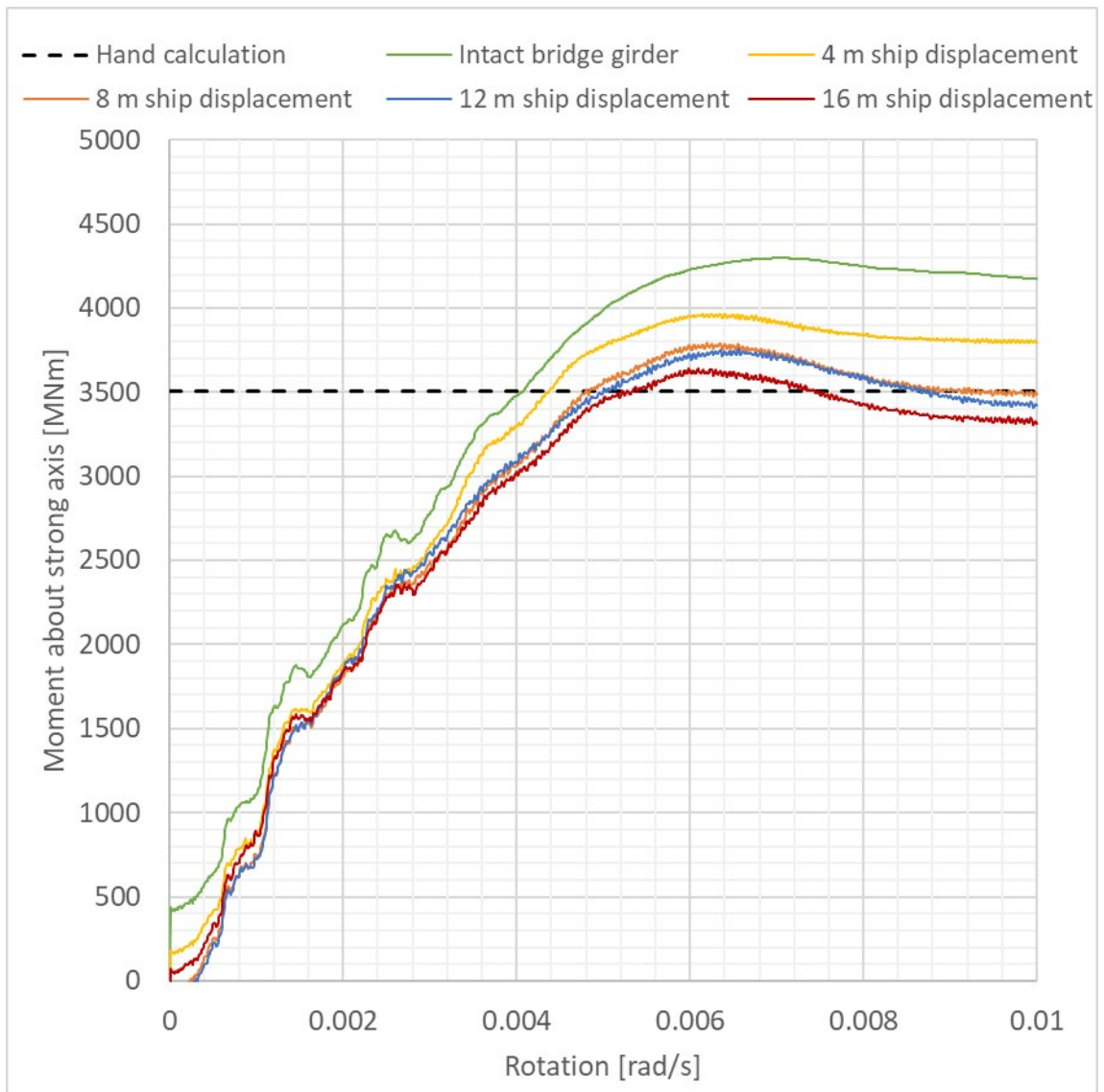


> Figure 4-35 Load-rotation curve for moment about strong axis

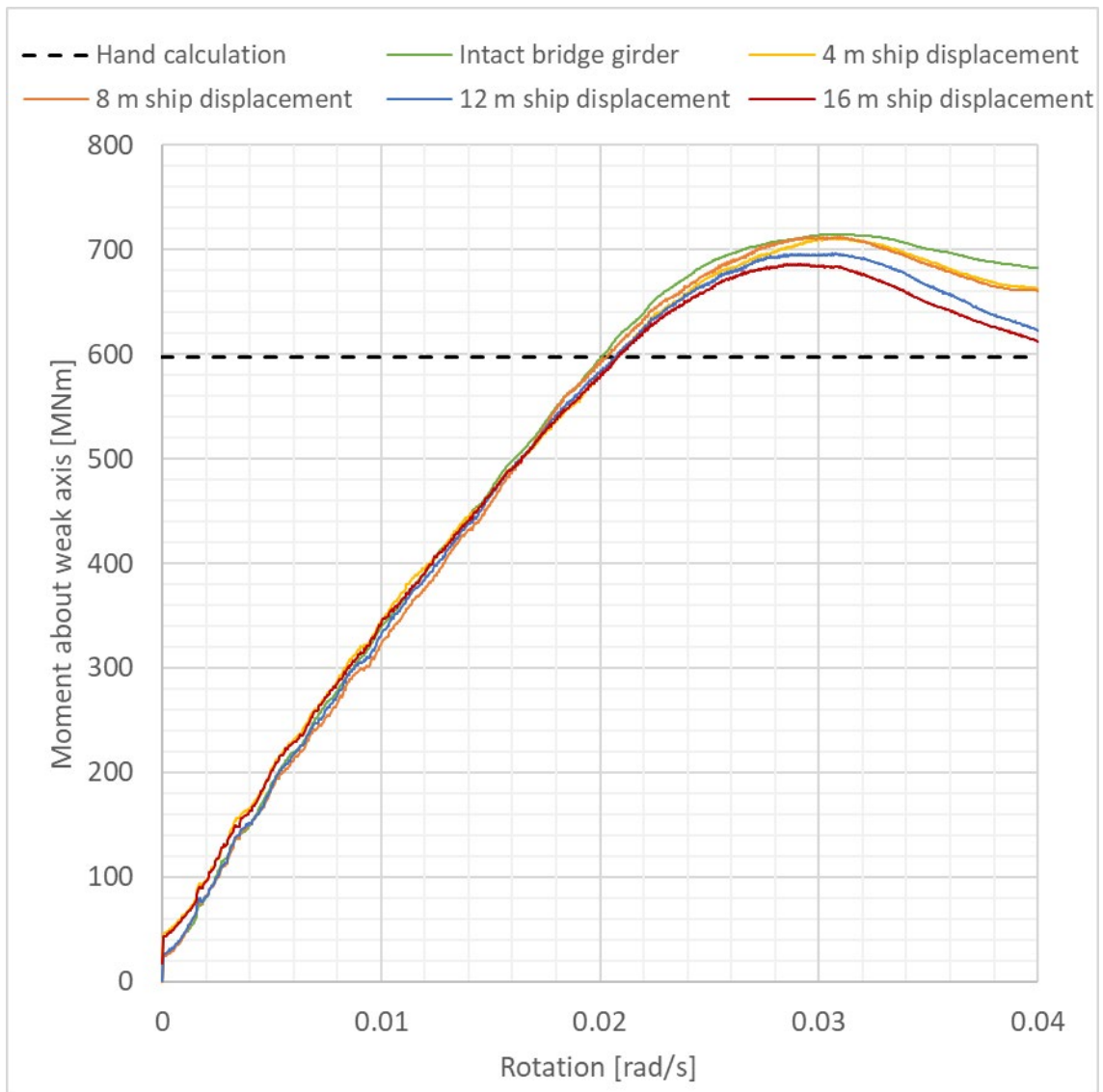


> Figure 4-36 Load-rotation curve for moment about weak axis

> Table 4-2 Residual capacity of bridge girder after ship impact

	Moment about strong axis	Moment about weak axis
Intact bridge girder	100 %	100 %
4 m ship displacement	92.3 %	99.6 %
8 m ship displacement	88.2 %	99.6 %
12 m ship displacement	87.4 %	97.4 %
16 m ship displacement	84.7 %	96.0 %

4.4.4 Global response

The analysis model for global ship impact response is equal to the models for environmental loads, with equal cross section properties and boundary conditions, see description in chapter 4.1. The model consists of wires only, hence the elements used are beam elements of the type B31, except for the stay cables which are B31H. The geometry is imported to Abaqus by a Python-script from the ".json"-input. All section properties are elastic, but second order forces are handled by Abaqus with the "nlgeom=on". The global element size is approximately 10 m, except from the stay cables which are modeled as one element per cable.

Some properties and features are added to the model to behave as correct as possible and to be able to simulate the ship impact. Post-tensioning of the stay cables (by temperature), buoyancy loads, water plane stiffness, structural pontoon mass, added mass and viscous damping on the pontoons and "side anchor springs" (K12-K14) are features that needs to be added for the model to behave correctly. The damping in the model consists of viscous damping only, with a drag coefficient of 0,4 for longitudinal translations and 1,8 for transverse translations. Potential damping is neglected due to low-frequent motions. Added mass is applied to the pontoons as constant masses, set to infinite period (slow motions). Gravity is included in all results.

The ship impact is an implicit dynamic analysis, where the ship is represented by a point mass with an initial velocity. The force-indentation-curve obtained from the local analysis is used to control the force transferred between the ship and the pontoon in the global model. The "ship" is restricted to translations in the horizontal plane only, with very low stiffness for translation orthogonal to the impact direction. The recorded impulse between the ship and pontoon depends on the dynamics and is taken care of by the global model. When all the kinetic energy is transferred from the ship to the bridge, the bridge will "push" the ship away due to elastic strain energy – there is no attachment between ship and bridge after the impact.

Several ship impact analyses have been run with a connector as described above in order to obtain a library of impulse loads, which are later used as input to the global screening analysis. Here, representative impulse loads have been added to the bridge in several impact points in order to record the maximum response of the bridge. See a selection of relevant impulse loads in Figure 4-37 below.

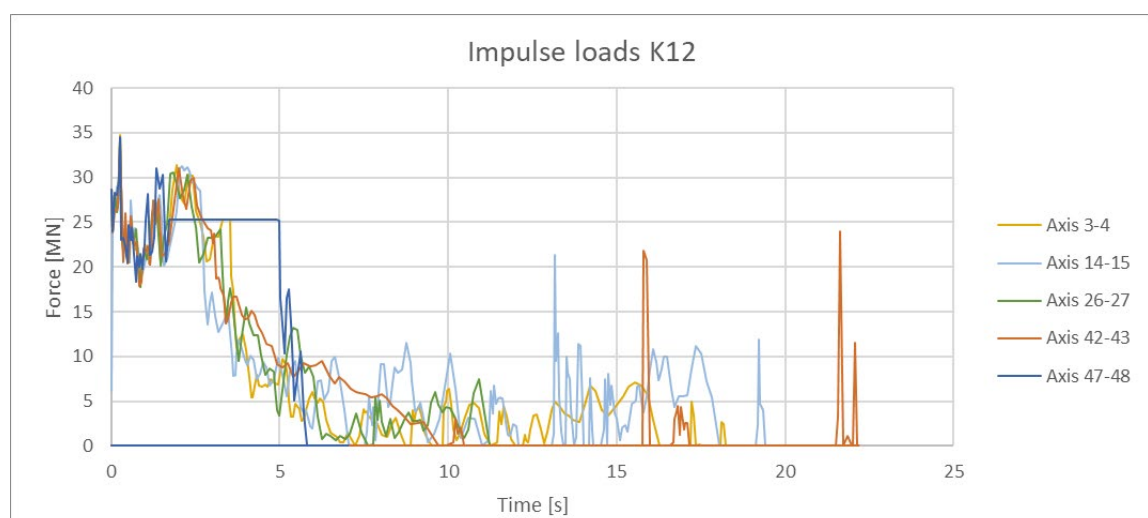


> Figure 4-37 Relevant impulse loads on bridge K12.

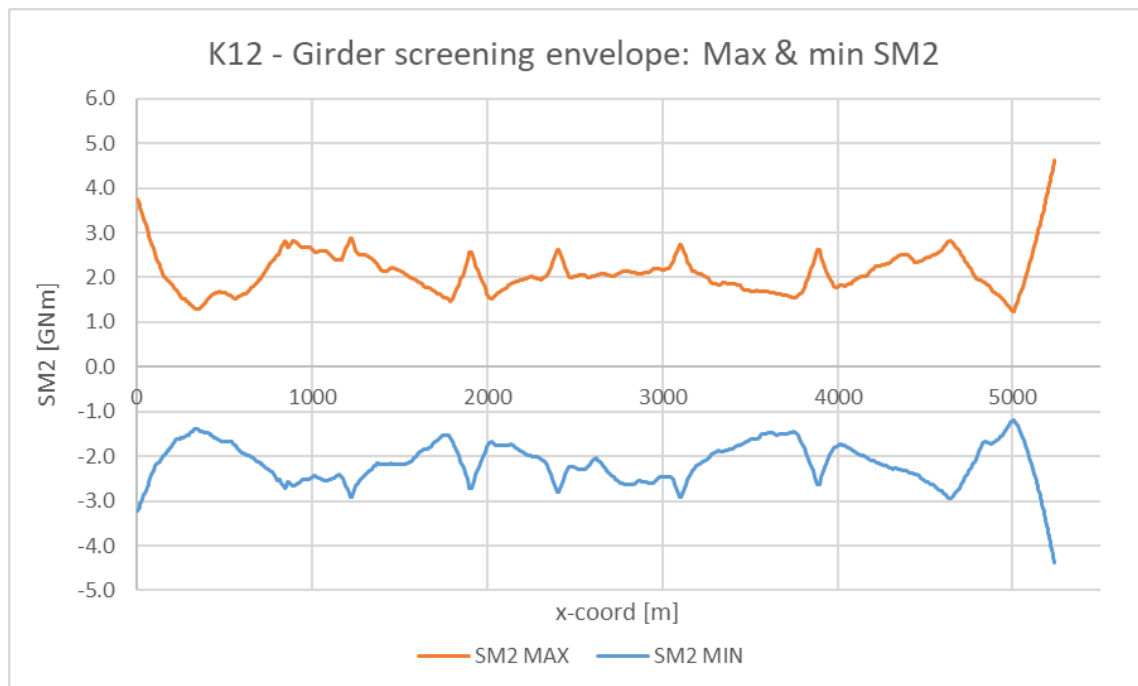
The response presented in this report is the response that is regarded as relevant when comparing the different bridge concepts. These are

- Bridge girder strong axis bending moment
- Maximum displacement of anchor point (K12-K14) – gives maximum elongation of anchor line
- Horizontal displacement of bridge girder at bridge tower, orthogonal to bridge girder.

Important assumptions made at this stage:

- Traffic loads are neglected – these are considered to not change the response between the concepts.
- For screening analysis, there has only been considered impacts to the bridge girder, as this is the impact with most energy and will transfer the most energy to global girder motions.

Results from the screening analysis are presented below. The strong axis bending moments is quite equal along the whole girder – except from the fixpoints at the two bridge ends, where the northern end naturally gives highest bending moments.



- > *Figure 4-38 Global bridge response: maximum and minimum strong axis bending moment in girder.*

The maximum strong axis bending moment is quite similar along the bridge length. A screening with more impact points would have equalized the peaks in the span.

Bridge response results from screening are shown in Table 4-3.

- > *Table 4-3 Bridge girder responses from screening*

Measure parameter	Maximum response
Strong axis bending moment in south end	3,76 GNm
Strong axis bending moment in "span"	2,99 GNm

Strong axis bending moment in north end	4,63 GNm
Maximum displacement anchor line and position anchor line	13,9 m – group axis 32-35
Maximum horizontal displacement of girder at bridge tower, orthogonal to girder.	5,5 m

The global bridge response of the girder is not very sensitive to small changes in the impulse load if the impact energy is unchanged. The response are slow motions, leading to oscillations of large masses.

4.5 Fatigue assessment

4.5.1 Overview

The work flow for calculating fatigue life for each concept is shown below:

1. Creation of relevant FE analysis models:
 - a. Global analysis models of the bridge to calculate section forces from the different fatigue load cases; environmental loads, tidal loads and traffic loads³.
 - b. Local FE models for calculation of stress transfer factors from unit loads at specific points, see Figure 4-40.
2. Establish fatigue specific parameters, i.e. detail categories, design fatigue factors and stress concentration factors, see Table 4-4.
3. Create script that calculates fatigue life for specific points for the entire length of the bridge girder based on the abovementioned points:
 - a. Calculation of local stresses from global loads based on stress transfer factors from unit load model.
 - b. Rainflow count of the stress data for all load cases
 - c. Damage calculation for load types separately and with combined stresses (for comparison purposes)
 - d. Combination of damage from environmental, tidal and traffic loads according to ref. Design basis [4] and DNV GL Fatigue methodology [14].

This procedure has been used to calculate fatigue life at midspan between all axes and at each axis, see Figure 4-39. Points checked on the girder are shown in Figure 4-40.

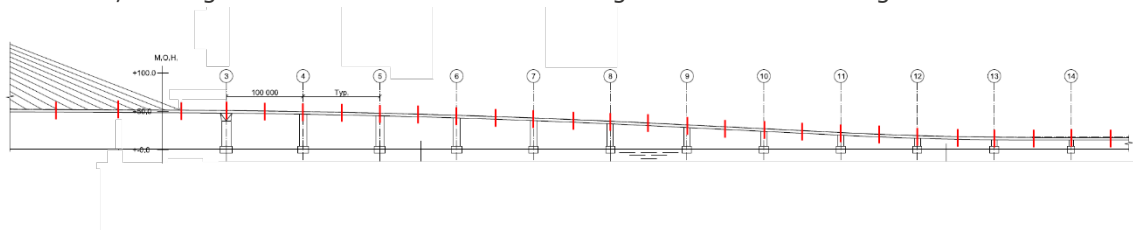


> Figure 4-39: Areas checked for fatigue damage along the entire length of the bridge

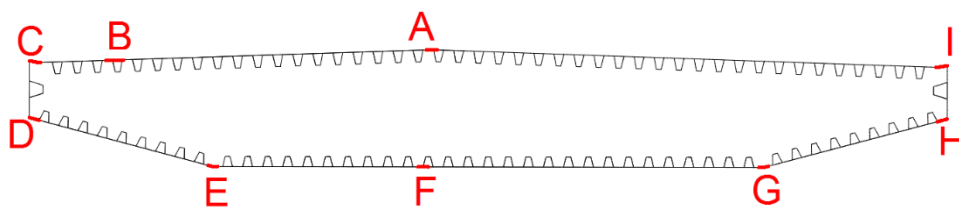


> Figure 4-40: Points that have been checked for fatigue damage at all midspans and axes.

³ Fatigue damage from local wheel pressure has not been included at this stage as this will be similar for all concepts.

4.5.2 Design parameters

Detail categories

Detail categories have been chosen according to DNVGL-RP-C203 [15]. The outer plates are assumed to be welded with two-sided butt and detail category D is used. The stiffeners are assumed to be welded from one side and detail category F is used.

Design fatigue factor

Design fatigue factors (DFF) have been chosen according to the design basis. A DFF of 2,5 has been chosen for all details on the bridge girder at this stage. All details are regarded as low consequence for failure and are open for inspection from the inside of the bridge girder.

Stress concentration factors

Stress concentration factors (SCFs) for the butt welds that have been checked are calculated in accordance with DNVGL-RP-C203, see Table 4-4. A misalignment, δ_m , of 2 mm and δ_0 of $0,1 \cdot t$ is used for all plate thicknesses.

**DNVGL noted that in the new, unreleased, revision of RP-C203, $\delta_0 = 0,05t$ is recommended. It was decided to keep the April 2016 edition in this phase.*

Cross-sections

Different types of cross-sections have been used in the global analysis models and each cross-section have been checked for fatigue. At the north end of the bridge there may be geometric stress concentrations due to differences in the shape of the cross-sections. These have not been calculated but an estimated SCF has been used to account for this – generally thicker plates are assumed in this area. See Figure 4-41 for an overview of the location of all cross-sections.

Outer plates and longitudinal stiffeners have been checked, and it was found that the stiffeners are governing with respect to fatigue life due to having detail category F and higher SCFs. Results for the stiffeners are therefore shown here for concept rating purposes.

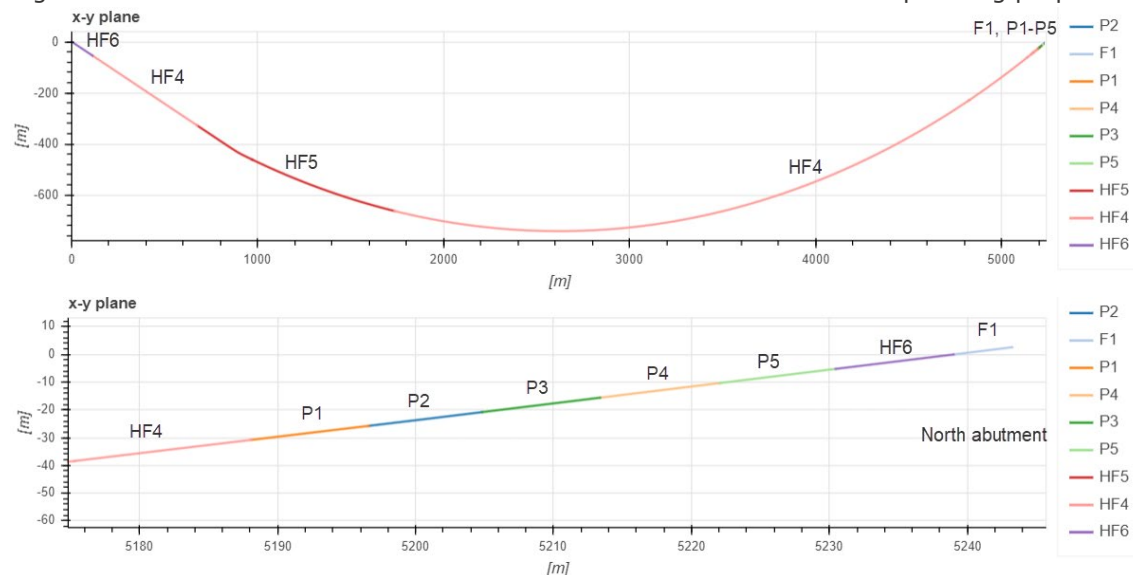


> Figure 4-41: Overview cross-sections

> Table 4-4: Overview of fatigue design parameters K12

Point	Detail type	Detail category	DFF	Girder section	Plate thickness	SCF
-------	-------------	-----------------	-----	----------------	-----------------	-----

A B C I	Stiffener top	F	2,5	HF4	8 mm	1,45
D E F G H	Stiffener bottom	F	2,5	HF4	7 mm	1,56
A B C I	Stiffener top	F	2,5	HF5	12 mm	1,2
D E F G H	Stiffener bottom	F	2,5	HF5	10 mm	1,3
A B C D E F G H I	Stiffener top and bottom	F	2,5	P1-P5, F1 HF6	Varying	1,5
A B C I	Outer plate top	D	2,5	HF4	14 mm	1,13
D E F G H	Outer plate bottom	D	2,5	HF4	12 mm	1,2
A B C I	Outer plate top	D	2,5	HF5	14 mm	1,13
D E F G H	Outer plate bottom	D	2,5	HF5	12 mm	1,2
A B C D E F G H I	Outer plate top and bottom	D	2,5	P1-P5, F1 HF6	Varying	1,5

4.5.3 Calculation of stresses

Nominal stresses have been calculated by creating a local finite element model of the bridge girder in Abaqus to calculate nominal stresses (stress transfer factors) from unit loads at certain points along the bridge girder (see Figure 4-40). These stress transfer factors are used to calculate stresses from section forces from the global analyses.

This procedure has been done for cross section type HF4/5. Stress transfer factors for other cross sections have been calculated by scaling the factors with the second area moment for respective cross sections.

Nominal stresses in combination with the appropriate detail category have been assessed to give satisfactory results due to all loads being “global loads” (local stresses from traffic being omitted as these are not different for the different concepts) for concept rating. Hot spot models have therefore not been included in this report, but hot spots e.g. in details around columns may be significant and will be assessed further.

Shear lag has the same impact on all concepts and a preliminary assessment shows a limited effect, hence it has been excluded in the calculations at this stage. It will be studied further in the final report.

4.5.4 Global analyses

The quasi-static fatigue loads such as traffic and tidal variations are calculated in Sofistik based on the fatigue loads defined in design basis [4].

The dynamic environmental load effects are calculated in the frequency domain with DynNO [3]. The scatter diagrams for the joint probability distributions of the environmental loads

provided in the MetOcean design basis [4] has been discretized to 119 wind sea combinations and 30 swell cases. The swell cases are randomized together with the wind sea combinations to establish the full environmental loads combinations.

To be able to calculate the fatigue damage using the rainflow count procedure, section force time series are generated from the complex response spectral density matrix from the multimodal frequency domain response calculations. In this way the computational efficiency advantage with a frequency domain response calculation can be combined with the best recognized fatigue damage calculation procedure.

4.5.5 Results

Fatigue life is shown for all load types separately for four specific points (B, C F and H) to show the variation in contribution to fatigue damage for separate load types. In addition, the combined fatigue life is shown for all points, A-I. The different cross sections are marked at the bottom of the plot with colours according to the sections given in the legend.

Fatigue life is generally over 150 years for the entirety of the bridge with the chosen design parameters except for the north abutment, where more work needs to be done.

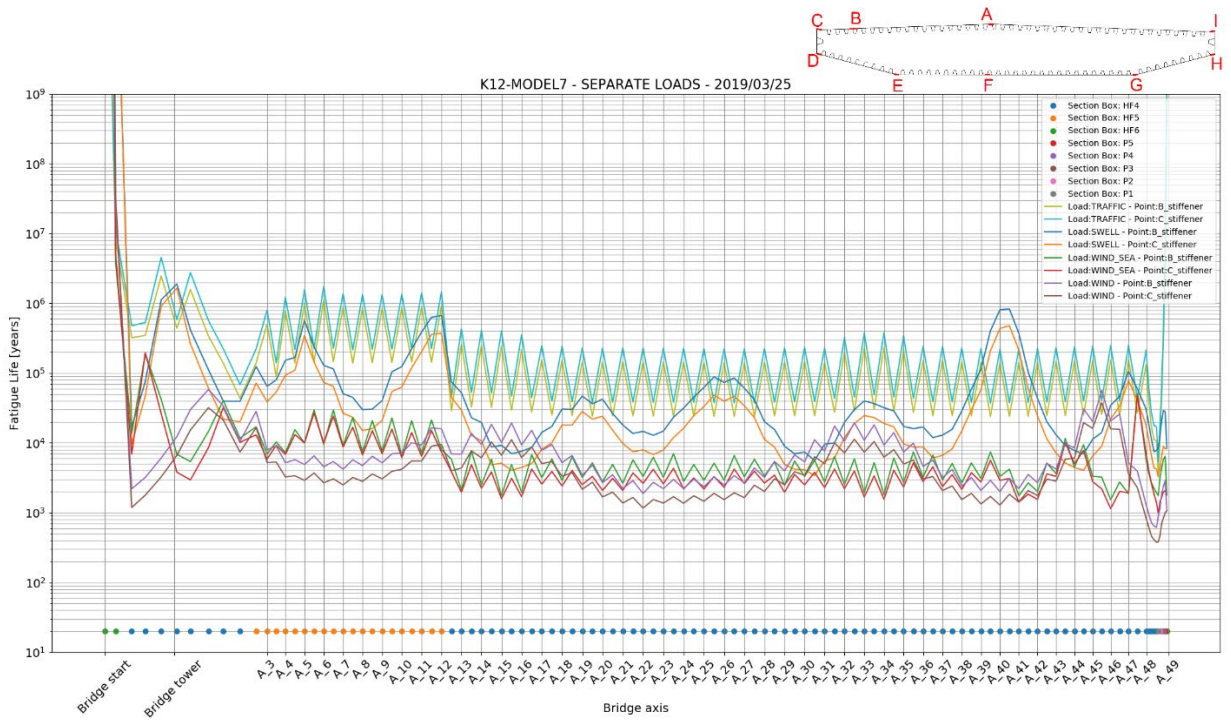


> Figure 4-42: Fatigue life for separate load types, point B and C

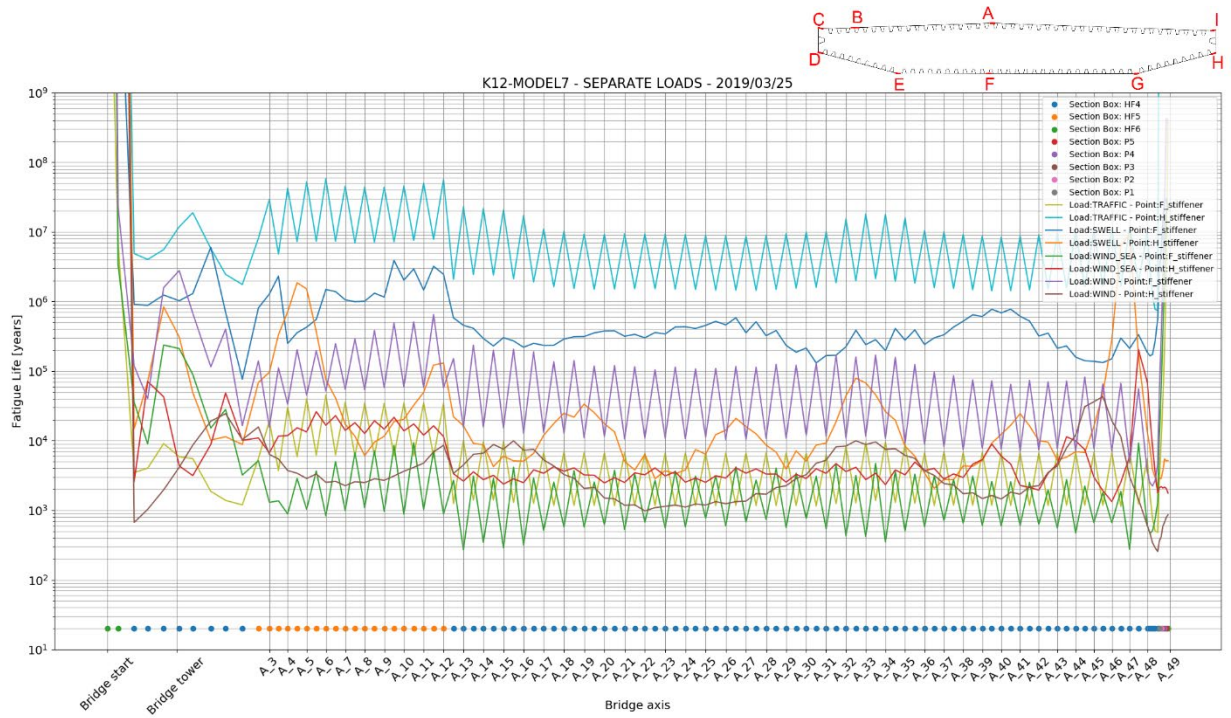


> Figure 4-43: Fatigue life for separate load types, point F and H

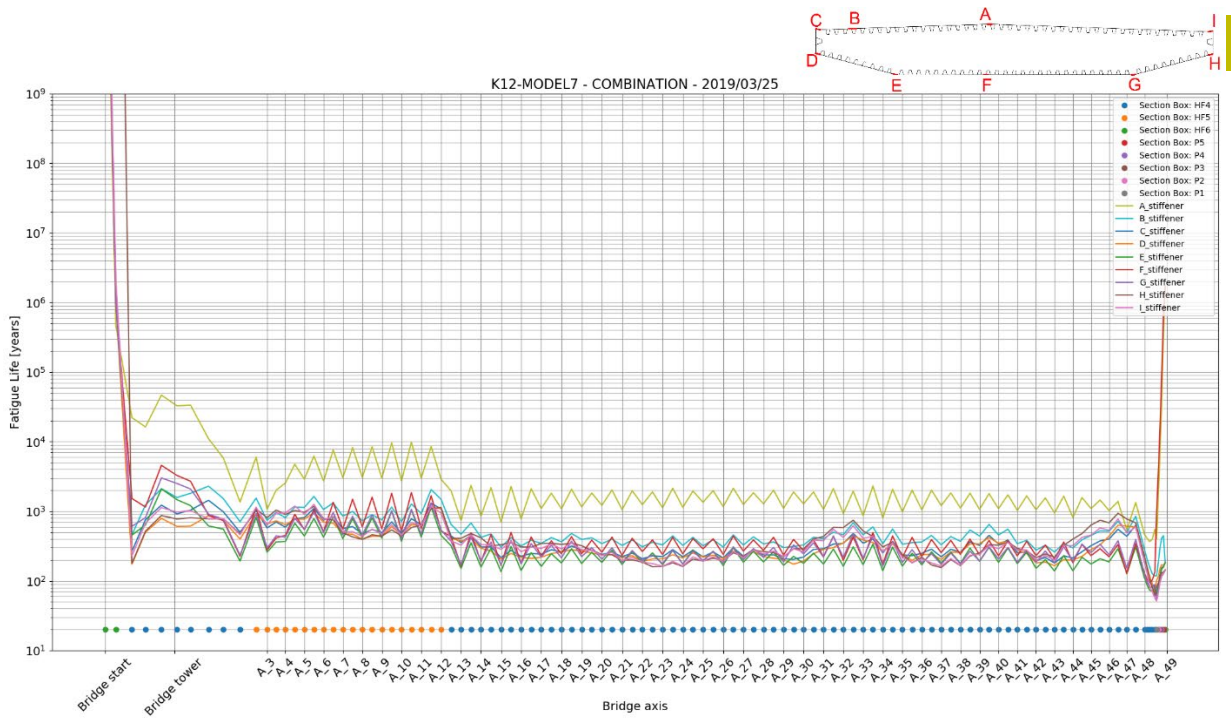


> Figure 4-44: Fatigue life from all load types combined

5 STRUCTURAL DESIGN

5.1 Design of bridge deck girder

5.1.1 General

The bridge girder is briefly described in chapter 2.4. In this chapter some preliminary design checks are presented. The box girder is a plated bridge structure subjected to buckling and should be designed according to . The girder will be subjected to both global and local actions and should be designed in ULS, ALS and FLS. The fatigue life of the girder for global actions is presented in chapter 4.5. Fatigue damage due to local traffic loads are not yet considered. The main accidental load, ship impact, is considered in chapter 4.4.

5.1.2 Global actions

The bridge girder is analyzed for global actions. The results of these analysis are presented in chapter 4.2 for the quasi-static analyses and in chapter 4.3 for the dynamic analysis. Combination of loads is described in chapter 3.5. In this section the results from the ULS load combinations are presented.

From the global analysis the axial stress at several points around the cross section is estimated. The axial stress is calculated according to beam theory by the simple formula:

$$S_x = F_x / A + M_y * z / I_y + M_z * y / I_z$$

where:

- F_x is the axial force in the girder
- M_y and M_z is the weak and strong axis bending moments
- A is the cross-section area
- I_y and I_z is the second moments of area about the weak and strong axis
- y and z is the coordinates of the stress point related to the neutral axis

Due to plate buckling and shear-lag effects these stresses cannot be directly compared with the yield stress of the material to get the correct utilization ratio of the cross-section. At this stage of the project the stress levels are reported directly without the effects of shear lag and plate buckling. The stress levels are used for comparing the four different concepts.

The figure on the next page shows the maximum and minimum axial stress level in the bridge girder from global actions in the worst ULS combination. The stress level plotted is the maximum and minimum of all the stress points around the cross section. It is seen that the stress levels in the different concepts are quite similar. It should be mentioned that K11 has a reinforced cross-section with more cross-section area compared to the other concepts.

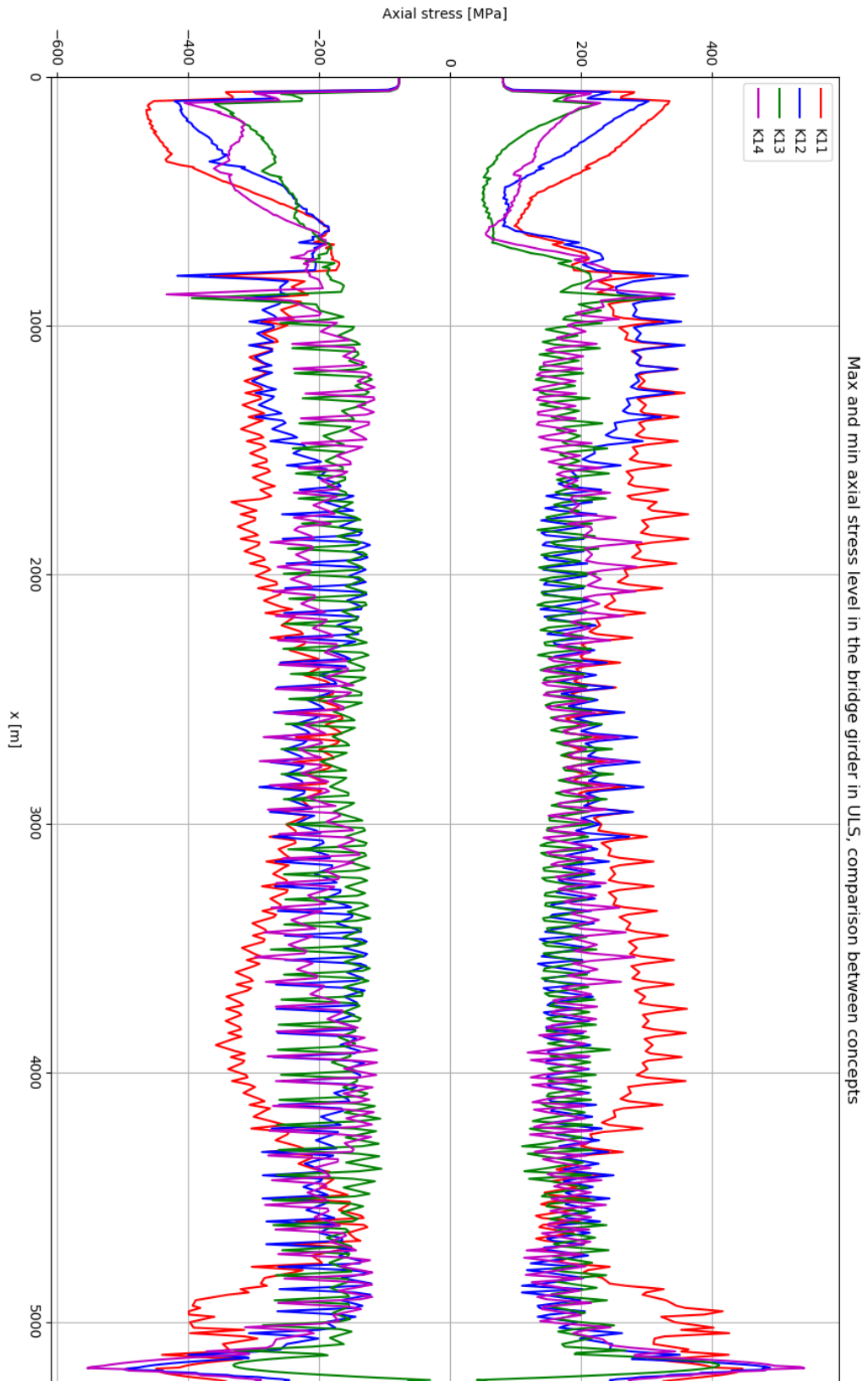


> Figure 5-1 Plot of axial stress levels from global actions

5.1.3 Local actions

Local traffic actions on the top deck plate of the bridge girder is analyzed with a combined shell and beam model in abaqus. The capacity of the deck plate with stiffeners and the transverse girders with bracings are monitored by the model shown in the figure below.

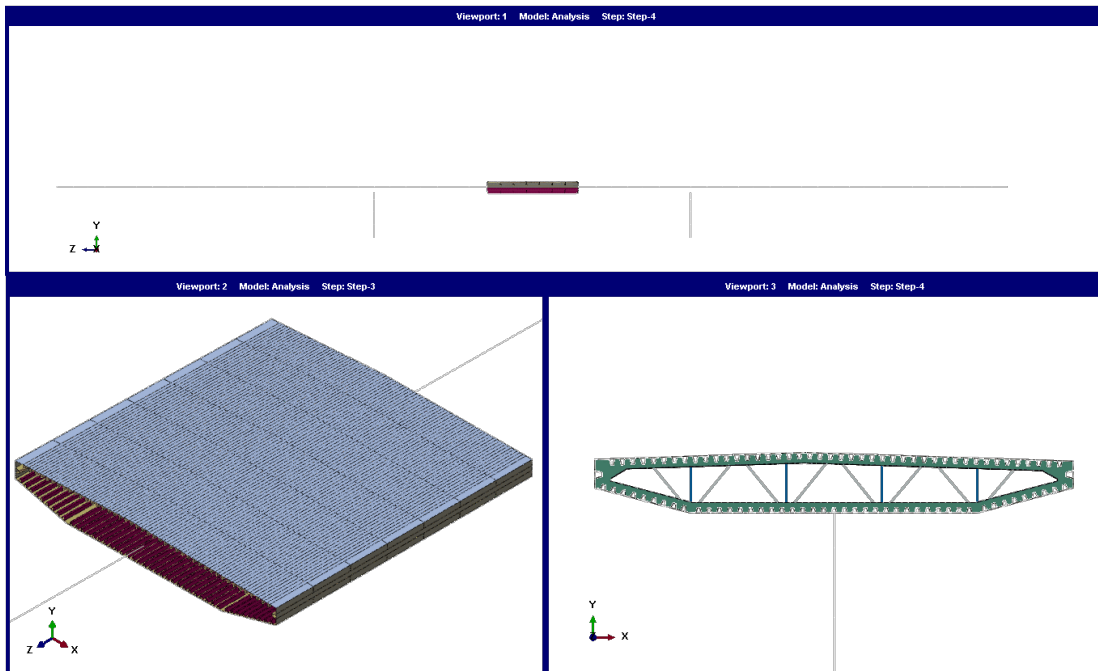


> Figure 5-2 Analysis model for local traffic actions

Load model 1 from [15] is used for the traffic loads. Traffic lanes are placed in the worst sideways position. The rest of the bridge deck, including the pedestrian lane, is loaded with a distributed load equal to $2,5 \text{ kN/m}^2$. Two different locations of the axel loads in the longitudinal direction are considered; axels placed to give maximum force in the transverse girder and axels placed to give maximum bending moments in the stiffeners of the top deck. Structural dead load and weight of asphalt is included. Load factor for traffic loads is 1,35 and load factor for dead load is 1,2.

The figure below shows the von Mises stress level in the top deck plate and stiffener under a local wheel pressure. It is concluded that the bridge deck has sufficient capacity for local traffic actions in ULS.

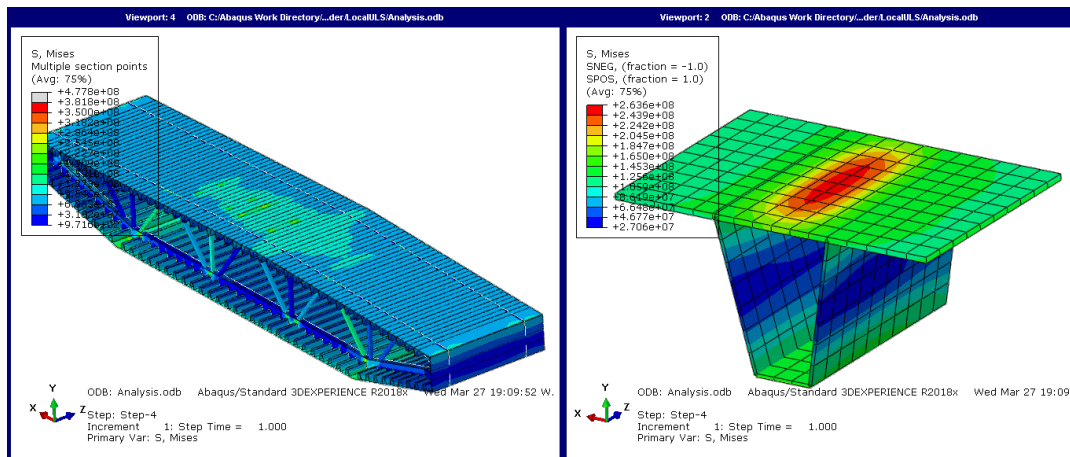


> Figure 5-3 Von Mises stress levels in the top deck plate due to traffic actions, ULS

The figure below shows the von Mises stress levels in the transverse girders and the axial force in the bracings. The overall stress level in the transverse girder is far below the yield strength of the material. Although there are some peak values. This mainly due to modeling simplification where the beam elements of the bracing are connected to the shell elements.

The maximum axial force level in the bracings is $N_{Ed} = 341,6$ kN (compression) for the vertical members, and $N_{Ed} = 709,5$ kN (compression) for the diagonals. Axial capacity of RHS 150x150x5 mm with buckling length of 2,3 m is calculated to $N_{b,Rd} = 993,7$ kN. Axial capacity of RHS 150x150x8 mm with buckling length of 2,9 m is calculated to $N_{b,Rd} = 1427,2$ kN.

It is concluded that the transverse girders have sufficient capacity.

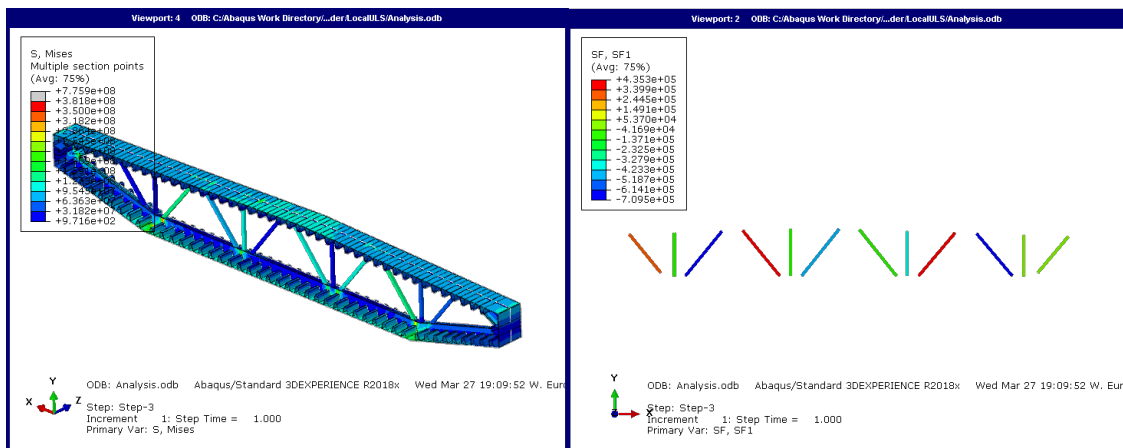


> Figure 5-4 Von Mises stress levels and axial force in the transverse girders, ULS

5.1.4 Connection between bridge girder and columns

The connections between the girder and the columns can be subjected to relatively large accidental loads from ship impact. Detailing of these connections is still on going and the ship impact loads needs to be revised in the next stage of the project. Some analysis has been carried out to investigate the structural behavior of these connections subjected to ship impact at the pontoons parallel to the bridge axis.

A full nonlinear FE-analysis with an elasto-plastic material model according to [9] has been used to simulate the behavior of the connection. The ship impact load is assumed to be a quasi-static force of 31,0 MN. The point of load application is assumed to be 21,0 m eccentric from the column center. The connection is modeled with shell elements. Beam elements are used for the rest of the structure. The model is shown in the figure below.

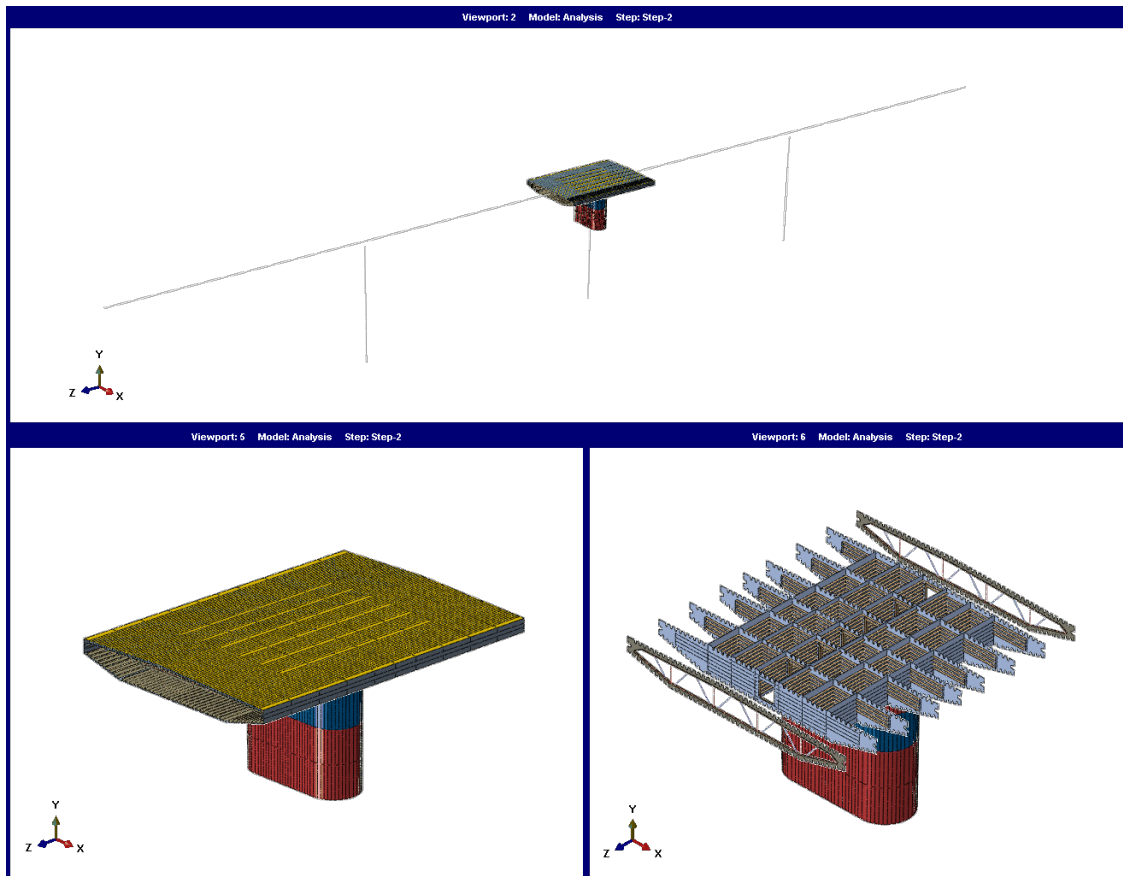


> Figure 5-5 FE-model of connection between girder and column, ALS

The results from the analysis shows that the girder will undergo large plastic deformations while the column is almost completely elastic. The analysis stopped after a load application of $0,8023 \times 31 \text{ MN} = 24,9 \text{ MN}$ due to large non-linearities. At this stage the bottom of the column reached a displacement of 4,7 m. The energy absorbed by the structure was approximately 100 MJ. Further investigation of these connections needs to be done in the next stage of the project. The results from the analysis is shown in the figure below.

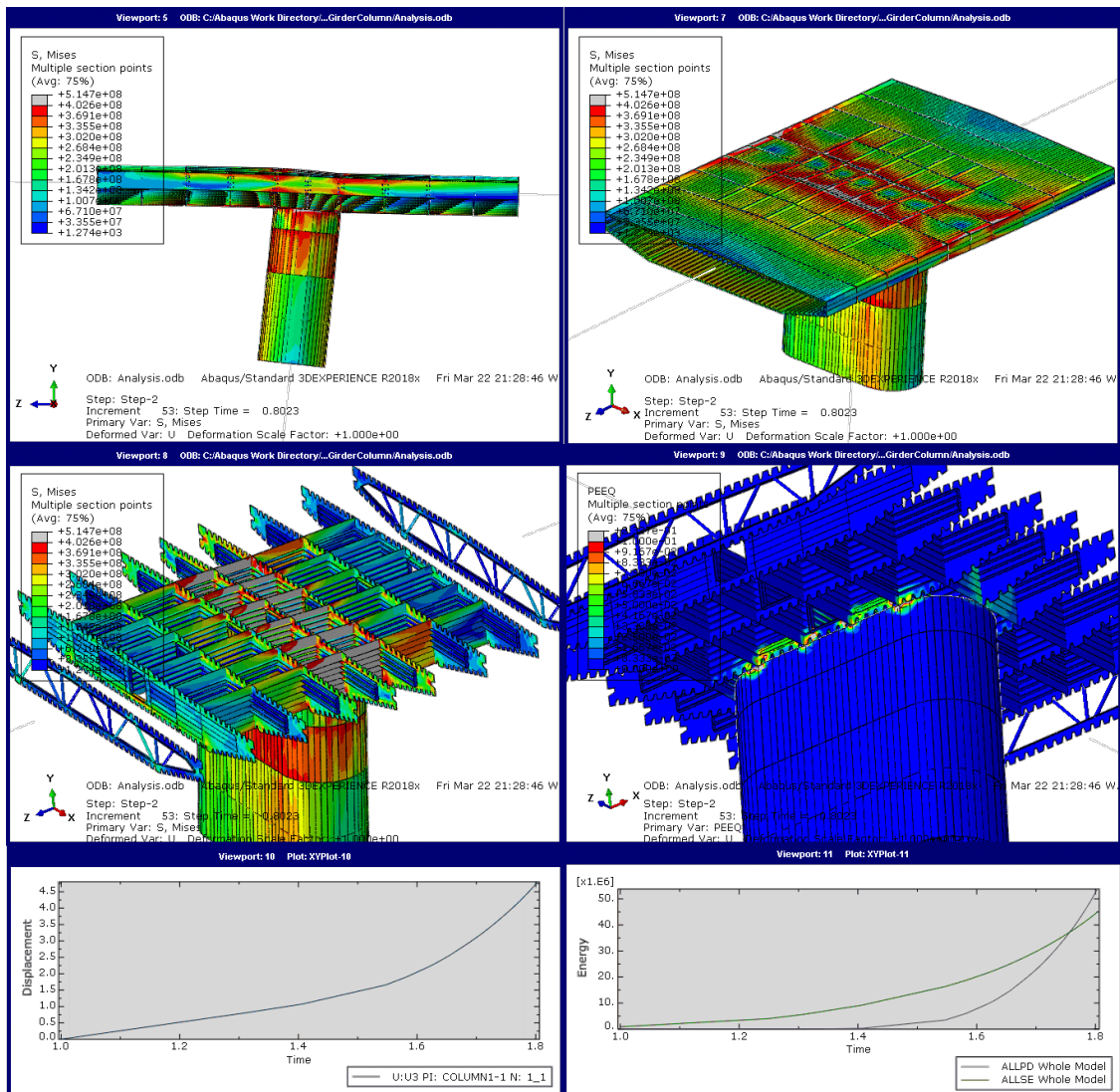


> Figure 5-6 Connection between girder and column, results for ship impact load applied to the pontoons, ALS

5.2 Design of pontoons and columns

5.2.1 Limit States and Assumptions

The pontoon and columns will be designed for both FLS, ULS and ALS. FLS has not been analyzed yet. However, large parts of the column and some parts of the pontoon have ship impact as the governing design load, and dynamic FLS loads are believed to be small in comparison to the ship impact loads. The pontoon skin, bottom- and top plate as well as the bulkheads are reduced 1mm thickness compared with design in previous phase.

5.2.2 ALS Ship Impact

Ship impact is handled by applying a ship impact force equal to 30MN on the pontoon. The ship impact force can have different directions and locations. One of the critical ship impact forces will be ship impact close to the pontoon end perpendicular to the pontoon longitudinal direction. Such a ship impact scenario will induce a large torsional moment in the column, a

large bending moment at the top of the column and a constant transverse shear force in the column.

The ship impact force is applied by giving the outermost pontoon wall with full breadth, located 21 meters in front of pontoon center, a shear stress equal to 0.2083MPa. With an area of 144m² the total transverse ship impact force becomes 30MN.

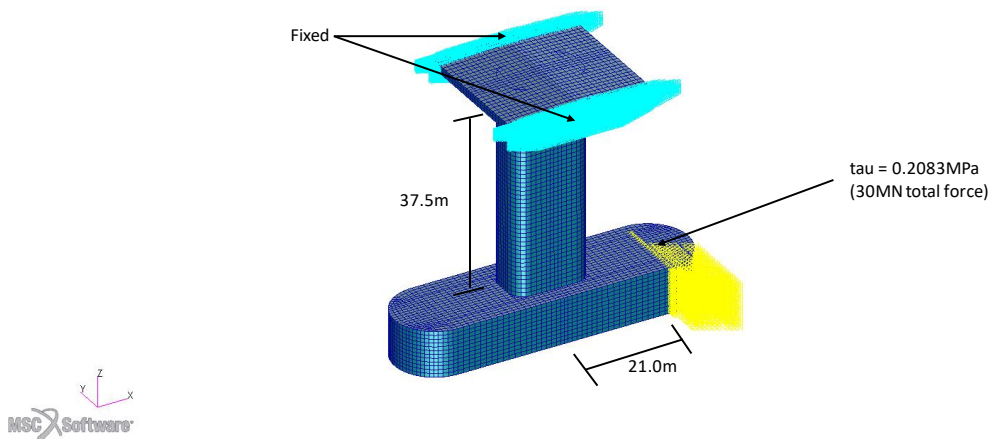


> Figure 5-1 Application of ship impact force

The ship impact force is combined with static water pressure and wave loads. The static water pressure consists of 5.0m normal draught plus 1.0m adjustment draught, giving a total static water pressure of 6 meters.

Wave load is considered with a return period of 100 years. Simplified pressure loads are found by assuming a significant wave height of 2.5m and multiplying the significant wave height with a factor of 2.12*1.2.

$$h_{100} = 2.12 \cdot 1.2 \cdot H_s = 2.12 \cdot 1.2 \cdot 2.5m = 6.36m$$

Summing the static water pressure height with the dynamic water pressure height gives the total water pressure height:

$$h_{water} = h_{static} + h_{100} = 6.0m + 6.36m = 12.36m$$

For ALS the load factor for water pressure is 1.0. Maximum total water pressure at pontoon bottom becomes 0.124MPa.

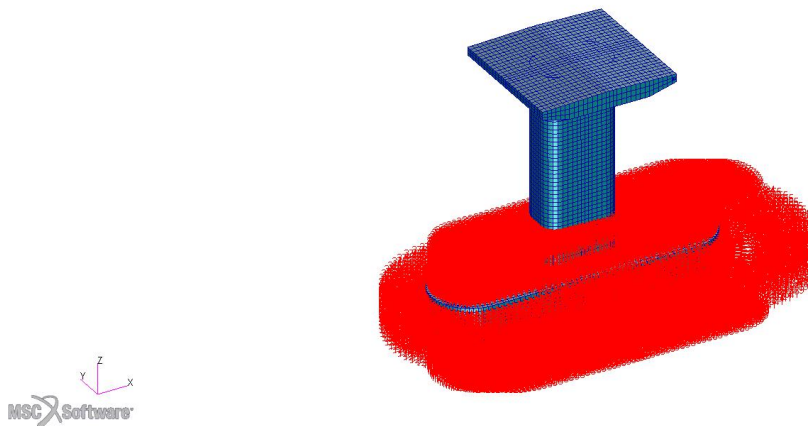


> Figure 5-2 Application of ALS water pressure

A non-linear FE-model is used to calculate structural ALS utilization. Permanent damage and large strains are allowed. However, sufficient post-ALS bridge girder load carrying capacity must be assured.

For the pontoon acceptable ALS structural utilization is found for all parts not directly hit by the ship impact. The column has acceptable ALS structural utilization in lower parts but struggles in the interface area with the bridge girder. The geometry for the column-bridge girder interface area is still under development.

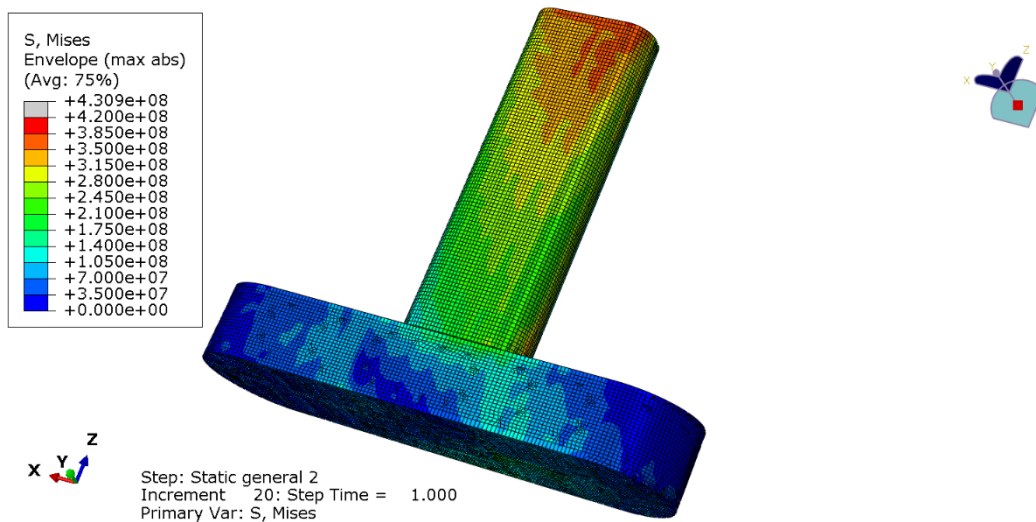


> Figure 5-3 ALS von Mises stresses

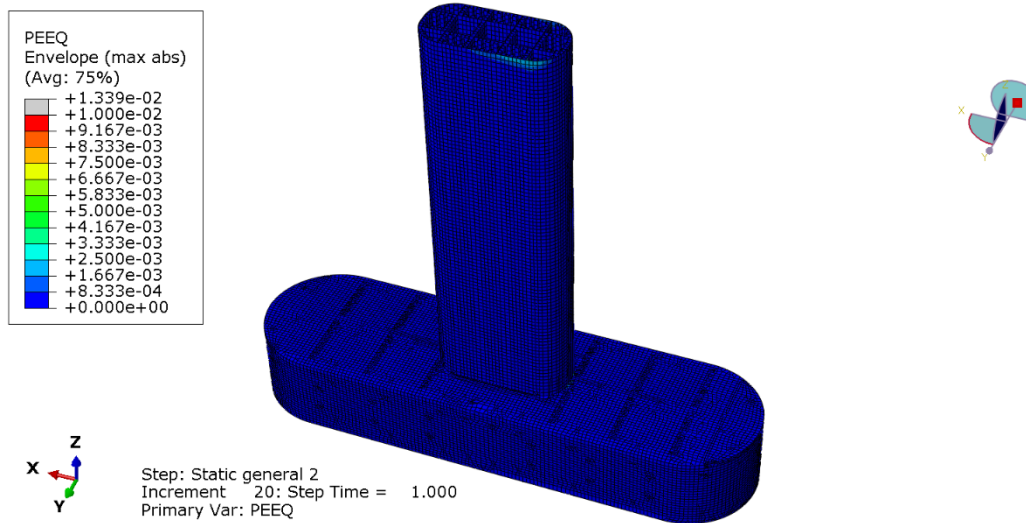


> Figure 5-4 ALS plastic strains

5.2.3 ULS analysis

The ULS analysis carried out is local and quasi-static. The total water pressure height, as calculated in Chapter 5.2.2, is used.

The load factor for ULS-analysis is set to 1.6. This is a conservative approach. The permanent static part of the water pressure could have been given a load factor equal to 1.35. Because not all loads from global behavior are included, the increased load factor for static loads is expected to compensate for some of the missing global loading. The maximum pressure at pontoon bottom becomes 0.199MPa.

For calculating ULS utilization a non-linear analysis is used. Stresses in some bottom plate stiffeners close to the pontoon bow and stern are high, but the stresses are believed to become acceptable if a somewhat stronger stiffener is used. The stresses are also very high for the longitudinal bulkhead in the compartment closest towards the column, where the stresses are believed to become acceptable if a thicker bulkhead is used for this compartment.

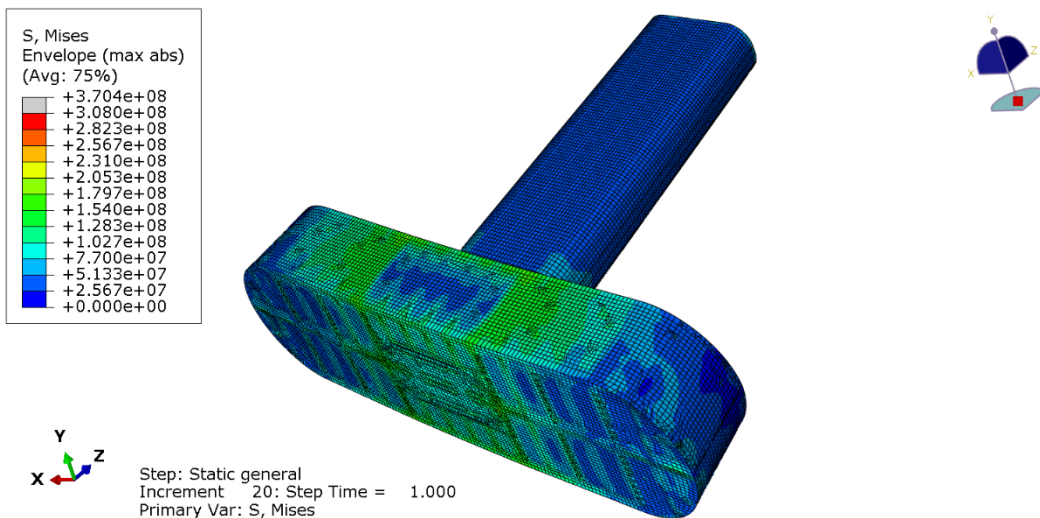


> Figure 5-5 ULS von mises stresses

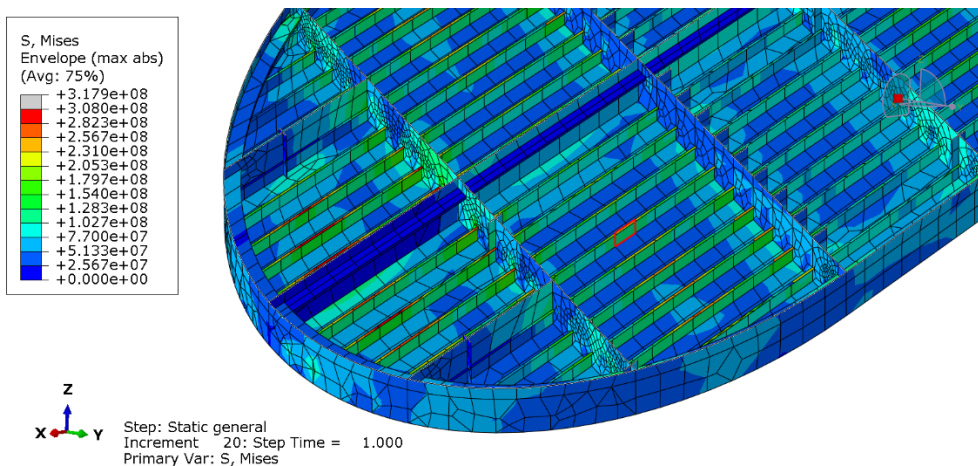


> Figure 5-6 ULS von mises stresses in pontoon bow bottom plate and stiffeners.

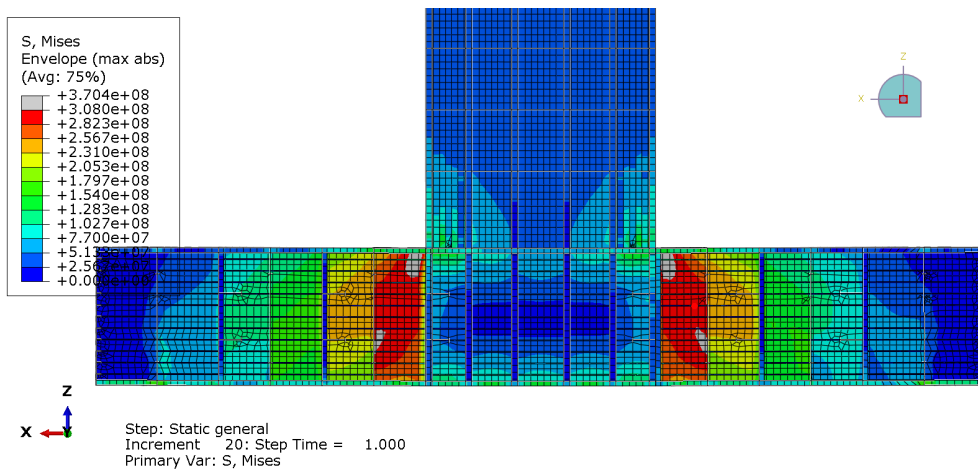


> Figure 5-7 ULS von mises stresses shown for a cut of the pontoon showing the longitudinal bulkhead.

5.3 Design of cable stayed bridge

As mentioned in paragraph 2.5, the cable stayed bridge has been kept approximate unchanged from the previous phase and consequently no detailed analyses have been carried out so far in this phase. The bridge still has one single pylon, a side span of 310 meters and a main span of 510 meters.

However, some changes have been made, especially in connection with the cable configuration and the pylon.

Therefore, several simple and approximate 2-D analyses have been carried out with different cable configurations to compare with the original solution and to establish an optimal geometry. Gathering the stays in groups, see paragraph 2.5, lead to a more flexible structure which was desirable to meet the movements of the floating bridge.

Furthermore, quite a few analyses of the pylon are carried out with different shapes, (diamond-shape, A-shape and H-shape), and with different possibilities for the girder to move sideways. All these shapes are relevant, and the choice is more of an architectural matter.

In the further work, several separate analyses must be done. The updated structure must be integrated in the different global models of the complete bridge for the final control and dimensioning. Secondly, the construction phase has to be investigated thoroughly because it uses to be a critical phase for a cable stayed bridge.

5.4 Design of abutments

5.4.1 General description

An FE-model is developed for the abutment concept for monolithic bridge end connection as well as for the alternative solution with the hinged connection by flexural plates. Both concepts are gravity based boxed structures as described in section 2.8.1, but the cellular configuration and the post-tensioning layout differs. The flexural plate connection is applicable for the north abutment only. Figure 5-8 shows the model for the monolithic connection.

Generally, the north abutment is subjected to the highest end reactions. Consequently, if nothing else is mentioned the subsequent design resumé concerns the north abutment.

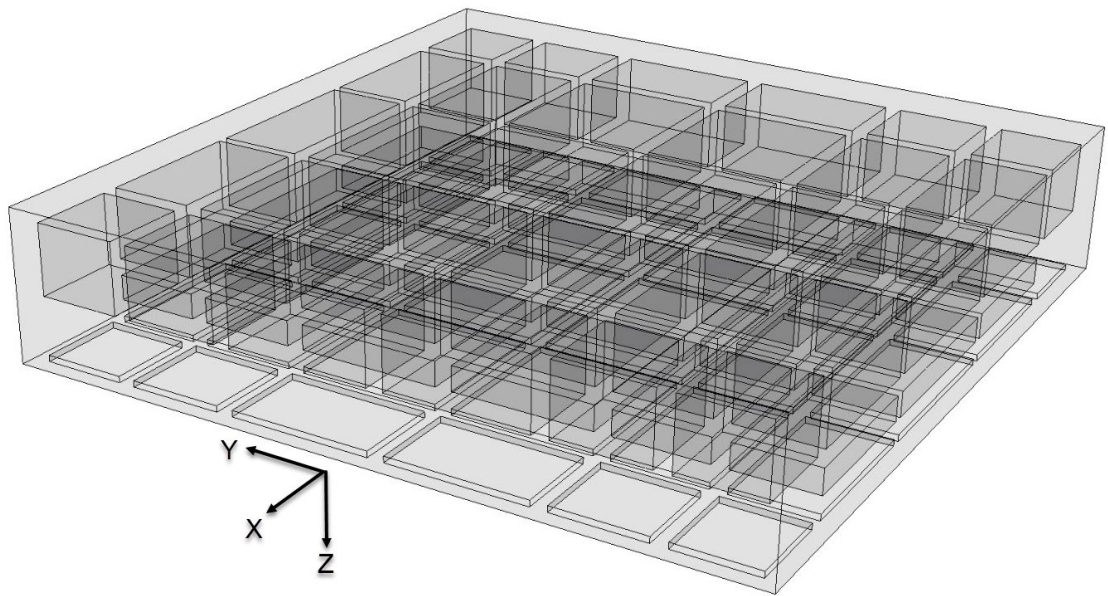


Figure 5-8 FE-model for the configuration for the monolithic connection. North abutment.

5.4.2 Bridge end connection - monolithic

In the girder-to-abutment connection the bridge terminal end is coupled to the abutment front face. The bridge girder is cast integrally with the abutment by the pre-installation of a bridge girder transition segment. A cast-in-place joint is deemed necessary to assure uniform distribution of the contact forces and to allow ample time (> 8 weeks) for placement and stressing of the PT tendons.

Figure 2-12 shows the key concept for the direct, integral connection between the bridge girder and the abutment. The superstructure is monolithically connected to the abutment by means of unbonded post-tensioning cables.

Verification of axial force and bending resistance

The design criteria for the prestressing cables in the intersection between the bridge and the abutment is that tension across the joint interface is not allowed for any ULS load combination. The maximum allowed utilization of the concrete compression capacity is set to approximately 80% to have some reserves for stress concentrations that may occur locally behind the plate stiffeners.

The normal stress distribution in the joint is calculated according to linear-elastic theory. Due to the high compression stress level concrete grade B85 with a design compressive strength of 48.2 MPa is required in the front and rear part of the abutment (areas closest to the PT anchors).

For the north abutment a total of approximately 184 pcs. of 6-37 cables is needed to suppress tensile stresses over the joint, with a total prestressing force equal to 1 424 MN (before losses). With potential for optimization of the PT layout, the tendons are arranged symmetrically about both axes. The anchors will be spread out in the rear end of the abutment, to achieve enough space for the stressing jacks. The center distance can be increased towards the mid axis.

The end frame plate has a general width of 800 mm matching the thickness of the adjoining concrete slabs and walls. The net contact area is 70.5 m² when accounting for the holes for the PT trumpets (net-to-gross ratio ~0.91) at abutment north.

The average concrete compressive stress resulting from prestressing is approximately 17 MPa at abutment north. For both joints the compressive stresses at service load level is well within the limits to avoid longitudinal cracks, micro-cracks and excessive creep.

To provide the necessary moment capacity and to achieve enough space for the post-tensioning arrangement, the bridge box girder cross-section must be extended at the connection. An increase to 36 meters width combined with an increase to 5.0 meters height gives the capacity and PT space needed for abutment north.

The cross-section height increase introduces a weak axis moment, due to the resulting vertical eccentricity (≈ 0.75 m) of the axial force in the bridge girder. However, the magnitude of this moment is small compared to the overall weak axis moment and will not affect the design significantly.

Verification of shear and torsion resistance

The shear forces are transferred from the steel bridge girder to the concrete by means of steel shear keys welded to the back of the end plate. The shear key configuration, complying with intended interface acc. to NS-EN 1992 6.2.5 [16], has ample capacity to resist the design shear stress loads due to biaxial shear and torsion.

5.4.3 Bridge end connection – flexural plates

The alternative solution with the plate hinge (for the north abutment), is releasing the weak axis moment in the connection. The release is provided by an arrangement of four flexural cast steel plates that are connected into the abutment by post-tensioning cables and bolted into the bridge box girder, see Figure 2-13.

The post-tensioning intensity is 24 pcs. of 6-37 cables at each plate, which makes a total number of 96 cables in the connection. Hence the total PT level is 705 MN (before losses), which is significantly lower than for the monolithic connection. Concrete grade B75 ($f_{cd} = 42.5$ MPa) is required in the areas behind the flexural plates, to resist the stresses in the joint in ULS.

The cross-section of the bridge box girder does not have to be increased in height as is the case for the monolithic connection. A slight increase (approximately 2 m) of the width may be necessary.

Each of the four plates are 5.0 m wide and 3.5 m long (flexible length, end flanges comes in addition) and the total width measured between the left and right extreme edge is 28 m. The end flange connected to the abutment is 2 m high and the plate thickness is maximum 150 mm.

The maximum ULS steel stress in the outer plates reaches approximately 370 MPa. Making the plates more flexural (i.e. increasing length and/or reducing thickness) will reduce the stress level but rapidly increase the buckling utilization.

Cast steel G24Mn6 (according to EN 10293:2015) with yield stress $f_{p0.2k} = 400$ MPa (for thickness ≤ 150 mm) is assumed suitable for the purpose.

5.4.4 Ultimate joint resistance

Using unbonded post-tensioning cables anchored at the rear end of the abutment, the bridge end joint can undergo large nonlinear deformations without yielding the post-tensioning steel and without a significant loss in self-centering capability. The predicted moment – curvature relationships investigated for the monolithic connection in the previous project phase indicates that the joint has a significant ULS loading capacity reserve to compensate for potential uncertainties in dynamic response, material strength, geometric deviations, inaccuracies in the design model or quality of workmanship. The ultimate resistance is governed by concrete compression failure for both axes.

5.4.5 Abutment design – monolithic connection

General

The abutment structures and the distribution of the base reactions used in the global stability control is predicted by means of the 3-dimensional solid FE-model and the results are extracted by using ShellDesign.

Ballast with density 20 kN/m³ is used. Heavier ballast is possible to use if needed (up to 30 kN/m³).

The connection with flexural plates represents an alternative solution. The cellular configuration will differ and there will be less post-tensioning, but the overall size will be comparable. In the subsequent sections, design results will not be provided for this alternative.

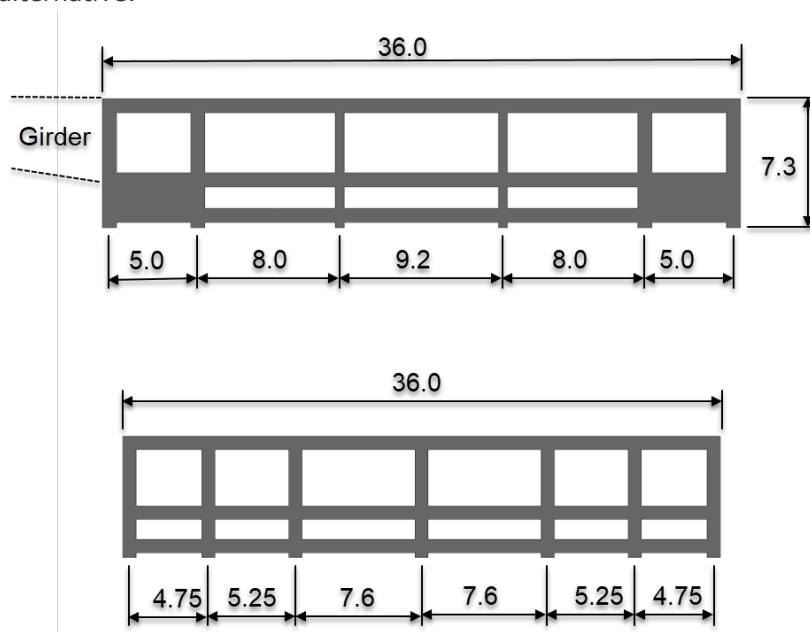


> Figure 5-9 Longitudinal (upper plot) and transversal (lower plot) cross section of north abutment FE-model. All walls and slabs have 800 mm thickness. The front and rear lower cells are filled with concrete (upper plot).

Sliding resistance

Vertical forces (N) and horizontal shear in both directions (T , V_2 and V_3) are integrated for each load case over the ground contact area, and the relation $N / V_{res} \geq 1$ means that the sliding resistance is fulfilled (friction coefficient $\mu = 1.0$). See Figure 5-10 for definition of beam section forces.

The lowest ratio found is 1.03 for abutment north (1.01 for south). The general check against sliding based on the beam section forces at the bottom of the abutment is conservative compared to a more detailed approach investigating the difference between axial and shear force in each result point in the FEM model towards the bottom. In this stage the overall check is used to predict sliding, whereas the point for point approach are used randomly as control. The contribution from rock anchors is not included.

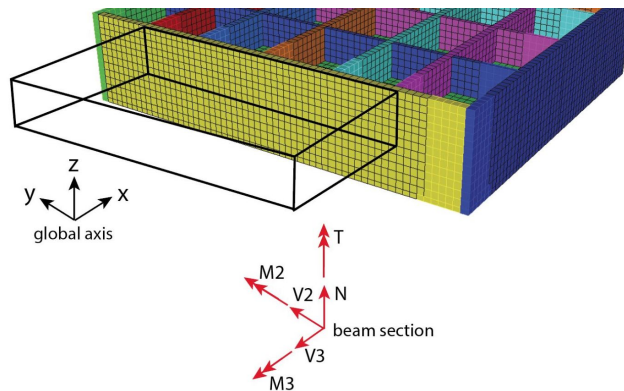


> Figure 5-10 Definition of beam section forces.

Overturning resistance

Normal compression stress from vertical forces (σ_N) and tension stress from overturning moment in both directions (σ_{M2} and σ_{M3}) are checked in the worst points, and the relation $\sigma_N / (\sigma_{M2} + \sigma_{M3})$ is checked. $\sigma_N / (\sigma_{M2} + \sigma_{M3}) \geq 1$ means that the overturning resistance is fulfilled.

The lowest ratio found is 1.22 for north abutment (1.35 for south). The contribution from rock anchors is not included, hence the result is conservative.

Abutment south

The south abutment will be larger than the north, because of smaller vertical loads in combination with the strong axis moment. Hence the sliding and overturning moment resistance will govern the overall dimensions.

Caisson concrete design

Overall measurements of the FE-model for the north abutment is shown in the plots in Figure 5-9.

Some utilization plots are provided in Figure 5-11. Concrete compression utilization is low/moderate in the central parts of the abutments with some local areas of overutilization that can be seen in the outer parts (upper plot). The same applies for horizontal reinforcement (lower plot). This can be handled by locally increasing reinforcement intensities and wall- and slab thicknesses.

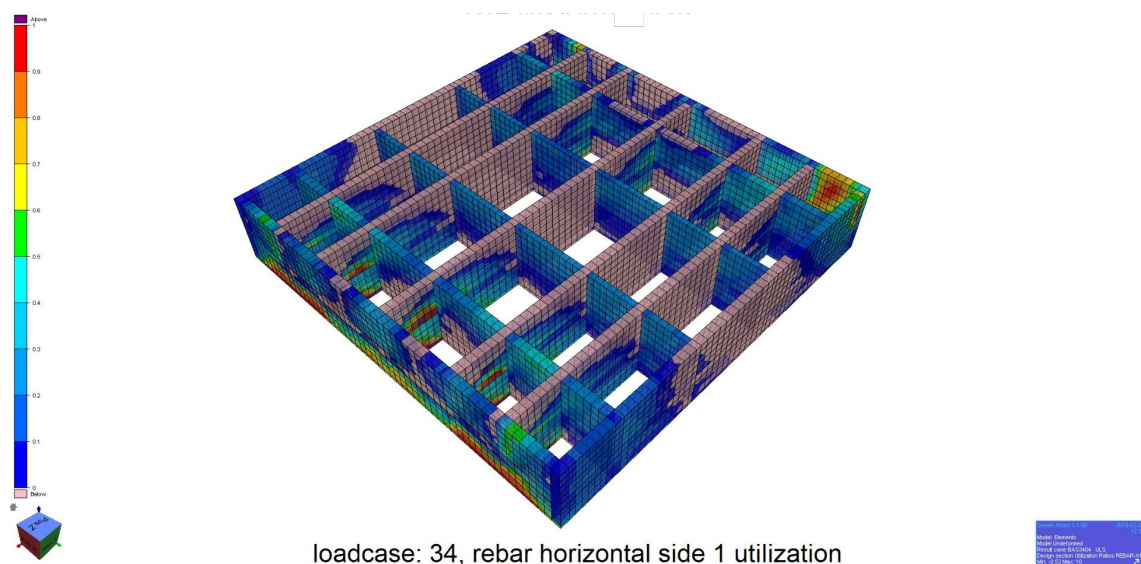
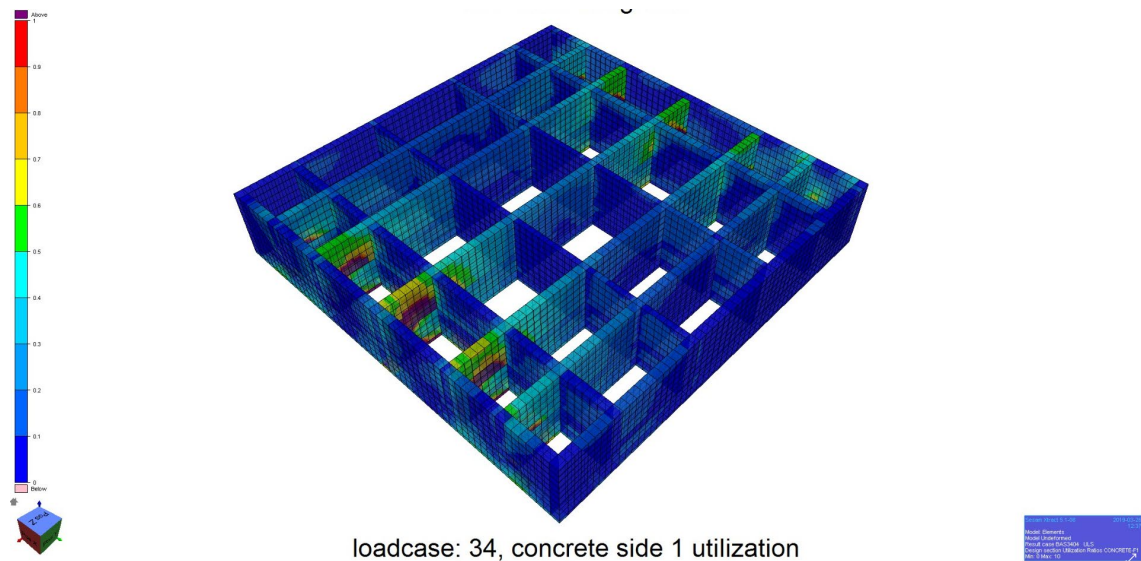
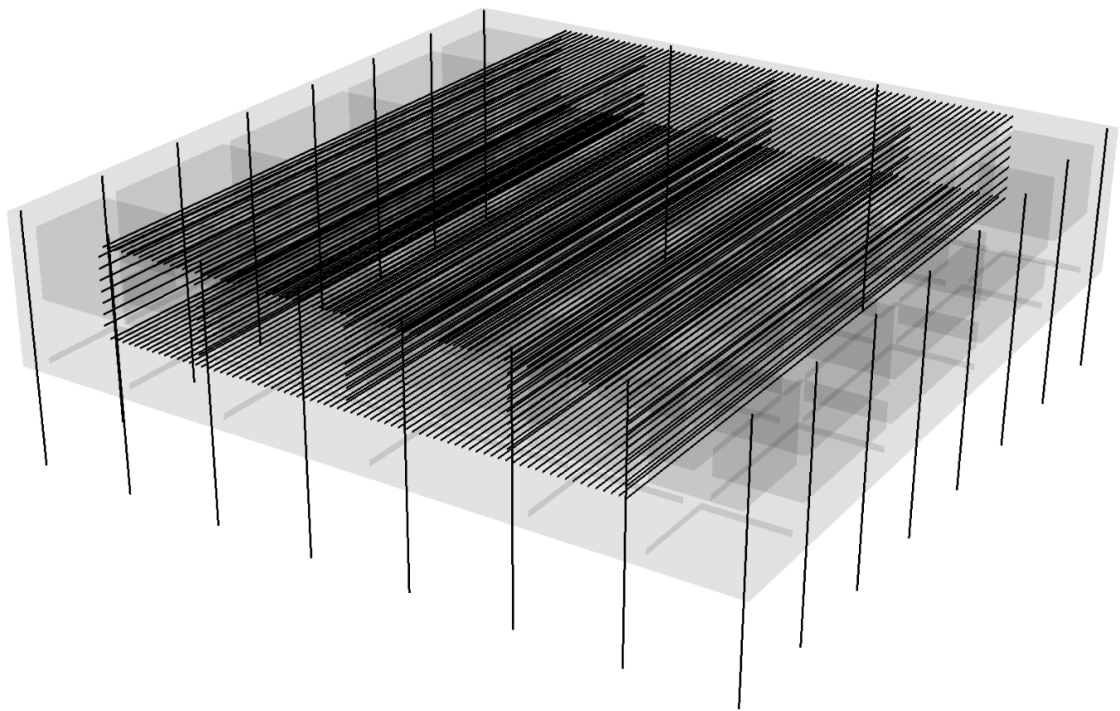


> Figure 5-11 Utilization plot showing concrete compression utilization (upper plot) and utilization of horizontal reinforcement (lower plot). Abutment north.

The post-tensioning and rock anchor design is shown in Figure 5-12. There is a total of 24 rock anchors with an assumed length of 20 m each. Horizontal post-tensioning is 6-37 tendons while the rock anchors are 6-19 tendons.



- > Figure 5-12 Horizontal post-tensioning (6-37 tendons) and rock anchors (6-19 tendons). Abutment north.

5.4.6 Bill of quantities – abutment for monolithic connection

- > Table 5-1: Material quantities for abutment North

BoQ	Concrete	Reinforcement	Post-tensioning	Rock anchors
	m ³	t	MNm	MNm
Total	4 940	1 482	51 250	1 907

- > Table 5-2: Material quantities for abutment South

BoQ	Concrete	Reinforcement	Post-tensioning	Rock anchors
	m ³	t	MNm	MNm
Total	7 294	2 188	39 258	1 907

5.5 Design of mooring

5.5.1 Design philosophy

A brief description of the mooring system is given in Sec. 2.6 of this document. The philosophy for design of the main components follows DNV-OS-E301 for determining ultimate capacity of the main components. Consequence class 2 is chosen. For intact ULS condition it is the target to avoid utilizations above 70% in the fibre rope in order to limit fatigue issues with polyester ropes.

The ULS loads for the mooring lines are obtained from the global analyses model. An additional increase in ULS loads of 25% is expected to account for planned maintenance and replacement of anchors/lines, where two lines is out of service for two years. This increase is not governing for design of the system as we allow for utilizations above 70% for this particular event. The factor of 25% is based on preliminary evaluations of the system and will be further evaluated in the next phase.

For determining minimum pretension to avoid slack, the philosophy of NS-EN 1990 is adapted, where a factor of 0.9 is used for favorable loads (EQU). To account for further uncertainties (i.e measurement of prestressing during installation, long time performance), the factor is set to 0.85. Avoiding slack is important to maintain the desired stiffness of the anchor groups during the operational phases.

The capacity of the main components (fibre rope and chain) is given by DNV-OS-E301 as $S_c = 0.95 * S_{mbs}$, where S_{mbs} is the minimum breaking strength of the component. Corrosion allowance of chain and steel components is included in the design.

Other components in the system such as connecting links, terminations, fairlead, chain stoppers will be designed to have strength exceeding the characteristic strength of the main body in the mooring line.

The principles used for selecting dimensions are illustrate with an example of load and load combinations for one line in Figure 5-13.

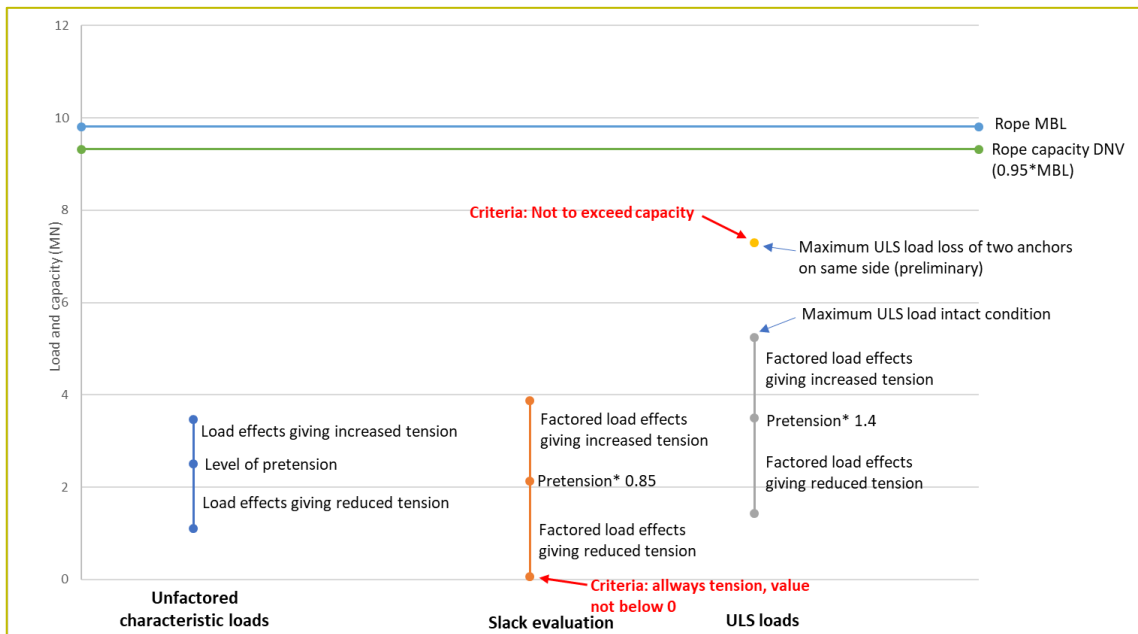


> Figure 5-13 Load contribution and combination

The resulting line geometry, components, prestressing and loads, and utilizations are further summarized for all lines.

5.5.2 Overall line geometry and preliminary main component dimensions

> Table 5-3: Mooring line geometry and components

Line No.	Hor. angle (local)*	Hor. length (m)	Anchor depth (m)	Vertical angle (deg)	Dimension Anchor chain		Fibre rope		Top chain	
	(deg)				Dim. (mm)	Length (m)	Dim. (mm)	Length (m)	Dim. (mm)	Length (m)
1	4.8	956	-561	30.2	111	50	177	1006	111	50
2	5.1	898	-560	31.7	111	50	177	956	111	50
3	5.7	886	-560	32.1	111	50	177	946	111	50
4	4.6	946	-561	30.5	111	50	177	998	111	50
5	199.3	628	-457	35.7	111	50	177	673	111	50
6	192.3	593	-461	37.6	97	50	155	648	97	50
7	211.2	500	-508	45.1	102	50	168	609	102	50
8	202.6	460	-511	47.8	102	50	168	584	102	50
9	347.9	1137	-123	5.9	111	50	177	1043	111	50
10	351.0	1157	-123	5.8	111	50	177	1063	111	50
11	350.2	818	-166	11.2	97	50	155	734	97	50

12	356.0	757	-167	12.1	97	50	155	674	97	50
13	178.0	435	-365	39.7	102	50	168	465	102	50
14	166.2	418	-353	39.8	102	50	168	444	102	50
15	179.2	494	-367	36.3	97	50	155	512	97	50
16	168.9	486	-366	36.6	97	50	155	505	97	50

*Horizontal angle is given in local pontoon coordinates, where 0 deg is defined normal to the bridge at the considered pontoon.

5.5.3 Loads and utilizations

> Table 5-4: Loads and utilizations

Line No.	Installed pretension	Max/min factored loads (without pretension)	ULS Intact (incl. load factors)		ULS maintenance (incl. load factors)	Utilization ratio ULS Intact / ULS maintenance	
			Min (MN)	Max (MN)		Fibre rope*	Chain**
	(MN)	From global analyses (MN)			Max (MN)		
1	2.5	1.7 / -2.1	0.0	5.2	6.6	0.56 / 0.70	0.55 / 0.69
2	2.0	1.5 / -1.7	0.0	4.3	5.4	0.46 / 0.58	0.45 / 0.56
3	1.6	1.3 / -1.3	0.0	3.5	5.3	0.38 / 0.48	0.37 / 0.46
4	1.5	1.4 / -1.3	0.0	3.5	5.2	0.37 / 0.46	0.36 / 0.45
5	2.8	2.1 / -1.6	0.8	6.0	7.0	0.65 / 0.81	0.63 / 0.79
6	2.2	1.7 / -1.4	0.5	4.8	6.5	0.64 / 0.80	0.66 / 0.83
7	2.2	1.4 / -1.2	0.7	4.6	5.8	0.54 / 0.68	0.57 / 0.71
8	2.1	1.6 / -1.3	0.4	4.5	5.9	0.53 / 0.66	0.56 / 0.70
9	2.1	1.9 / -1.7	0.0	4.8	4.4	0.52 / 0.65	0.50 / 0.63
10	1.9	1.8 / -1.6	0.0	4.4	4.3	0.47 / 0.59	0.46 / 0.58
11	1.8	1.7 / -1.5	0.0	4.2	7.6	0.56 / 0.70	0.58 / 0.73
12	1.8	1.6 / -1.5	0.0	4.2	6.0	0.56 / 0.70	0.57 / 0.71
13	2.7	1.9 / -1.9	0.3	5.6	5.7	0.67 / 0.84	0.70 / 0.88
14	2.5	1.7 / -1.7	0.4	5.2	5.6	0.62 / 0.78	0.64 / 0.80
15	2.2	1.6 / -1.7	0.1	4.6	6.0	0.62 / 0.78	0.64 / 0.80
16	2.2	1.6 / -1.6	0.3	4.7	5.5	0.63 / 0.79	0.65 / 0.81

* Fibre rope capacities used in evaluation from Lankhorst ropes. Some deviations in capacities is seen when comparing different suppliers.

**Assuming R4 studless chain, including corrosion allowance of 0.2mm/year, 50 years life time. Capacities in utilizations from Vicinay. Splash zone corrosion to be evaluated in the next phase.

The increase in mooring line loads due to loss of anchors in ULS/ALS condition will be further evaluated in the next phase. Preliminary calculations show that the increase in mooring line loads is approximately 25% in ULS for replacement and 55% in ALS for loss of two random anchors. In general, the lines have sufficient capacity for this extra load due to low utilization in the intact ULS condition and reduced load factors for ALS. If loads turn out to be are higher than expected this may result in adjustment of the line dimension for some of the lines with the highest utilization, but major changes to the configuration is not expected.

5.5.4 Fatigue

Preliminary analyses for evaluation of fatigue damage shows low utilizations, even when considering 50-100 years of life time. This indicates that corrosion is the governing limiting factor for life time evaluation, especially in the splash zone. Evaluation of the corrosion rates with respect to entrapped water in the chain fairleads and sheltered splash zone underneath the pontoon is ongoing and might need to an increase in corrosion allowance for the top chain. An increase in corrosion allowance might also imply a reduced design life for the top chain.

6.1 Background

Four different concepts for a floating bridge are currently being studied (*K11, K12, K13 & K14*). The differences in the concepts relate to the shape of the bridge and anchorage. Three different shapes of the bridge alignments result in three different landfalls on Svarvehella (in the south) and Røtinga in the north. However, the pivot-points at the southern bridge tower on Svarvhelleholmen and the northern landing on Gulholmane are the same for all four concepts, only with different rotation of the foundation.

Studies of the geological conditions for similar concepts in the near vicinity have been conducted by Norconsult and by geologists from the Norwegian Road Authority:

- *12149-00-R-011 Engineering geology evaluations – Reinertsen/Olav Olsen/Norconsult 2015-06-16*
- *Befaringsrapport Bjørnafjorden, Berggrunnsundersøkelser – Statens Vegvesen 2016-04-14*
- *Befaringsrapport Tunnelinnslag, Frøyne, Bjørnafjorden – Statens Vegvesen 2017-01-27*
- *E39 Bjørnafjorden, Engineering geological evaluations for foundations on Svarvhella, Svarvhelleholmen and Gulholmane – Norconsult 2017-05-30*

Although previous studies have not focused on the ground conditions at the exact locations relating to the current concepts, some of the data and evaluations are still considered relevant for evaluations of the new concepts. For further detailed studies for the relevant concept it is recommended to perform updated engineering geological mapping and relevant ground investigations.

In the following, a short presentation of the available information on ground conditions and engineering geological evaluations for foundation and anchoring at the pivot-points and for anchoring at the landfalls is summed up. Each concept is commented and presented in four separate reports, one for each concept.

6.2 Southern landfall/anchoring and bridge tower foundation

6.2.1 Geology of the project area

A geological map of the Svarvhelle area, issued by the Norwegian Geological Survey (NGU), is shown in Figure 6-1.

The southern landfall of bridge *K12* is located at Svarvhella, at the northern tip of the island Reksteren (Figure 6-1 and Figure 6-3). The bedrock in this area consists mainly of a greyish, coarse grained monzogranite with local occurrence of amphibole and some areas with red, biotite-rich granite (Håkre monzogranite).

Along the northern shore, a narrow dike intrusion of greenstone and basaltic lava with pillow structure is present.

The small island Svarvhelleholmen consists of green polymictic conglomerates, with lumps of gabbro greenstone, granitoids, diorites, and partly also marble and phyllitic or greenish greywacke. The rock types on this island are distinctly different from the ones found on Svarvehella, some 70 m to the south, thus, the shallow channel between the islands represent a clear geological boundary, possibly also a weakness structure.

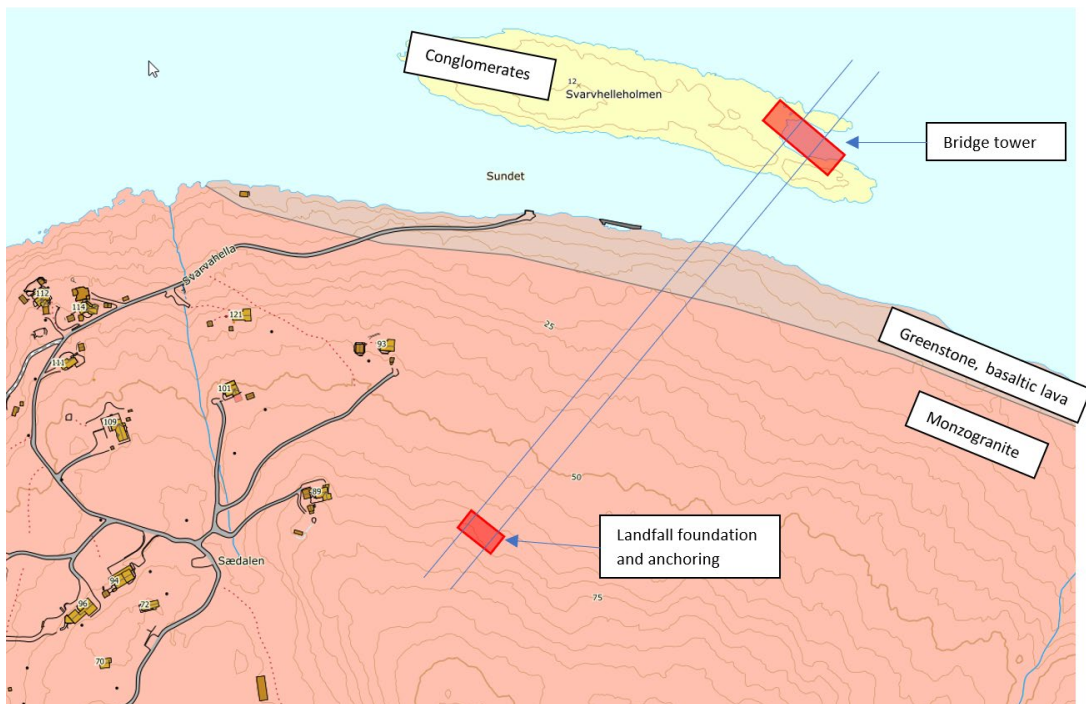


> Figure 6-1 Geological map of the southern landfall area – bridge elements for concept K12.

6.2.2 Engineering geological mapping (Norconsult, 2015)

In 2015 Norconsult carried out engineering geological mapping in this area, for the purpose of feasibility design of the landfall for a previous alternative alignment of the bridge. This alternative had a landfall to the west of Svarvhelleholmen. The current bridge concept K12 has an alignment crossing over the eastern part of Svarvhelleholmen, with a bridge tower on the eastern tip of the island and partly in the shallow waters in a bay of the island. The landfall for K12 is located some 100-200 m east of the previous bridge alternative, within the same geological formations according to the geological map. Observations from the detailed engineering geological mapping (at locations 1 – 4, ref. Figure 6-2) are presented in sections 6.2.3 - 6.2.6.

The geological conditions for the K12 landfall are expected to be fairly similar to that observed during field survey in 2015. However, it is recommended that the geological conditions at the final locations for foundations are investigated further.

According to Norconsult's observations in the field the boundary between the monzogranite and the greenstone and basaltic lava intrusion seems to be closer to the shore than that indicated on the geological map (Figure 6-1).

Engineering geological mapping of the Svarvhelleholmen includes observations from the western tip of the island, while the project area for the foundation is on the eastern tip. However, from pictures at the actual location for the foundation, the geology seems to be similar to that observed by Norconsult in 2015.

Figure 6-2 shows structures mapped at the previous location of the landfall. There is a distinct set of weakness zones with a strike in NNW direction and steeply dipping. It is reasonable to assume that similar structures may be repeated towards east, and thereby also at the new landfall location.

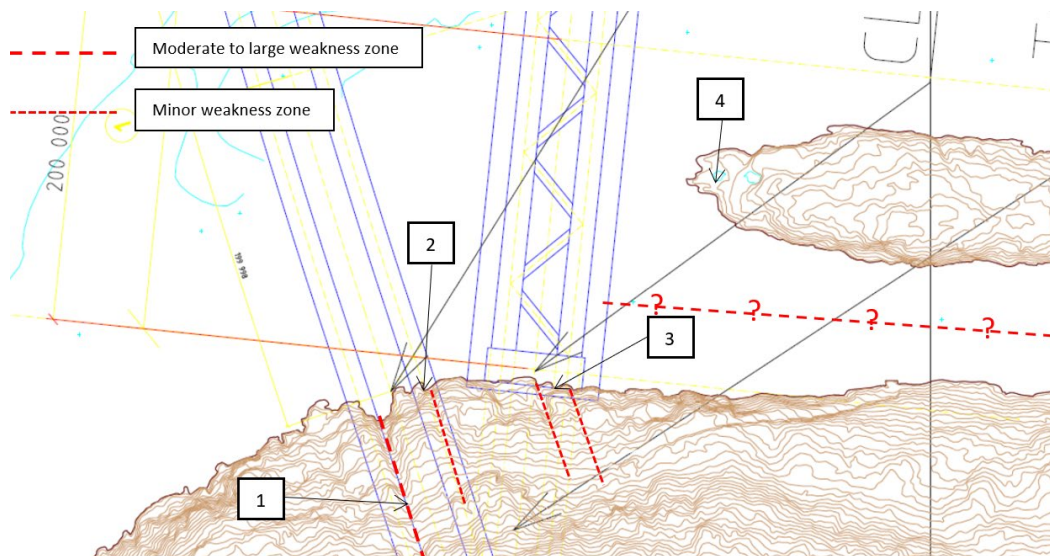


> Figure 6-2 The 4 locations for detailed geological mapping in the southern landfall area.

6.2.3 Location 1

The dominating rock type is monzogranite of fairly good overall quality. The rock mass in general appears as blocky, with an average block size of about 0.25 m³. Higher degrees of jointing and surface weathering were observed in the first 1-2 m in the exposed rock mass. Below this depth, the rock mass appears as relatively fresh and un-weathered. The most pronounced joint sets can be described as follows:

Joint set nr.	Avg. dip/dip direction	Joint surface	Spacing	Trace length
1	70-80°/70°	Planar, rather smooth	0.5 m	> 10 m
2	10°/80-90°	Planar to slightly undulating, rather smooth	0.5 - 1 m	1 - 10 m
3	75-80°/150-160°	Planar, slightly rough and irregular	0.5 - 1 m	1 - 10 m
Random joints	90°/0°	Planar, rough	2 m	1 - 10 m

6.2.4 Location 2

The dominating rock type is monzogranite. The greenstone/basalt intrusion emerges from the sea approximately about at this location. The most pronounced joint sets can be described as follows:

Joint set nr.	Avg. dip/dip direction	Joint surface	Spacing	Trace length
1	80°/345°	Planar, slightly rough	2 m	> 10 m
2	80°/80°	Planar, rough	1 - 1.5 m	1 - 10 m
3	0-5°/330°	Planar, slightly rough	1.5 m	1 - 10 m

6.2.5 Location 3

The dominating rock type is monzogranite, permeated by numerous syenitic dykes, up to 1 m wide. Joint frequency increases towards the sea. Greenstone/basalt is present on the first few meters of the shoreline. The most pronounced joint sets can be described as follows:

Joint set nr.	Avg. dip/dip direction	Joint surface	Spacing	Trace length
1	75-80°/100°	Planar, slightly rough and irregular	1.5 m	1 - 10 m
2	20-30°/150°	Slightly undulating, slightly rough	2 m	> 10 m
3	65°/345°	Planar, slightly rough	0.5 m	1 - 10 m

6.2.6 Location 4

Location 4 lies on the western end of the small island Svarhelleholmen. The dominating rock type is conglomerate with defined schistosity along joint set 1 and several veins of quartz, syenite and greenstone, mainly striking in the same direction as the foliation (approximately E-W). The rock surface is heavily weathered/eroded and has a bladdery texture. The most pronounced joint sets can be described as follows:

Joint set nr.	Avg. dip/dip direction	Joint surface	Spacing	Trace length
1 (foliation)	70-80°/175°	Undulating, rough and weathered	0.2 - 0.3 m	1 - 10 m
2	90±10°/120°	Undulating, rough and weathered	1.5 m	1 - 10 m
3	50°/70°	Undulating, rough and weathered	1.5 m	> 10 m
4	0-20°/250°	Undulating, rough and weathered	0.5 - 1 m	< 1 m

6.2.7 Landfall and anchoring on Svarvehella

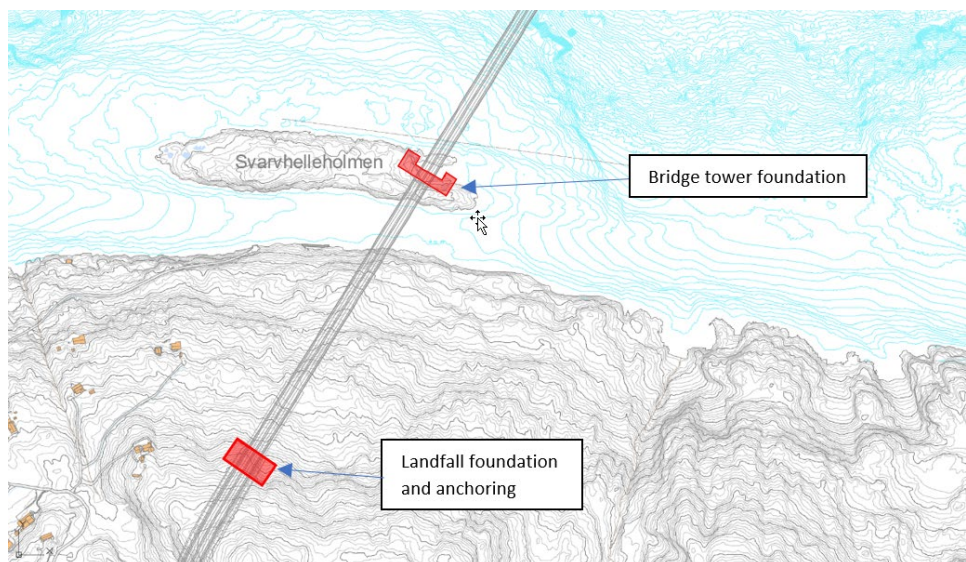


> Figure 6-3 K12 – bridge tower foundation and southern landfall.

The southern landfall of the bridge is indicated in Figure 6-3. The structures at this location will require a significant anchoring force, thus exposing the bedrock to very high loads. Although the local geology at the exact location of the landfall has not yet been surveyed in

detail, observations in the nearby area suggest that the intended methodology for anchoring will be feasible. The necessary anchoring capacity must be obtained by allowing sufficient dimensions of the anchors – thus, feasibility is expected to be a matter of calculating the adequate anchoring lengths.

The expected rock mass formation comprised of monzogranite will be well suited to sustain loads from for both foundation and anchors. The possible presence of local syenitic dykes and/or fracture zones must be further mapped. If necessary, such conditions should be either avoided or compensated for by increasing anchoring length or surface area of foundations.

6.2.8 Bridge tower foundation and anchoring on Svarvehelleholmen

The bridge tower foundation for *K12* is located on Svarvehelleholmen (Figure 6-3). The rock types on this island is of different characteristics than that on Svarvhelle to the south. The rock mass is weaker, deformed and has developed a high degree of schistosity. With regards to foundation and anchoring this rock mass is considered less suitable than the monzogranite to the south. For further detail design it will be necessary to perform investigations of the local structures and geological features at the exact location of the foundation.

The key issues for the design will be bearing capacity of the rock mass under the tower, and sufficient anchor capacity along the perimeter of the foundation. Both issues are considered to be feasible, based on the available information. Similar to the issue of landfall anchoring (ref. section 6.2.7), feasibility is expected to be a matter of establishing sufficient area of the foundation in order to obtain the necessary total bearing capacity, and calculating the adequate anchoring lengths.

Another important element related to foundations for a bridge tower is evaluation of the potential for land slide, either debris from higher ground striking the structure, or resulting in loss of stability of bearing capacity for the foundation. At the location of the *K12* bridge tower there are no higher grounds in the vicinity of the planned structure. Further, the foundation is located well inside a broad subsea shelf, with water depths less than 30 m, and about 130 m horizontal distance to the nearest steeper sub-marine slope (se Figure 6-4). Hence the issue of slope stability is not considered relevant for this location.

For more detailed information on the geological conditions, degree of jointing and rock mechanical properties, it is recommended to perform ground investigations in this area, preferably core drilling to depths of 40 – 60 m below the planed foundation.

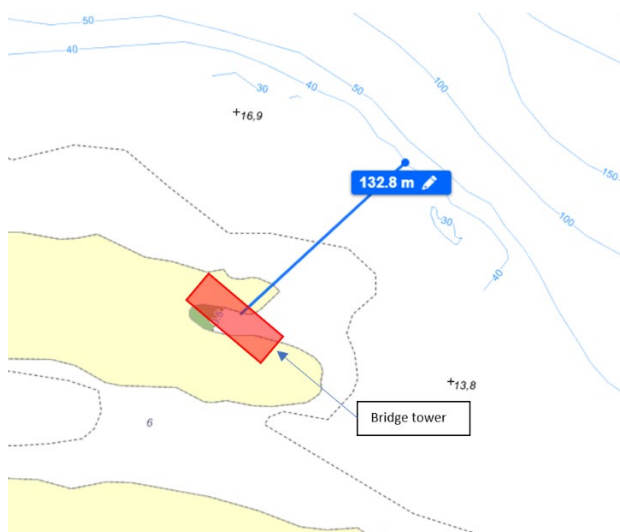


> Figure 6-4 Subsea map in the area of the *K12* bridge tower.

6.3 Northern landfall/anchoring

6.3.1 Geology of the project area

A geological map of the Svarvhelle area, issued by the Norwegian Geological Survey (NGU), is shown in Figure 6-5.

The northern landfall of bridge *K12* is located on Gullholmane, south-east of the island Røtinga (Figure 6-5 and Figure 6-7).

In previous alternatives of the project, the northern Landfalls were located at Fløholmen and Kobbholmane, some 500-800 m to the west of the current project location. The area of the mapping performed for the previous project by Norconsult in 2015 is indicated in the top left corner of the geological map in Figure 6-5. This mapping is not considered directly relevant for the new location, but parts of the constructions will be located in the same geological formation as before – a light coloured, foliated, garnet bearing trondhjemite (a variant of tonalite enriched in oligoclase, indicated by pink colour on the map in Figure 6-5). This trondhjemite is present on half of the island of Gulholmane, and also in the continued axis of the road/bridge on to the island of Reksteren. The other half of Gulholmane is comprised of a metatuff, a fine-grained metamorphic rock of volcanic ash origins.

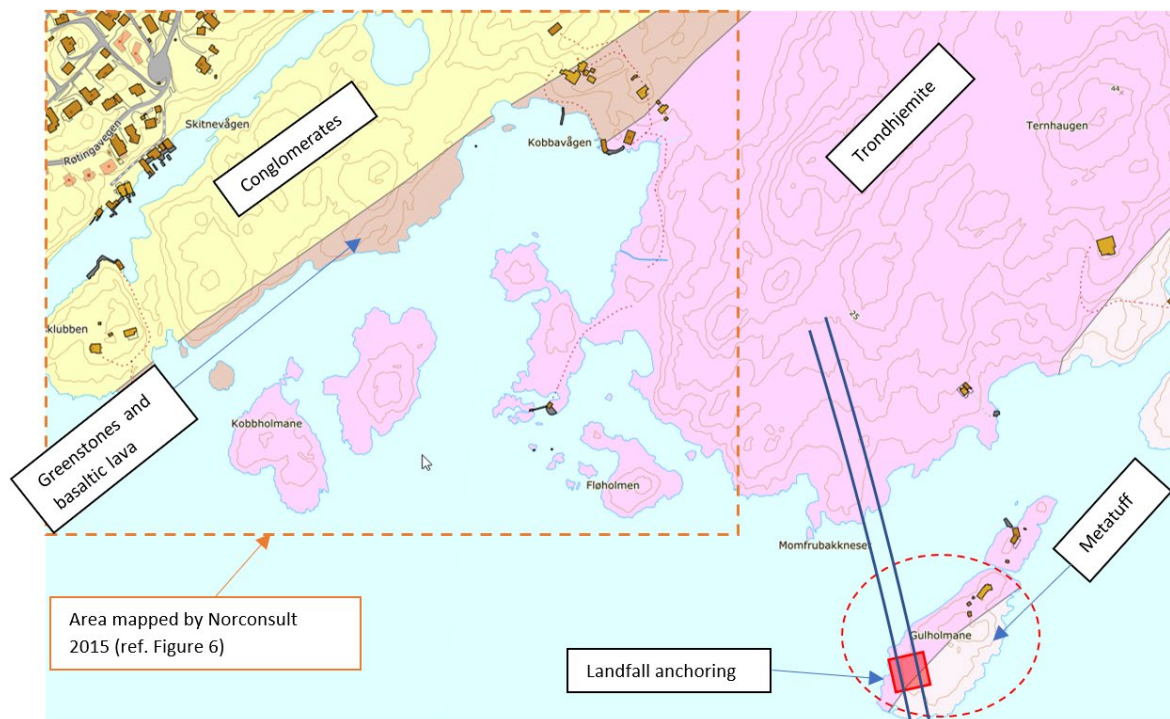


> Figure 6-5 Geological map of the area for the northern landfall at Røtinga/Gullholmane.

6.3.2 Engineering geological mapping (Norconsult, 2015)

From Norconsult's mapping in 2015, two detailed observations are located on Reksteren, some 150-200 m to the west of the *K12* alignment – denoted location 5 and 6 on Figure 6-6, with description and joint measurements in sections 6.3.3 and 6.3.4.

Figure 6-6 also shows structures/lineaments interpreted as weakness zones in the area west and north-west of the current landfall. Although the area of the landfall is not covered, it is expected that the same pattern of dominant lineaments, striking NW and NE, will also occur at the landfall area.

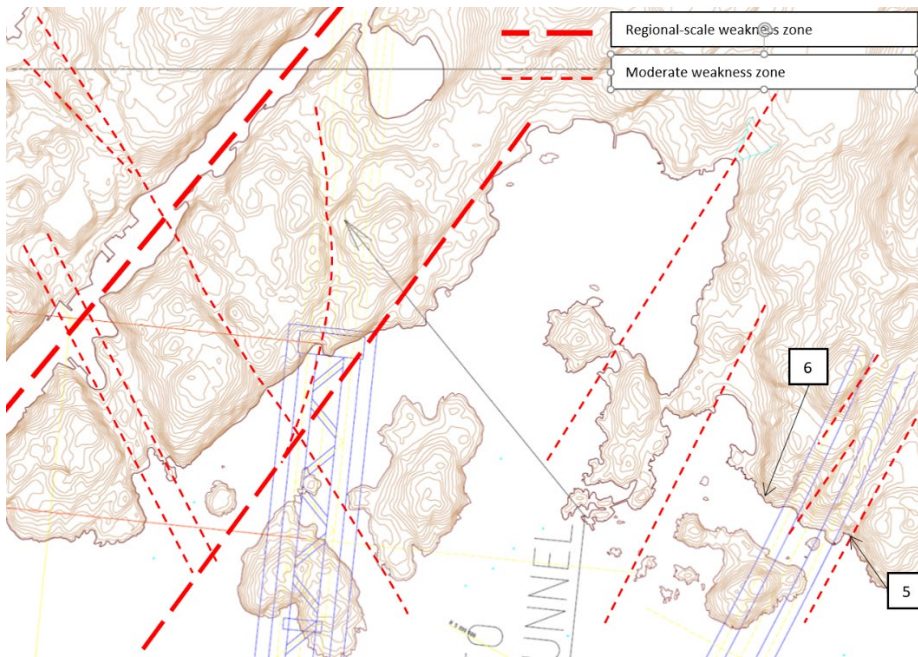


> Figure 6-6 Geological structures/weakness zones on Røtinga.

6.3.3 Location 5

The rock mass consists of trondhjemitic gneiss with a well-developed foliation along joint set 1 and good overall rock mass quality. A visible weakness zone runs through the bay east of this point and into the terrain. The joint frequency is significantly higher in the rock mass up to 15 m on either side of this zone. The most pronounced joint sets can be described as follows:

Joint set nr.	Avg. dip/dip direction	Joint surface	Spacing	Trace length
1 (foliation)	80-85°/300°	Planar, rough/irregular	1 m	> 10 m
2	45-55°/190-200°	Planar to slightly undulating, rough	0.5 - 1 m	1 - 10 m
3	55°/60°	Planar, slightly rough and irregular	0.5 - 1 m	1 - 10 m
4	35°/30°	Planar, rough to irregular	0.5 - 1 m	> 10 m

6.3.4 Location 6

The rock mass consists of trondhjemitic gneiss. The most pronounced joint sets can be described as follows:

Joint set nr.	Avg. dip/dip direction	Joint surface	Spacing	Trace length
1 (foliation)	80°/315°	Plane to undulating, rough	0.5 m	1 - 10 m
1	80°/60°	Planar, slightly rough	0.5 - 1 m	1 - 10 m
3	30-40°/240-270°	Undulating, rough	0.3 - 0.6 m	1 - 10 m
4	35°/30°	Planar, rough to irregular	0.5 - 1 m	> 10 m

6.3.5 Landfall and anchoring on Gulholmane

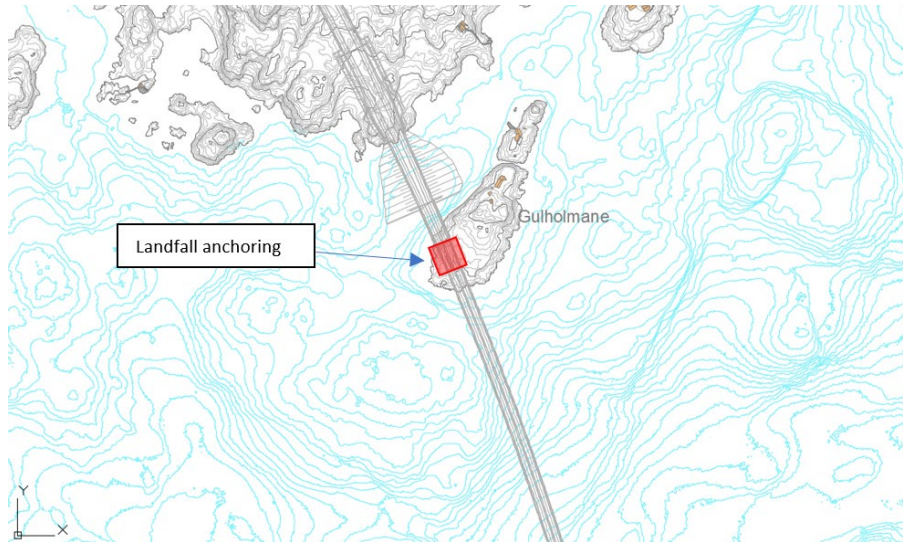


> *Figure 6-7 K12 – northern landfall.*

The landfall of the bridge will require a significant anchoring force, thus exposing the bedrock to very high loads. Preliminary observations and assessments suggest that the potential for land slide is not considered relevant with respect to landfall foundation at this location. The intended methodology for anchoring will be feasible. Similar as to the southern landfall, the necessary anchoring capacity must be obtained by allowing sufficient dimensions of the anchors – thus, feasibility is expected to be a matter of calculating the adequate anchoring lengths.

The surrounding waters of Gulholmane island are relatively shallow, less than 30 m depth, and with relatively gently dipping slopes. There are no higher grounds on the island. Thus, for further evaluation and detailed design, it is recommended to perform geological mapping and possibly ground investigations in the local area (core drilling, refraction seismic analyses, and possibly laboratory testing of samples).

7.1 Bathymetry and soil conditions

The bathymetry data illustrated in Figure 7-1 shows variable seabed conditions. The fjord is asymmetrical with undulating seabed. On the southern side there is a steep inclination down to the basin. The basin itself stretches out almost two thirds of the crossing distance and has depth of about -550m. The last part in the north, which is shallower from about -200m to -50m depth, consists mainly of exposed bedrock.

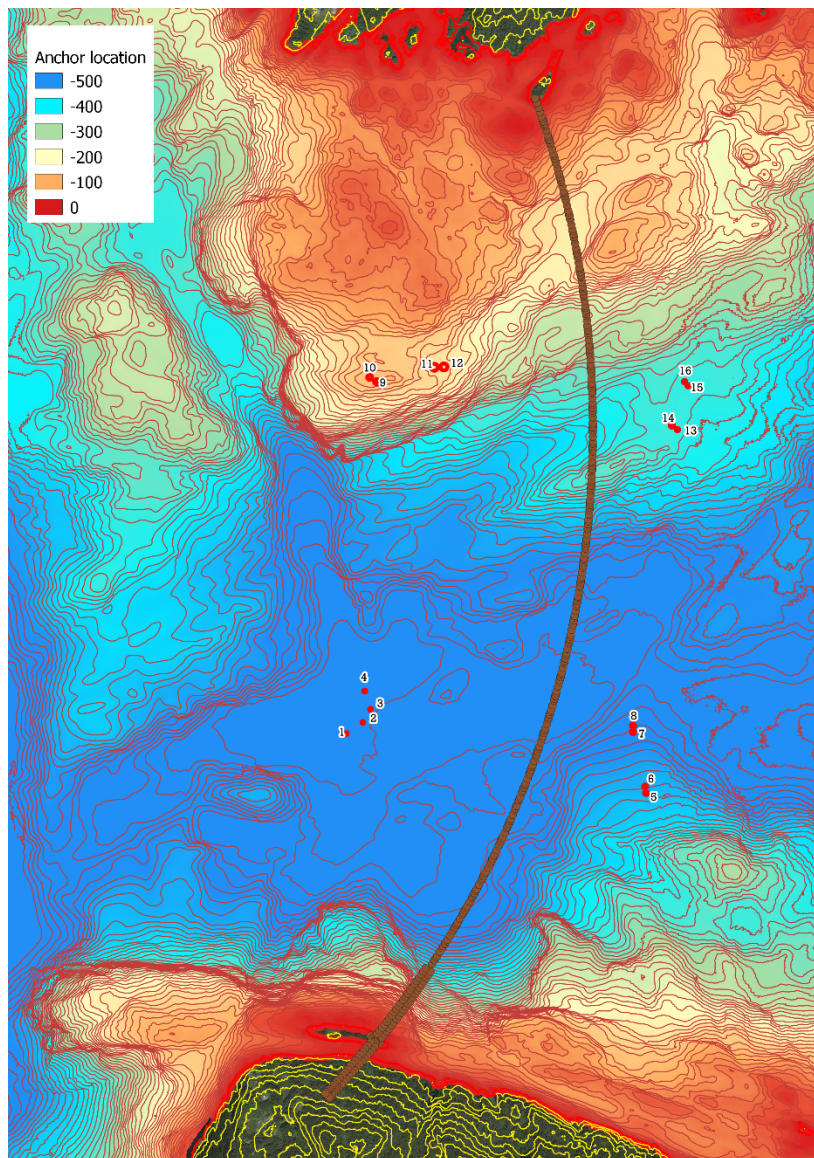


> Figure 7-1 – Bathymetry shown together with the bridge and anchor locations

The geotechnical data and soil samples are mainly taken from the basin and consists of NC-clay. The in-situ soundings and laboratory data show homogeneous soil conditions with low-sensitive NC-clay. The unit weight and undrained shear strength is increasing almost linearly with depth.

7.2 Anchor site evaluations with respect to slope stability and holding capacity

The major concern with anchor site evaluation is seabed landslides caused by earthquake, erosion or other changes in the in-situ conditions. Several areas in the Bjørnafjorden has poor slope stability and the risk of surface and deep plowing landslides is therefore high.

For anchor site evaluations the preliminary criteria given in the geotechnical design basis have been used. The criteria are with respect to seabed inclination and soil thickness and is mainly tied up to anchor holding capacity and installation requirements. In Figure 7-2 (a) possible anchor locations are shown where blue is areas suitable for gravity anchors, green having more than 25m of soil thickness and yellow being in between with less than 10 degrees in seabed inclination.

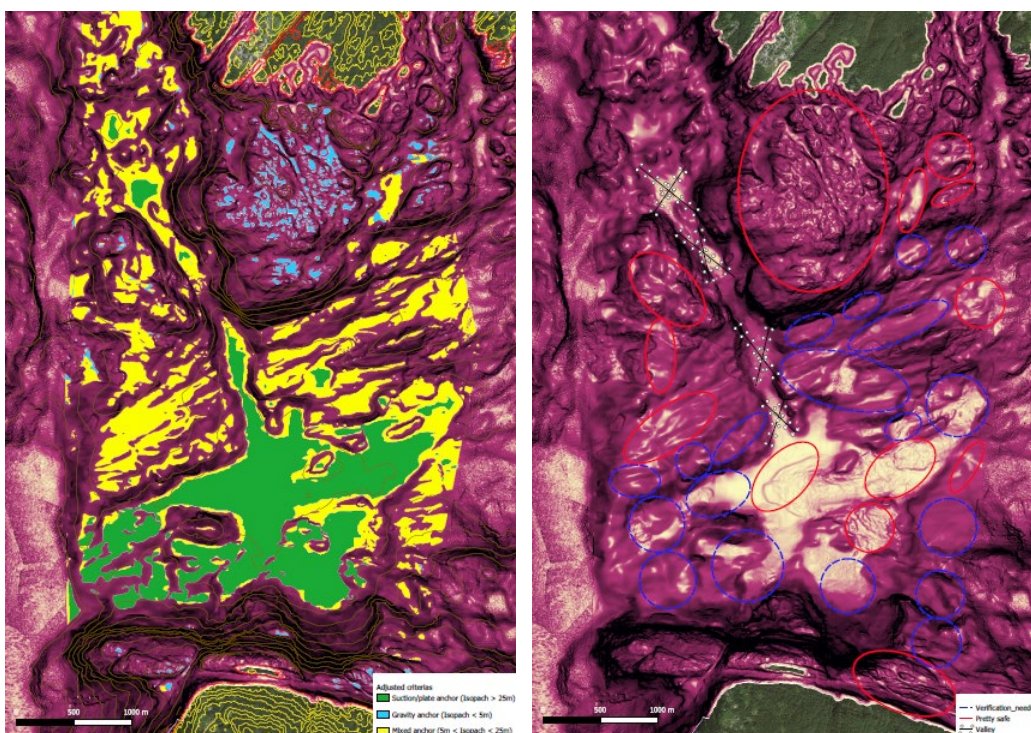


> Figure 7-2 Preliminary anchor location after certain criteria (a) and preliminary geohazard evaluation.

There is a strong correlation between the slope stability and the seabed inclination. Thus, for preliminary anchor site evaluation, areas with insufficient static factor of safety have been avoided. Valleys surrounded with poor slope stability are also avoided due to increased possible landslide sources. This is shown in Figure 7-2 (b), where the red rings indicate fairly safe areas and blue ellipses suggest areas with challenging ground conditions.

Anchors 1-4 is in the middle of the basin and therefore relatively safe, while anchors 5-8 is in the most exposed area with respect to possible landslides. Location of anchors are shown in Figure 7-1. The current position was chosen to avoid slopes with poor static safety factor in the south. However, due to installation issues it might be relevant to move the group further south if sufficient slope stability and holding capacity can be verified. Anchors 9-12 are located in an area with little or no sediment cover above bedrock. Anchors 13-16 is located on a plateau with little risk of slides up- and downstream.

7.3 Anchor holding capacity

The gravity anchors (anchor 9-12) are calculated according to common slide friction capacity. The equation proposed by Janbu is used to estimate the required submerged weight to achieve satisfactory frictional resistance. In the calculations it is assumed that the anchor line force is acting horizontally on the anchors. Crushed rock is used to even out the foundation area and is assumed to have a friction angle of 37° . The roughness factor used in Janbu's equation is set to 0.8. The material factor is set to 1.3 according to DNVGL-OS-C101.

Additional friction between the anchor and soil can be achieved by skirts if required. The gravity anchor is filled with olivine aggregate with an assumed porosity of 42%. This corresponds to a submerged unit weight of 13.2kN/m^3 . Structural capacity of the gravity anchors has not yet been verified.

For the suction anchors (anchor 1 – 8 and 13-16) the anchor holding capacity has been calculated with Plaxis 2D 2018. The design line loads are defined by the mooring analysis and the results are shown in Table 5-4. The anchor is modeled in plane strain with a width equal to the diameter according to DNVGL-RP-E303. The geometry is shown in Figure 7-3. Interfaces are used to simulate set-up after 1 year and to avoid numerical singularities. The capacity from side-shear is manually calculated using an average direct undrained shear strength and afterwards reduced due to set-up and material factor. Since the side-shear is direction independent, it can thus be subtracted from the design load. Bedrock presence beneath the foundations has not been included in the model and is expected to give a higher capacity for anchors close to the bedrock.

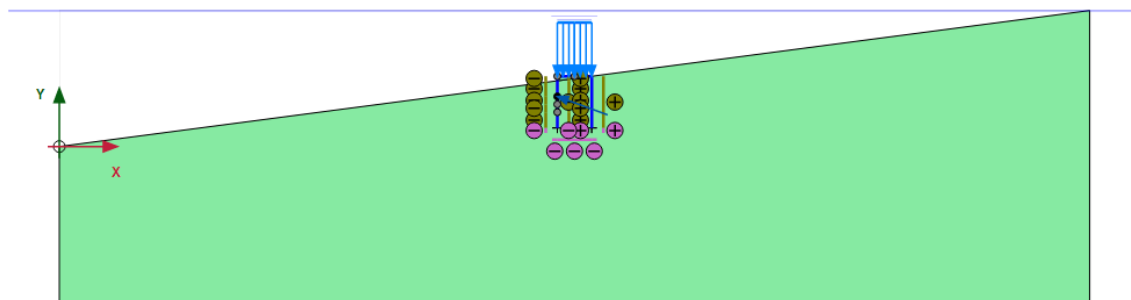


> *Figure 7-3 Plane strain model of suction anchor*

NGI-ADP, undrained C material has been used to calculate the holding capacity. Material parameters are according to the design brief. Due to the circular shape of the anchor, the plates can be assumed to be stiff in the plane strain model. The undrained shear strength is modeled to vary linearly with depth from terrain as shown in Figure 7-4.

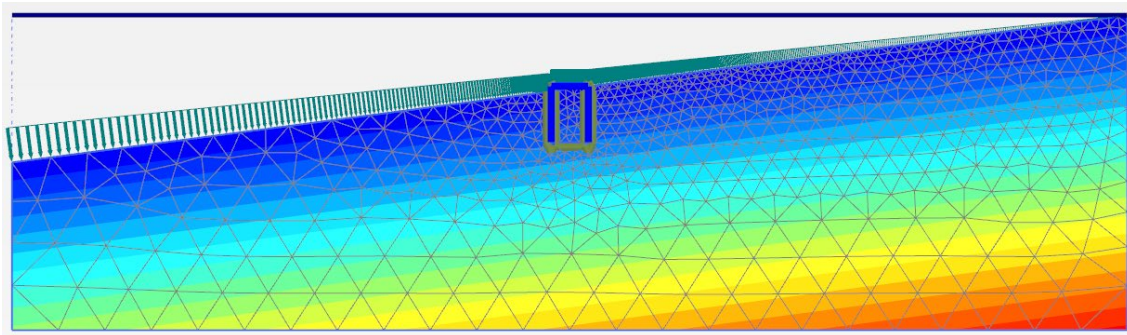


> *Figure 7-4 Undrained shear strength with depth*

The optimal padeye position depends both on the load and the seabed inclination. Several positions have therefore been evaluated to verify the capacity. After installation and prior to hook-up, the bearing capacity has been checked. Typical failure modes are shown in Figure 7-5.

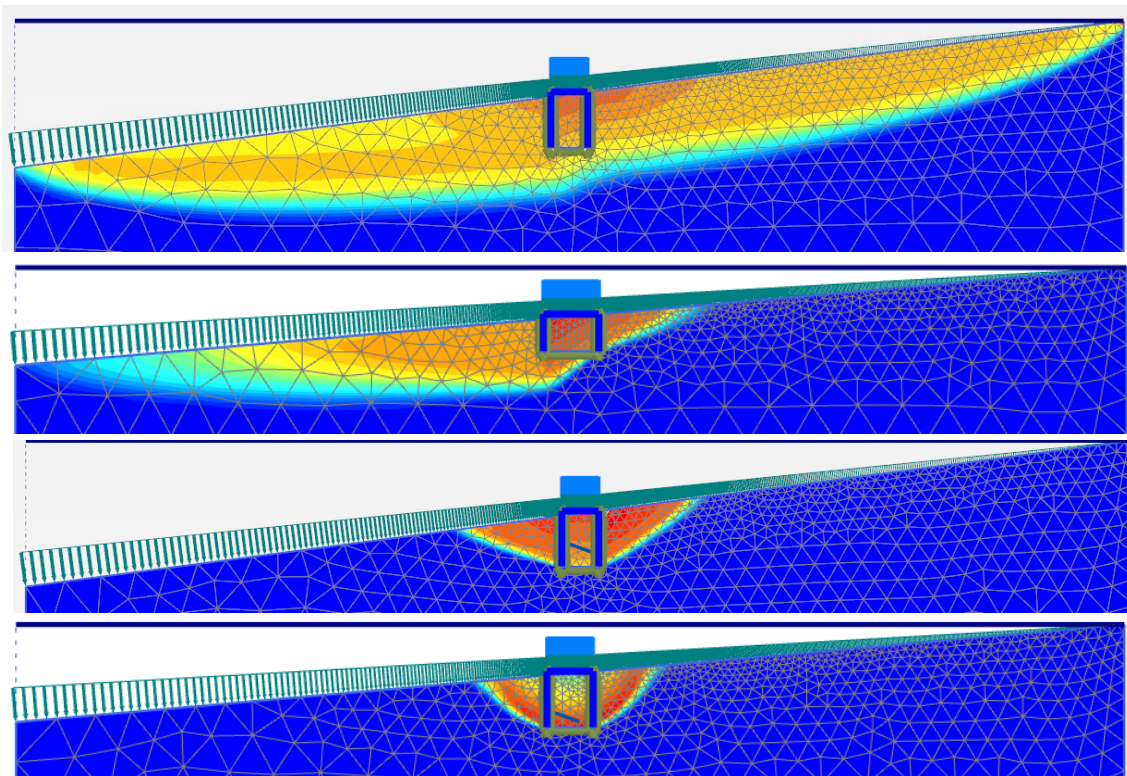


> *Figure 7-5*
 (a) *Slope failure due to infinite steep inclination $\alpha > 5^\circ$ and no bedrock*
 (b) *Bearing capacity failure due to self-weight of anchor*
 (c) *Holding capacity failure at optimal padlock position*
 (d) *Holding capacity failure where the padlock position causes rotation of the anchor*

8 CONSTRUCTION AND INSTALLATION

8.1 General

The project strategies for this Construction and Installation Plan includes the execution strategies for the safe engineering, procurement, prefabrication, assembly and installation, including marine operations. There are four alternative concepts in this study: K11, K12, K13 and K14. This report deals with alternative K12, which is an end-anchored arch with 16 support anchor lines arranged on 8 pontoons in two groups, see Figure 2-5.

The end-anchored bridge across the Bjørnafjord is split into the following major elements (subsystems):

- Abutment south (south support of cable stay bridge)
- Cable stayed-bridge tower
- Cable stayed-bridge (bridge girder and cables)
- Floating Bridge
 - Bridge girders (carriage way)
 - Pontoons
 - Columns (between pontoons and bridge girders)
- Anchors and mooring system
 - 16 mooring lines in two groups
 - anchors
- Abutment north (at Gulholmane)
- Filling and road north of Gulholmane

For concept description, structural dimensions and weights of the main elements reference is made to Sec. 2.

8.2 Floating bridge construction and installation

8.2.1 Work flow general

There are many possible fabrication strategies for the Bjørnafjorden fjord crossing project. The logistic chain for the steel works in the floating bridge is generally as follows:

- Steel plate delivery to prefabrication site
- Prefabrication at yards for pontoons, columns and bridge girder sections
- Transport of prefabricated sections/elements to Assembly site 1
- Joining of pontoons, columns and bridge girder 'superelements' at Assembly site 1
- Transport of 'superelements' to Assembly site 2
- Joining of 'superelements' as appropriate for the different concepts and storage at Assembly site 2
- Installation campaigns for Bjørnafjorden as specified for the different concepts
- Completion works for the bridge in Bjørnafjorden

Prefabrication of the steel structures for the Bjørnafjorden bridge may take place at many locations around the world. It is also closely connected to the market conditions at the time of project realization and the SVV selected contracting strategy. For this report prefabrication in Far East/China assumed.

8.2.2 Assembly site 1

Many suitable sites have been considered for assembly of the prefabricated structures. Among these are:

- Lutelandet
- Hanøytangen
- Kværner Verdal
- Dommersnes/Ålfjorden
- Kværner Stord

For this report Hanøytangen is selected as base case Assembly site 1 due to its vicinity and access for inshore towage to the Bjørnafjorden area.

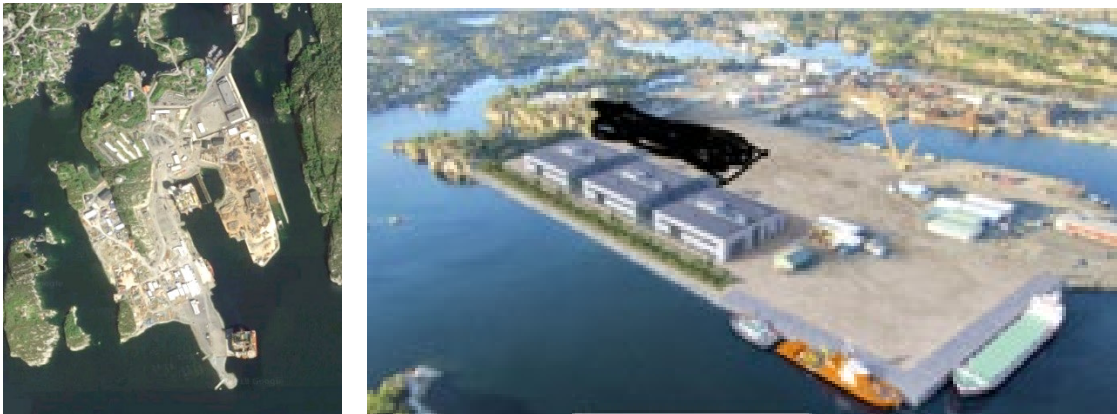


> *Figure 8-1 Hanøytangen yard: Aerial photo (left) and future plans for area and quays extension (right)*

8.2.3 Steel material delivery

For this case all steel materials for the pre-fabrication is assumed to be procured by the selected yard for prefabrication.

8.2.4 Prefabrication yards

In general, three arenas are specified for prefabrication:

- Prefabrication in Norway
- Prefabrication in Northern Europe
- Prefabrication in Far East:

For this report, prefabrication in Far East/China has been selected, and steel prefabrication is assumed to take place in China in Qingdao in the Shandong province.

All fabrication; bridge girder, pontoons and columns, is assumed to take place at the same yard. The box girder is generally assumed to be prefabricated in 100 m lengths for the floating bridge with curvature built into the sections. The cable stayed bridge girder is prefabricated in 50 and 100 m sections.

The pontoons are delivered from the fabricator with the columns installed. For the pontoons supporting the ramp part of the bridge the top part of the column will be installed at Assembly yard for floating stability reasons.

Strict specification for and control of fabrication tolerances must be exercised for the prefabrication process both for bridge girder sections to be joined and between the top of the columns and the girders. Here the design of the transition needs practical detailing. This should be carefully studied further in order to facilitate the assembly process. The main components of the bridge are listed in Table 8-1.

> *Table 8-1: Main components*

Component	Quantity	Comment
Pontoons	46	8 equipped with chain stopper and fairleads for 2 anchor lines
Columns	46	
Floating Bridge deck sections	3×16 = 48×100 = 4 800 m + 60 m	Girder sections to be pre-fabricated with hor. curvature $R_H = 5\,000\text{ m}$
Cable stayed Bridge sections	50 and 100 m long sections, total 835 m	Straight girder sections

Bridge girder prefabrication and transportation

- The bridge girders are standard steel construction structures suited for worldwide fabrication. Typically, the element lengths are 100 m with a corresponding weight of 1 350 – 1 400 tons which is considered a manageable size and weight for a range of ship yards as well as the assembly site(s).
- To simplify the section joining operations, there are no element joints above the columns from the pontoon. This special element includes internal reinforcements and will be fitted with a 'column starter' of about 0.3 – 0.5 m on the underside of the girder to simplify the column connection. Special considerations and design elaborations has to be developed for the tolerance aspect in the column/girder connection.
- For the Transportation of the floating bridge girder sections it is assumed that they arrive at HT in batches of 12 elements, delivered every 6th month to fit with the Assembly process.

Column prefabrication

- Columns are standard stiffened steel plated structures and thus well suited for fabrication at a large range of ship yards and fabrication methods.

Pontoon fabrication

- The pontoon design is standard ship type construction with minor internals and is suited for worldwide fabrication at a large range of qualified ship yards. It is vital to ensure that the ship yards adhere to the strict surface preparation and coating requirements and have the required welding procedures for welding the corrosion resistant splash zone
- The pontoons can be fabricated on land, on a slip way or in dock and can be transported on own keel (towed) or transported on a barge or transportation vessel.
- The fabrication method is not advised since this will be dependent on the selected yard facilities.

8.2.5 Transport from Prefabrication site to Assembly site 1

For the transportation of such a large quantity of structures, thorough studies of market conditions for transport vessels suitability and availability need to be performed. Also, the logistics at both ends has to be considered carefully. Suitable transport vessels considered in this case are:

- Boka Vanguard
- Blue Marlin
- White Marlin

→ BOKA Vanguard is selected in this case.

Pontoon and column transport from fabrication site to Assembly site 1 is assumed to take place in 3 batches for the floating bridge and one batch for the cable stayed bridge. Load out to the vessel and sea fastening to be executed by the prefabrication yard. It is assumed that SPMTs (Self Propelled Modular Transporters) will be used for load-out of the bridge girders and the pontoons, all stored on support stools on the transport vessel and secured with proper sea fastening.

8.2.6 Load-off and storage

SPMTs are assumed used for load-off of the girders and storage on land at Hanøytangen, whereas the pontoons are floated off and stored in the dock area.

The bridge girder sections for the for the Cable Stayed Bridge (CSB) is transported as the 4th batch and also stored at Hanøytangen prior to load out for installation. SPMTs are assumed used for load-off and load-out to the extent possible for the CSB.

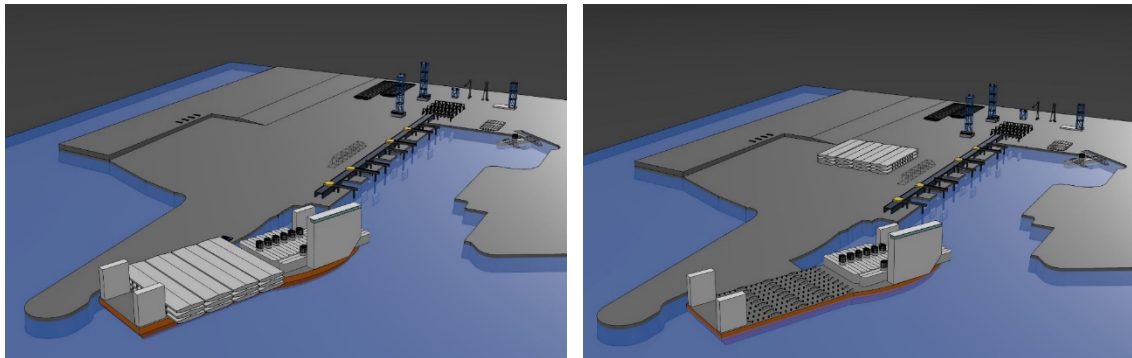


> *Figure 8-2: Transport vessel BOKA Vanguard at Hanøytangen (left). Load-off and storage of girder sections and pontoons (right).*

8.2.7 Assembly site 1

Rigging and modifications of Assembly site 1 at Hanøytangen comprise:

- Land storage area
- Keyside modifications for pontoon
- Skidways
- SPMTs and mobile cranes
- Lifting towers and temporary supports

- Facilities for workforce
- Offices

At Hanøytangen the bridge will be assembled in several floating sections. The length of one section will mainly be about 400 m, consisting of 4 pontoons, 4 columns and 4 × 100 m long deck sections.

The pontoons with columns installed will be grounded on concrete support foundations. These foundations will be cast on the bottom of the dock, on rock. In order to provide sufficient space in the dock, recesses in the key side wall will be provided. The pontoons will be water-ballasted down on the foundation support cushions located on the concrete foundations. The pontoon is secured, in addition to its own weight, by steel bracket guides. Fresh water will be used for ballasting the pontoons from a water tank on the site. For the low bridge, the columns will arrive to the assembly site with the columns already fixed to the pontoons. For the ramp part of the bridge the upper part of the columns are delivered separately from the pontoons and installed when the pontoons are positioned on the key side foundations.

For the low part of the floating bridge the following installation methods of deck-elements are considered:

- Transverse skidding
- Longitudinal skidding, incremental launching

Transverse skidding is further described in this report.

Transverse skidding Low bridge

Deck-elements stored on the site will be transported using multi-wheelers. The deck-elements have to be lifted up some 10 meters above the ground. Alongside the dock, a transport way has been erected consisting of two wagons running on rails. The deck-elements are lifted up and placed on sliding equipment on the wagons. From the rail way the element is skidded transversely on two skidding beams to be lined up with the columns. The gap between the ends of the elements will be closed by welded steel.

When the deck-elements are finished, the gap between the columns and deck is closed by welded steel structures. This operation will be repeated for interconnecting the bridge sections and connecting the girder with the column transition piece. The finished 400m long bridge section will then be de-ballasted and prepared for the tow to assembly site 2 in Eikelandsfjorden. The process is illustrated in the figures below.

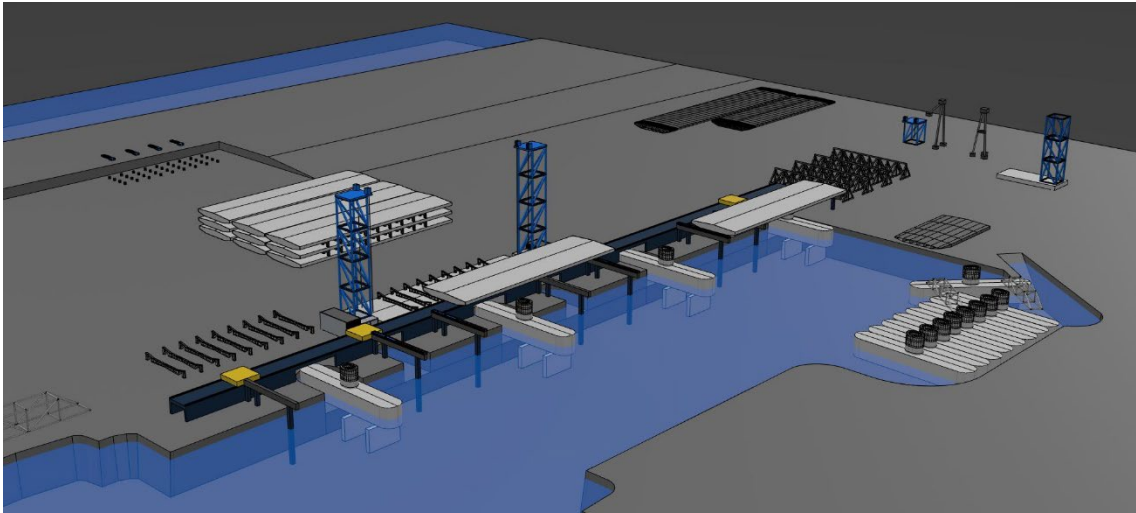


> *Figure 8-3: Low bridge transverse skidding*

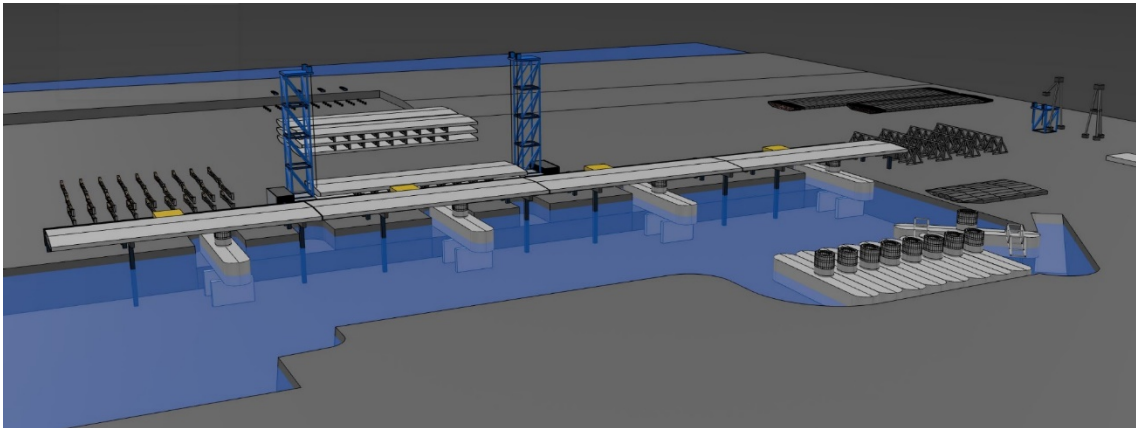


> *Figure 8-4: Superelement complete ready for towing to Assembly site 2*

Transverse skidding Ramp bridge

Due to the increased height of the columns, the upper part of the columns has to be installed when the pontoons are sitting on the concrete foundations. For the ramp part of the bridge the upper part of the columns are delivered separately from the pontoons and installed when the pontoons are positioned on the key side foundations. This can be performed by connecting two pontoons by two temporary girders, or by having a temporary smaller barge connected to the pontoon.

Before installation the pontoons, the deck element at the inner part of the dock, is skidded to position and hoisted by two hoisting towers. One of the towers is on land, at the end of the section, and the other tower is placed in the dock. This tower is placed on a purpose built pontoon, also grounded in the operation phase. The pontoons will be installed. In order to adjust the sagging curvature of the deck-element, an extra tower will be installed in the middle of the span. The other elements are then installed in similar procedures. The process is illustrated in the figures below.

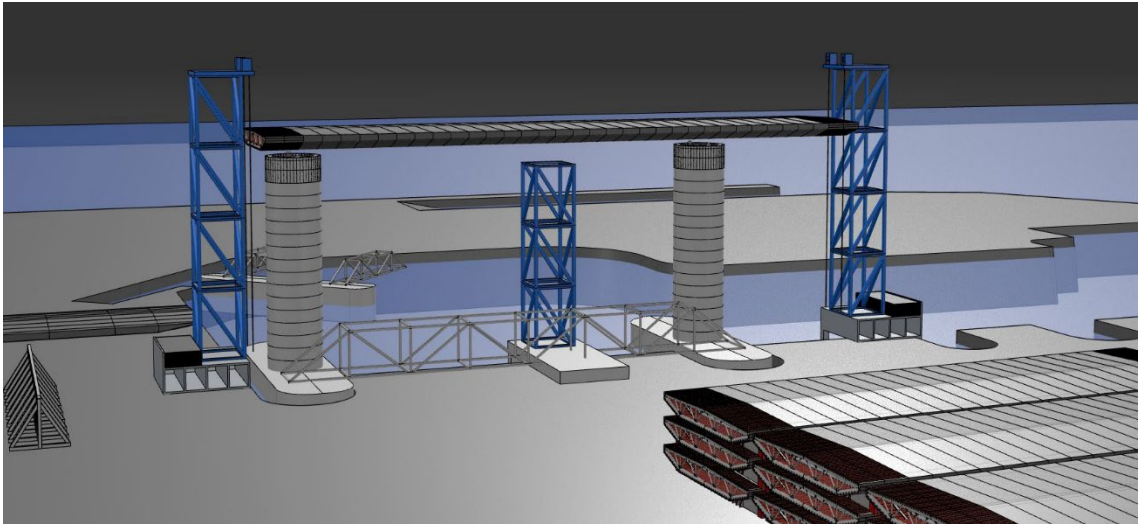


> Figure 8-5: Ramp Bridge assembly

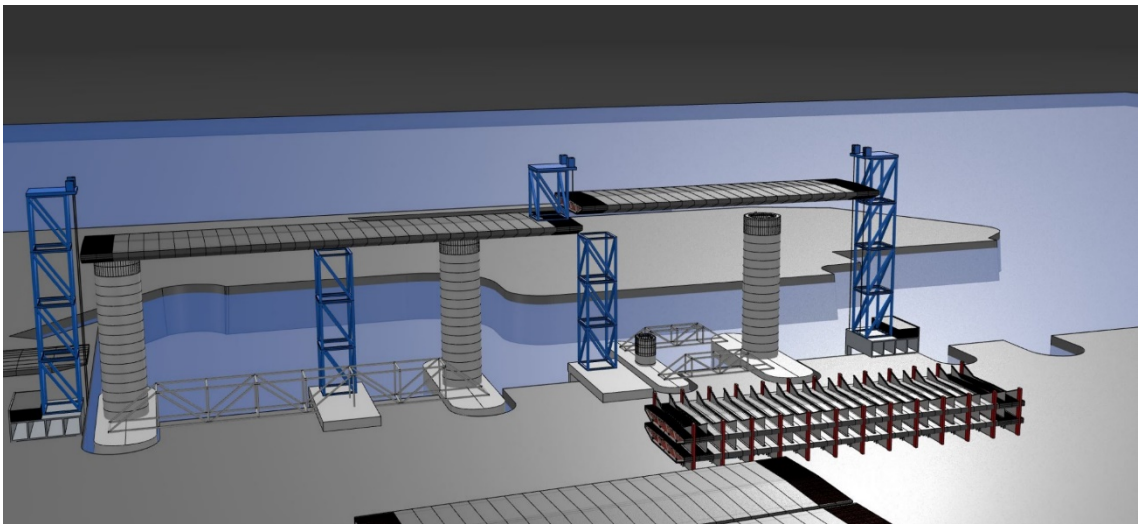


> Figure 8-6: Ramp Bridge assembly

> Table 8-2: Superelements

Superelements	Nos.	L (m)	Total length (m)	Location
High bridge	2	500	1 000	Axis 3 – 12
Low bridge	9	400	3 600	Axis 13 – 46
Abutment North Connection	1	260	260	Axis 47 – 49

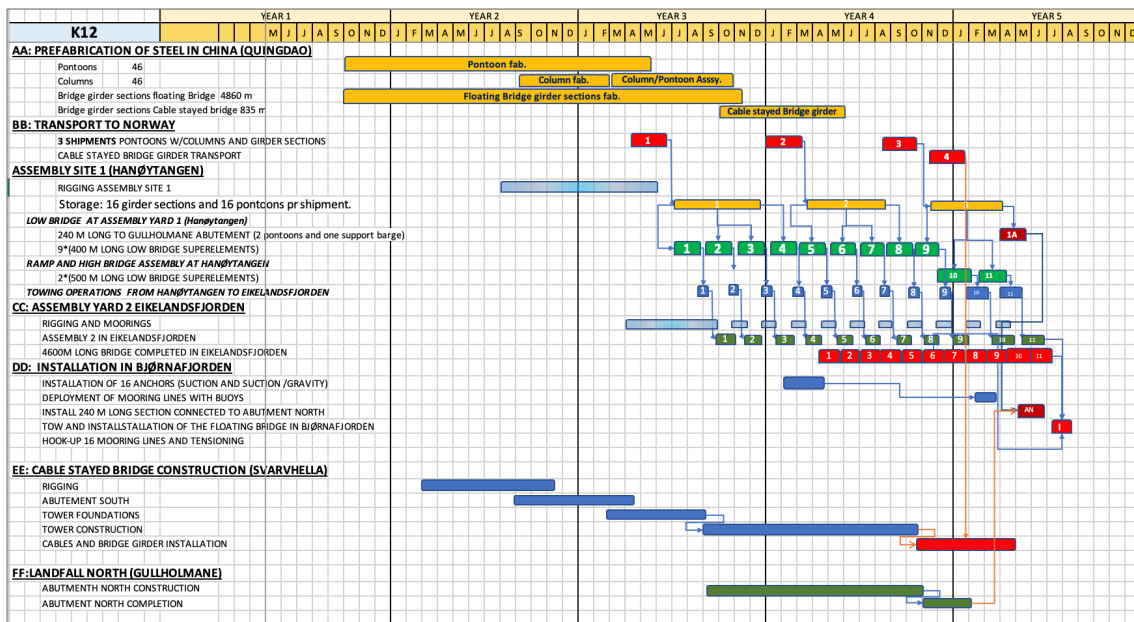


> Figure 8-7: K12 Prefabrication, Transport and Assembly LOGIC

8.2.8 Towing from Hanøytangen to Eikelandsfjorden

The superelements are transported on own keel from Hanøytangen to the bridge assembly site in Eikelandsfjorden along the inshore towing route shown in Figure 8-8. For this tow a tug fleet of 5 nos. 60 – 70 tonnes bollard pull tugs with the configuration as shown in Figure 8-9 is foreseen. The towing distance is approx. 35 NM. With an average towing speed of 2.5 knots the tow will be accomplished within 14 hours.



> Figure 8-8: Towing route (left) and towing of superelement through Vatløstraumen (right).

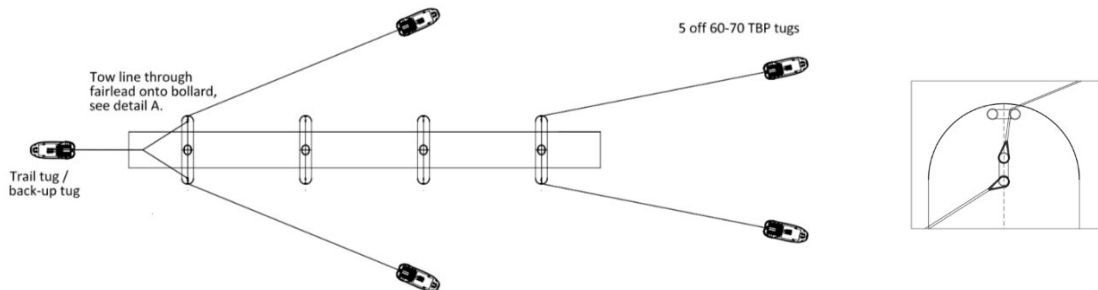


> Figure 8-9: Towing configuration for superelements

8.2.9 Assembly Site 2: Eiklandsfjorden

For assembly of the superelements arriving from Hanøytangen, a special purpose rig as shown in Figure 8-10 above is utilized. The same rig will be used both for the ramp section and also for the south connection to the CSB in Bjørnafjorden. The assembly procedure is shown in Figure 8-12.

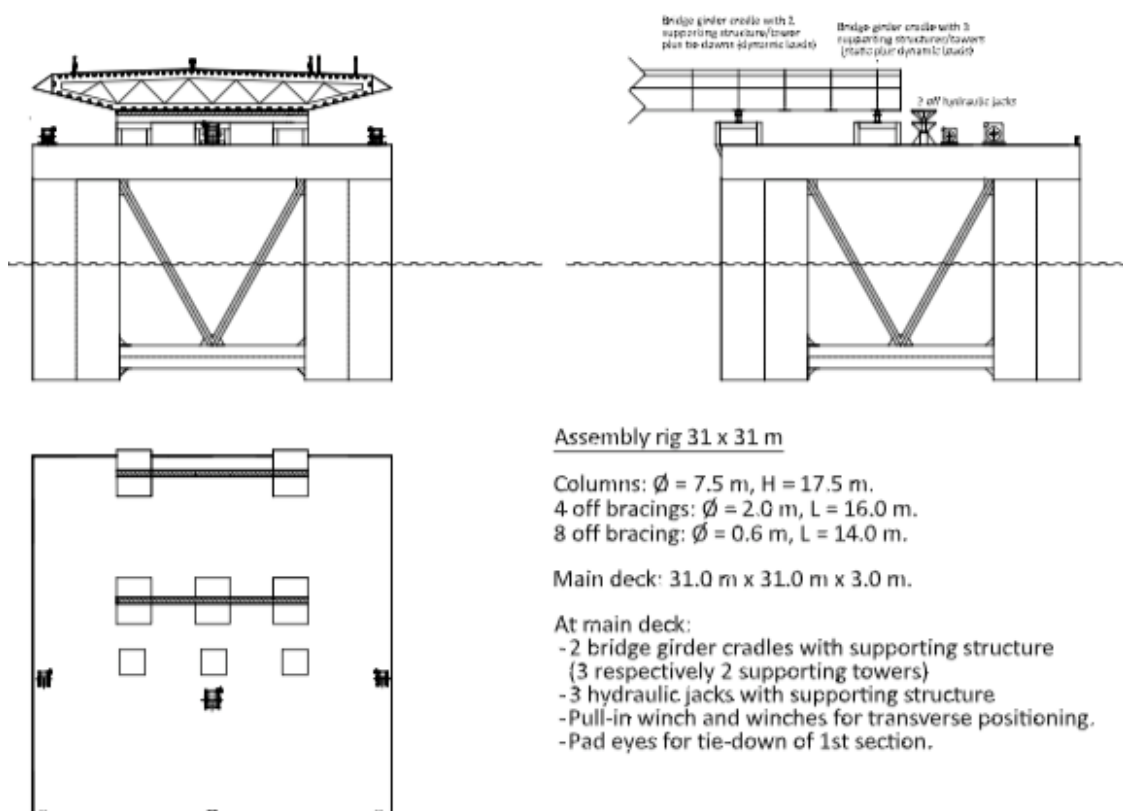


> Figure 8-10 Semi-submersible Assembly rig (here rigged for low bridge superelement connection)

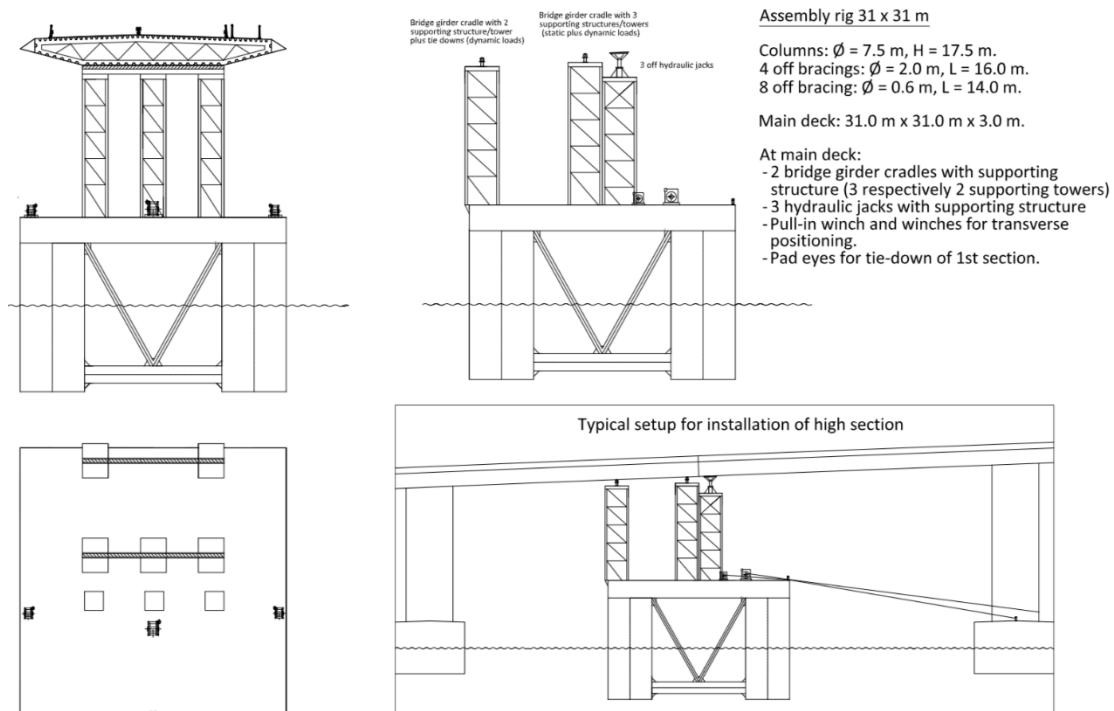


> Figure 8-11: Ramp Bridge assembly at Eikelandsfjorden

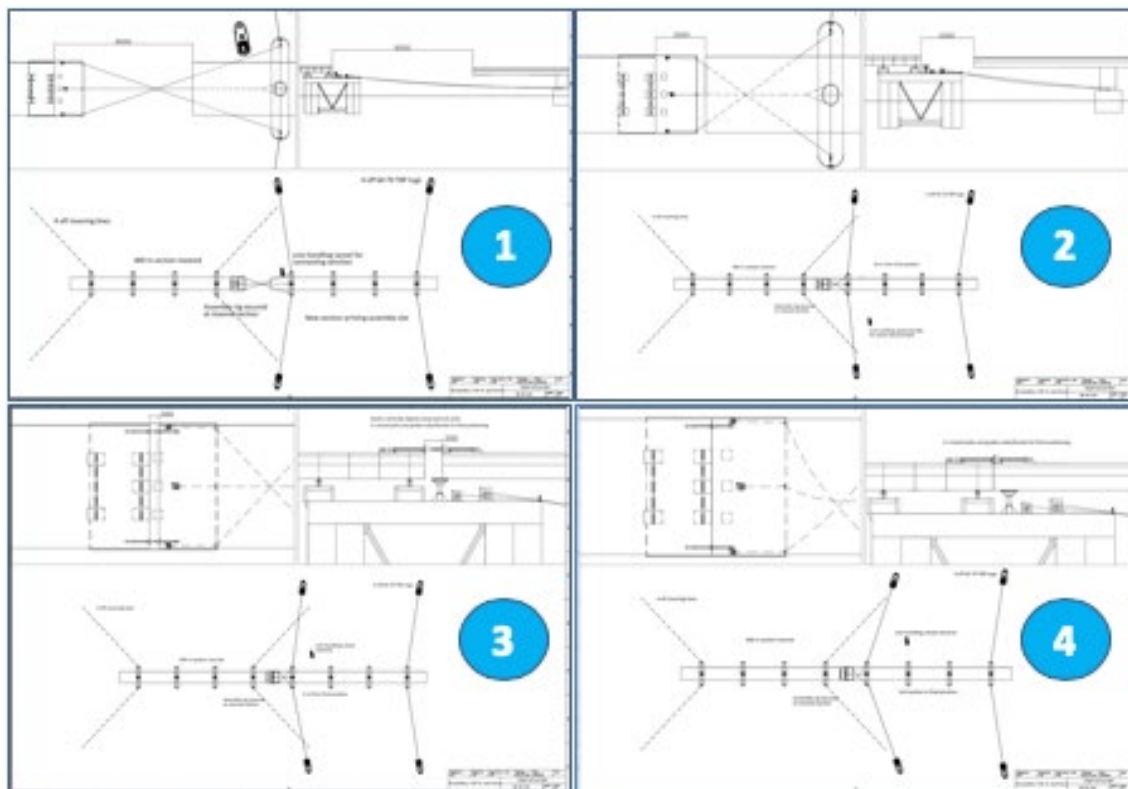


> Figure 8-12 Low bridge assembly using semi Assembly rig

For K12 the arch will be built up from west towards east as the superelements are arriving from Hanøytangen. The assembled string is shown in Figure 8-13 below. No mooring lines are indicated, but have to be considered at a later stage. There are power cables in the fjord, which has to be avoided. Also, the fish farming facilities have to be taken into consideration.

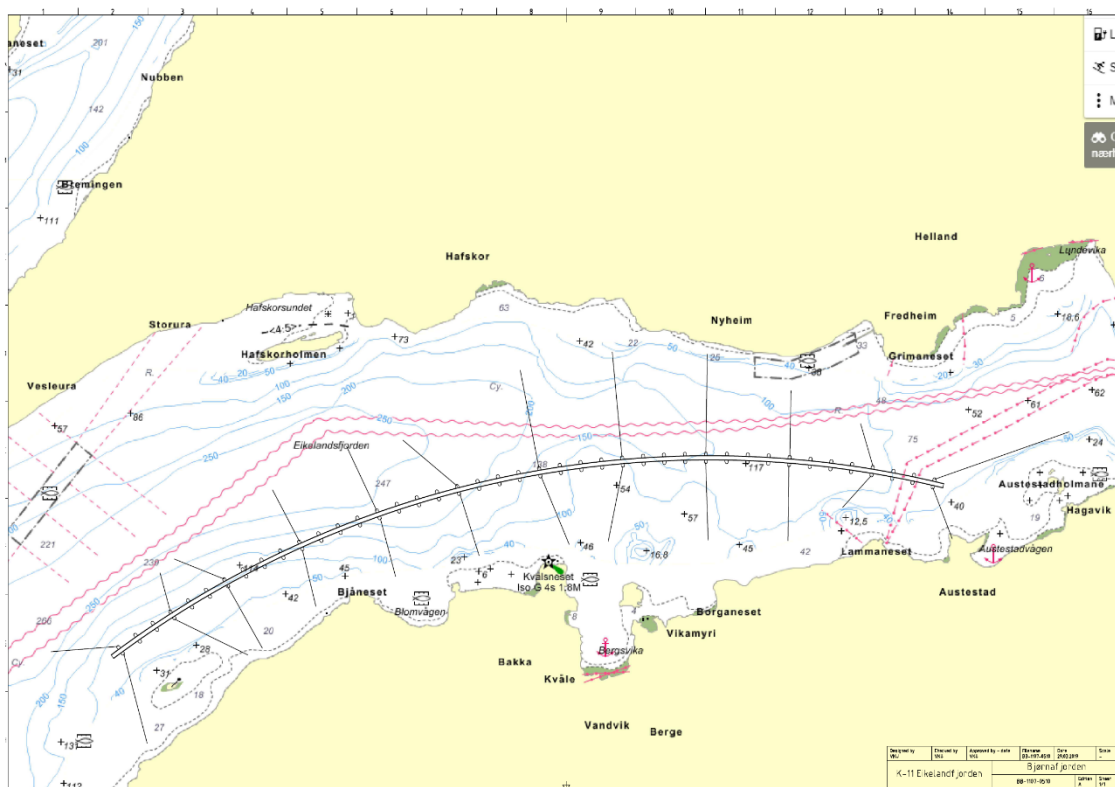


> Figure 8-13 K12 floating bridge assembled at Eikelandsfjorden; Ramp bridge towards east

8.2.10 Installation in Bjørnafjorden

As shown in Figure 8-17, the floating bridge is proposed to be installed in two parts, one 260 m segment connected to the north abutment and one 4 600 m segment between this element and the cable stayed bridge. The main reason for the installation of the short section is to minimize/eliminate the effect of tide at one of the interface points to simplify the connection operation of the long bridge.

Installation of the Bridge section at Abutment North

The bridge section to be connected to the abutment located at Gullholmane is towed from the storage area at Hanøytangen and to Bjørnafjorden. The installation sequence is shown on Figure 8-14 below.

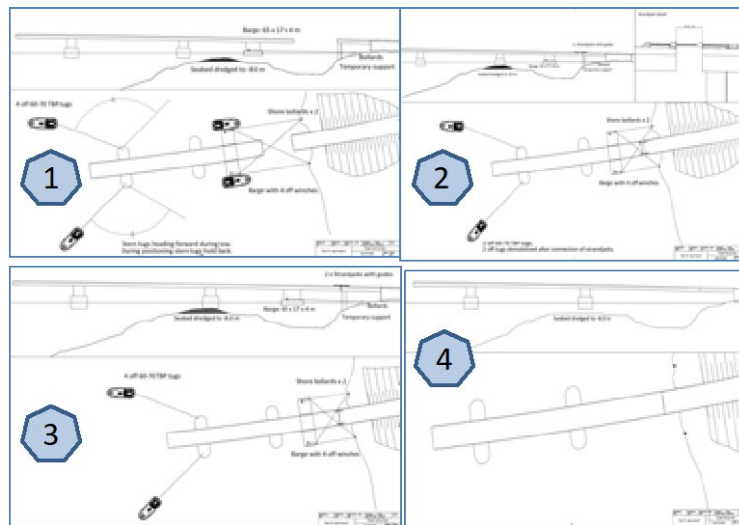


> Figure 8-14 Installing bridge section at Abutment North

Main Bridge installation

Due to the relatively short tow from Assembly site to the final bridge site in the Bjørnafjord (Figure 8-15), the tugs will be connected such that there is no need for reconnection for the turning and installation or even holding.

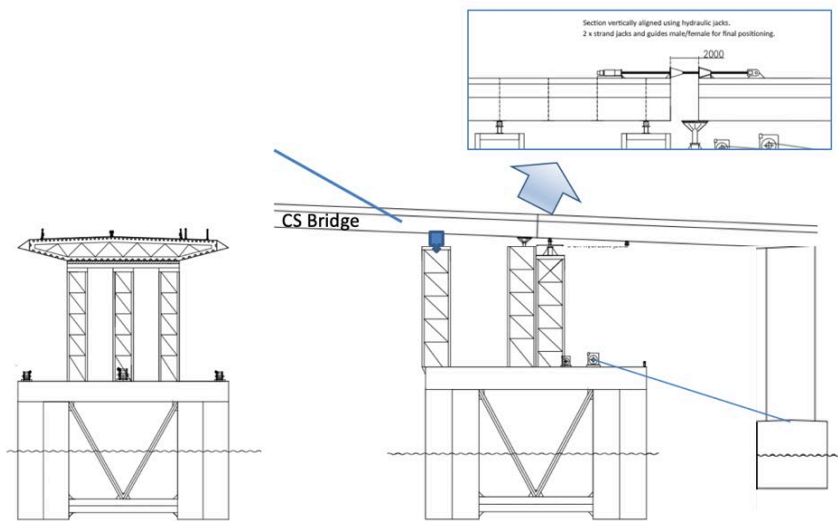


> Figure 8-15 Towing route from Eikelandsosen to Bjørnafjorden installation site. Towing distance is 13.4 NM.

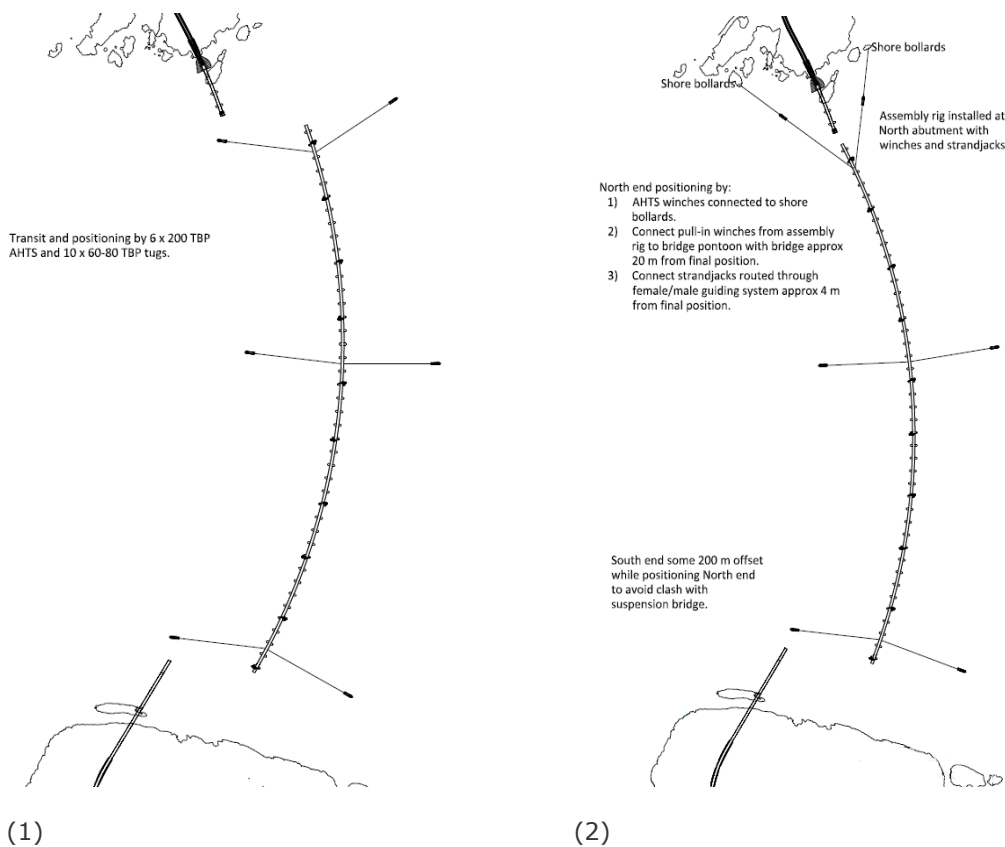
The final installation is shown in Figure 8-17, where the main sequences are described as:

- (1) Approach free floating controlled by tug fleet
- (2) Winching in and connecting to abutment
- (3) Swing in and pull into quick connecting structures at CS bridge
- (4) Making up permanent connections using special purpose semi rig

The cable stayed bridge is erected with and pre-equipped with arrangements and guiding structures at the northern end for pulling in and making up the quick connection, prior to the arrival of the floating bridge. Logistic support from land over the bridge is assumed.



> Figure 8-16 Connecting Cable stayed Bridge and Floating Bridge using a purpose built semi-submersible construction rig looking west.



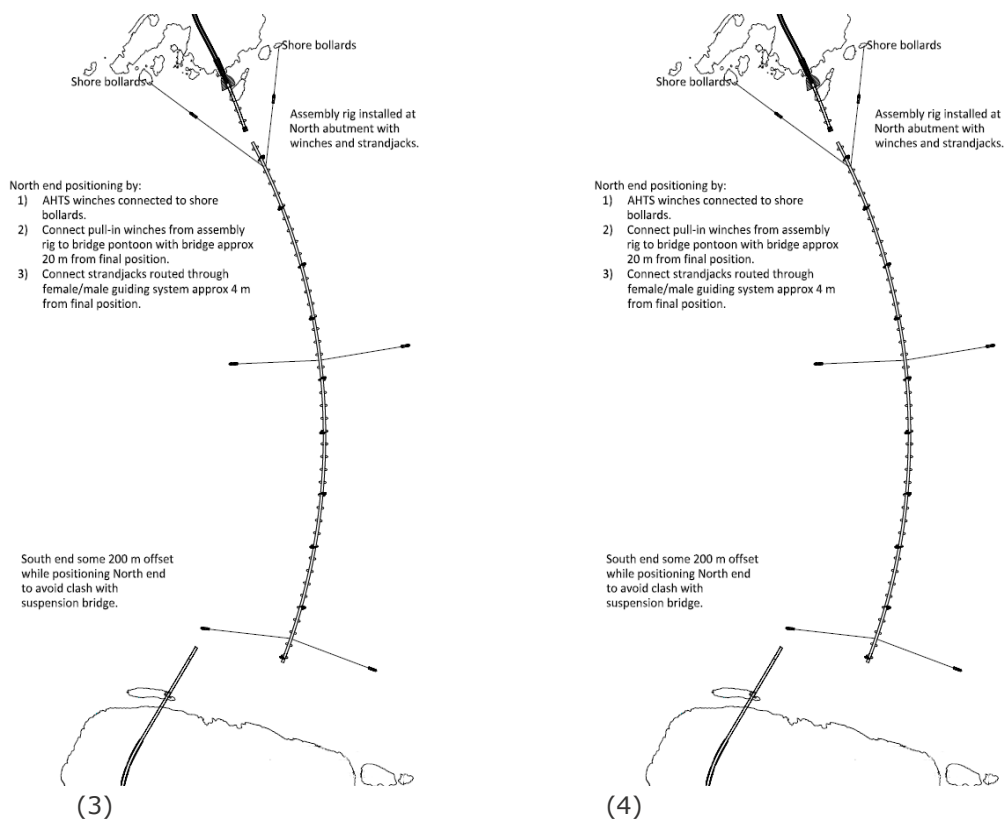


> Figure 8-17 Installation sequence of the floating bridge

8.2.11 Deploying mooring lines in Bjørnafjorden

Alternative K12 has in total 16 mooring lines connected in pair to 8 pontoons and located as shown in Figure 2-9. Anchors are either suction type or combination of suction/gravity depending on sea bed conditions. The sea bed is uneven and the thickness of the soft soil is varying. It has been challenging to identify proper locations for the anchors. However, for K12, proper locations are identified as shown in Figure 8-18. The anchors are installed one year prior to hooking up and tensioning mooring lines. The mooring lines are deployed and buoyed off as shown on Figure 8-19 below.

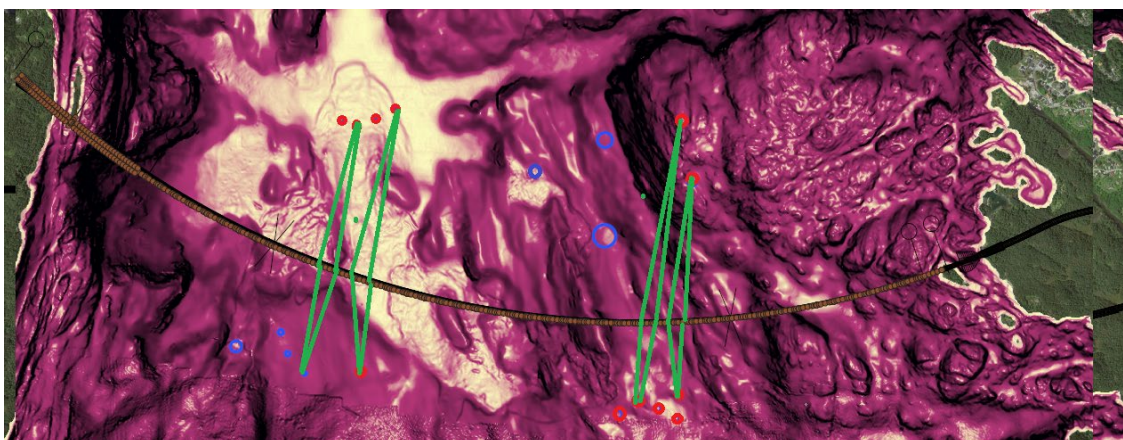


> Figure 8-18 Anchor locations for concept K12

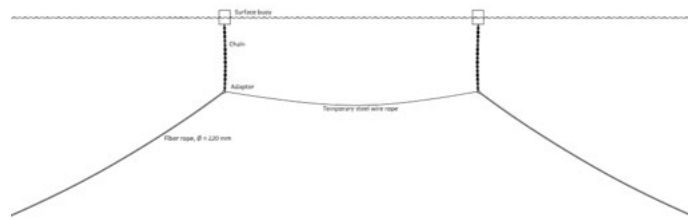


> Figure 8-19 Mooring lines

8.2.12 Hookup in Pre-installed Mooring System

When the K12 floating bridge is secured at the end positions, hooking up in the mooring system will start. The mooring lines have to be connected to the pontoon symmetrically. The pontoons are pre-rigged with anchor chains as shown on Figure 8-20 below.

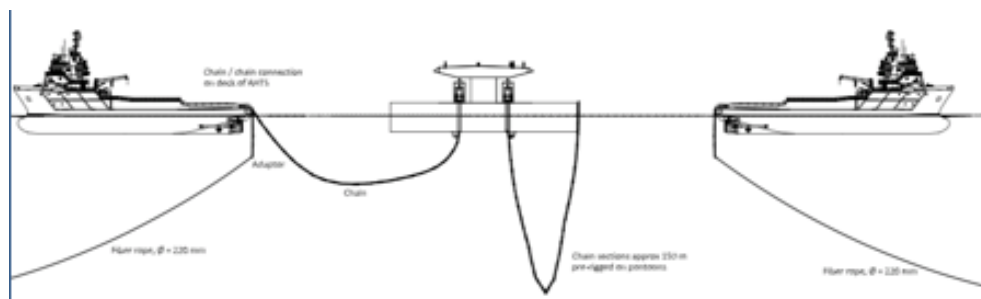


> Figure 8-20 Hook-up of pontoon mooring.

The tensioners with power pack and handling gear are mounted on the pontoon. This equipment has to be moved to the next pontoon when the operation is finished.

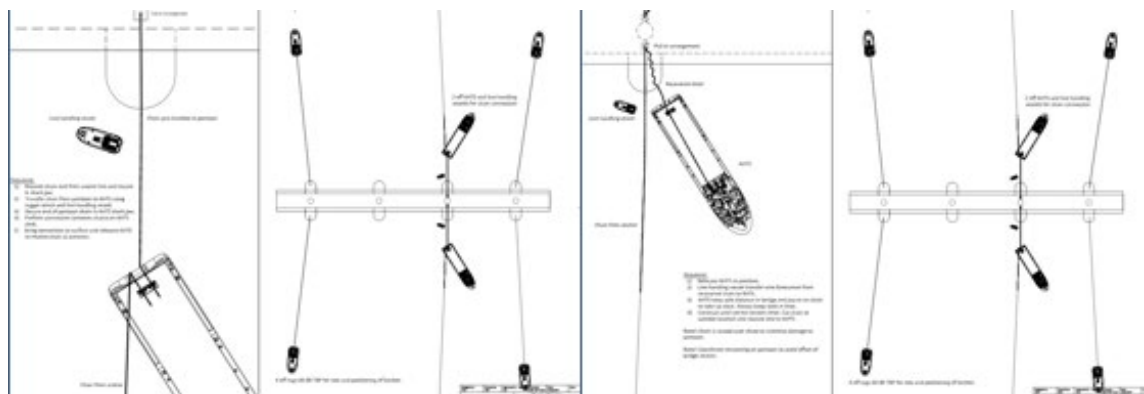


> Figure 8-21 Tensioning the mooring lines

8.3 Cable-stayed bridge

8.3.1 Construction

The cable stayed bridge consists of the main components:

- Main tower
- Anchor structure

- Bridge deck on land
- Bridge deck on sea

8.3.2 Rigging on site

It is assumed that the access tunnel or road is finished, in sufficient quality, that it can be used for the construction of the bridge. A rigging area close to the site will be established. Following will be performed:

- A construction jetty
- Barracks
- Warehouse
- Offices
- Concrete mixing station
- Steel/reinforcement yard

8.3.3 Construction of cable stayed bridge

The construction of the south abutment with anchoring structures and the tower will start first and independently of each other. The tower is supposed to be constructed utilizing slip-forming or climbing scaffolding techniques.

The bridge girder for the cable stayed bridge will be prefabricated in China in sections of 50 to 100 m. On the landside 50 m long elements will be lifted on to a steel scaffolding structure from the by a floating crane and skidded to the abutment, see Figure 8-22. The deck elements, 50 m in length, is lifted onto a platform at the seaside of the tower. The deck element is here placed on a wagon and transported on the steel structure to the rear part of the bridge. The element is lifted off the wagon, by jacks, and the wagon is released to continue to the transport of the elements. The elements will then be inter-connected by welding.

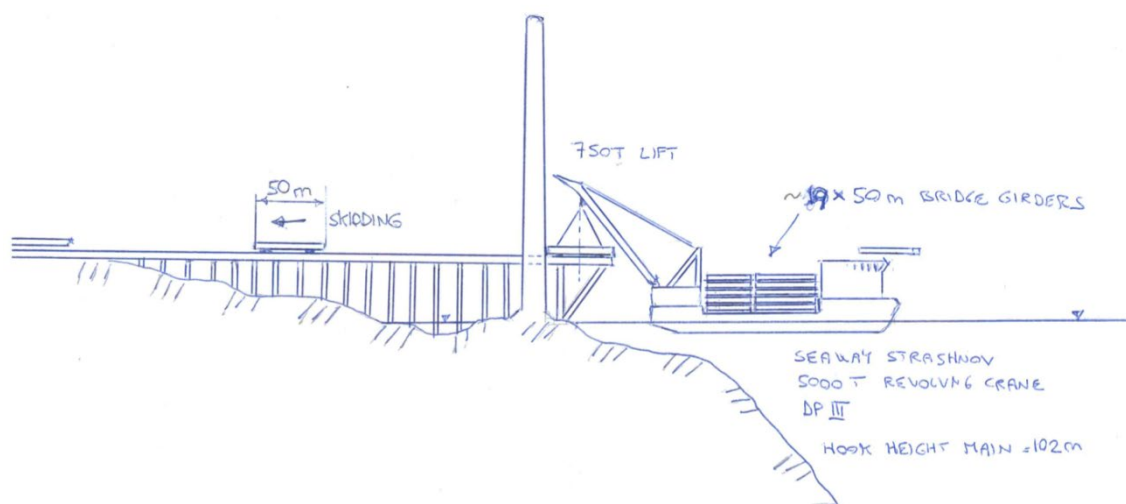


> Figure 8-22: Installation of Cable Stayed Bridge Land side girders

The deck-elements at the seaside will be lifted up in position, temporarily connected to the existing deck-end and connected to temporarily cable-stays. After adjustments final

connection and final stays will be performed. The deck elements will be in length of 100 m. When the seaside of the bridge is finished, the scaffolding structure on the landside will be removed.

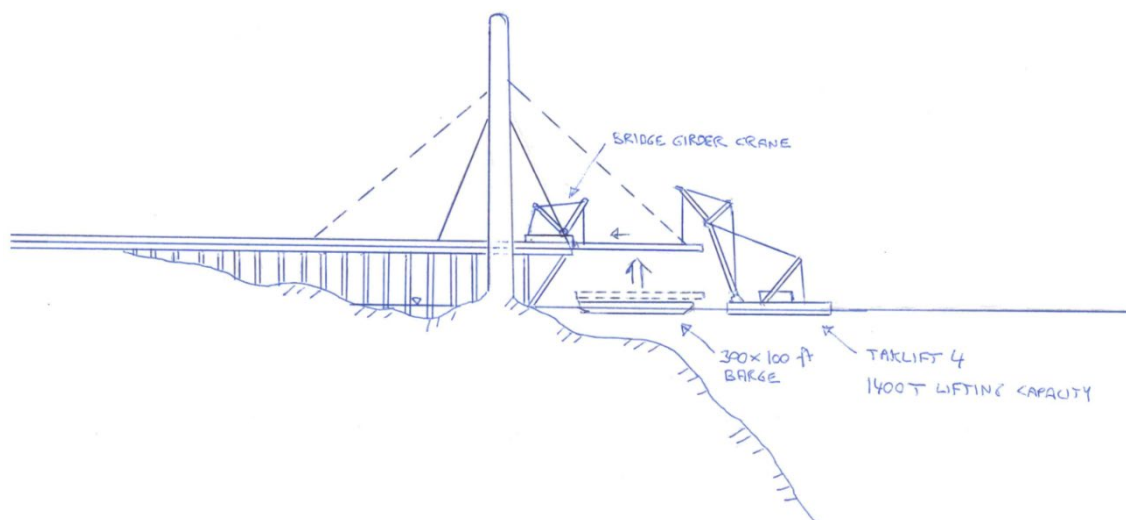


> Figure 8-23: Installation of Cable Stayed Bridge outer girders in 100 m sections

8.4 Abutments

8.4.1 Rigging at the bridge site

It is assumed that the access roads/tunnels in both ends are finished and can be used by the contractor for the project. Necessary rigging at the Northern abutment site will be:

- Access rock-filling to the island
- Small construction jetty
- Warehouse
- Office
- Misc.

In addition, a temporary mooring system will be installed. The rigging for the Southern abutment is included in the rig for the cable stayed tower described in 8.3.2

8.4.2 Construction

The abutment on Gulholmane is located on dryland and is founded directly on the bed rock with level base established at el. +2.0 m. Preparation of the 1 500 m² base involves blasting and excavation of some 4 500 m³ of hard rock. The box-shaped caisson structure is constructed by 'standard' civil construction method. The caisson is foreseen cast with modular wall formwork system in two lifts to allow for solid ballasting of the cellar compartments. A total concrete volume of approx. 5 000 m³ implies ~700 ready-mix truck deliveries via the hard rock tunnel.

The steel box girder is cast integrally with the abutment by installing a bridge girder transition segment as outlined Sec. 8.2.10. A cast-in-place joint is deemed necessary to allow ample time, approx. 8 weeks, for placement and stressing of the PT tendons.

The southern abutment is constructed in connection with the cable stayed bridge; Refer cable stayed bridge Sec. 8.3.

8.5 Completion

- Outfitting systems
- Ballasting and drying
- Maintenance systems
- Asphalt and rails
- Paint systems and touch-up
- Marine growth and corrosion prevention systems

9 CONCEPT ROBUSTNESS

9.1 General Robustness Evaluation

Bad quality environmental data, error in the analysis process, and unforeseen effects not covered by the design basis dominates the resulting robustness consequence for all concepts, though in a varying degree. Following is a group of incidents requiring major repair, like ship collision, bad maintenance and welding errors in production. Most of these incidents can be attributed to the point that the bridge is a first-off, but also that the consequence of major repairs is evaluated to be highly uncertain, resulting in a large spread and contribution on the 85 percentiles. This is further elaborated in chapter 9.2 and summarised in Figure 9-2.

Combined with the relatively poor track-record for first-off structures, typically requiring repairs and amendments more often than traditional structures, it would be beneficial to focus more effort on how and when large repairs could be performed.

The use of mooring system and for what purpose has been a significant focus in the project, as reflected by the resulting concept variations. Whether the concept relies on or just receive support from a mooring system is important. In a generalised perspective, relying on a mooring system add complexity and maintenance constraints. The general belief that a mooring system will perform for 25 years is low, so is the belief the maintenance process will be performed at a sufficient level. This is clearly shown in the resulting data, and was also a discussion of high frequency in the group discussions.

The results are produced after finishing workshop 8 (25.03.2019), that last part of the planned robustness assessment process. 21 events were evaluated for K11, K12, K13 and K14 and the resulting consequence distribution has been computed and shown in this chapter. An overview of the results is shown in Table 9-1.

> *Table 9-1: Resulting consequence in MNOK for each of the concepts. Lower cost is better.*

Concept	P10	P50	P90	P85	EV
K11	993	1 580	2 735	2 450	1 766
K12	883	1 422	2 554	2 270	1 625
K13	1 299	1 984	3 321	2 992	2 202
K14	1 198	1 867	3 114	2 813	2 063

The results summarised in Table 9-1 are elaborated with a histogram in Figure 9-1, showing the resulting distributions for each of the concepts. K11 and K12 have quite similar shape and almost identical expected cost, however, K11 has more inherent uncertainty that result in a more significant distance at the 85 percentiles, leaving K12 as the definitive most robust concept. K13 and K14 have similar results at the 85 percentiles, but the K13 has a significantly larger expected cost as a result of having the highest complexity and number of critical parts.

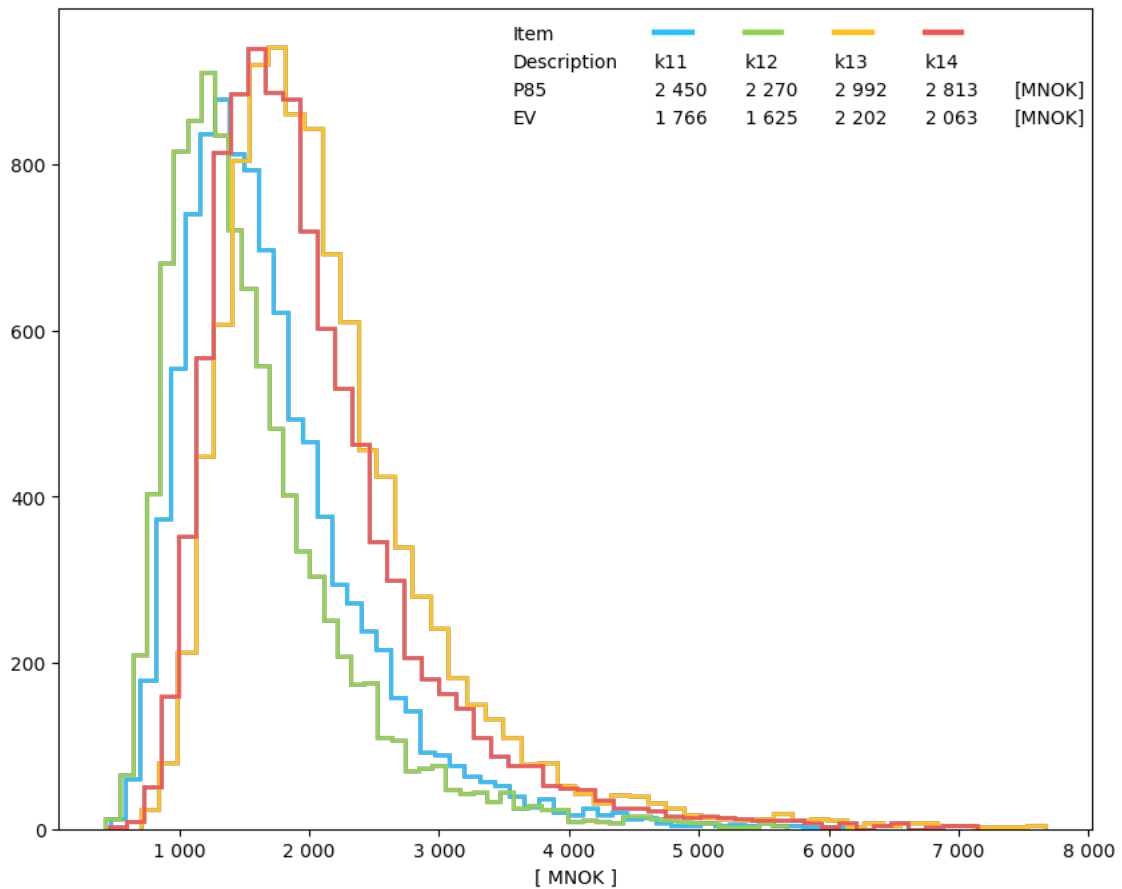


> Figure 9-1: Histogram of total consequence for all concepts

9.2 Resulting Consequence Components for K12

Components of the resulting consequences are shown in pie-charts in Figure 9-2. The overall distribution of elements is good, and there are no single contributing events that dominate any of the concept results. This strengthens then confidence in the result and the total sum has low sensitivity to possible errors in data processing or data collection process. The quality of the environmental data, possible analysis error, and unforeseen effects not covered by the Design Basis dominate the results.

K11 and K12 have similar expected total cost from robustness. K12 performs significantly better on the main contributors, with an 8 % reduction on impact from environmental data and an analysis error. This is mostly caused by increased flexibility having a mooring system that aid in extreme situations. However, the addition of a mooring system also increases maintenance requirements and cost from ship impact within design space due to increased repair costs.

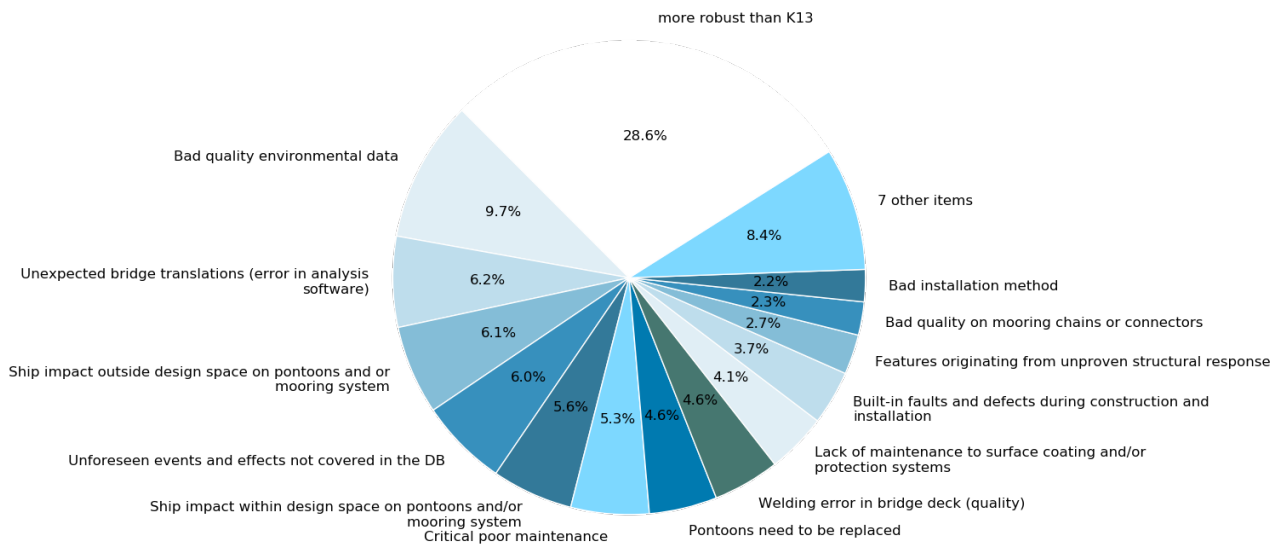


> Figure 9-2: Pie-chart of the contributing events to consequence in NOK for K12.

9.3 Resulting Consequence Sensitivities for K12

Tornado diagrams (violin plots) are shown in Figure 9-3. A tornado diagram is a type of sensitivity analysis that provides a graphical representation of the degree to which the result is sensitive to the specified independent variables (comparing the relative importance of variables). The calculations are done by holding all but one variable fixed at some base value, while the single inputs are varied.

Bad quality environmental data, error in the analysis process, and unforeseen effects not covered by the design basis dominates the resulting robustness consequence for all concepts, though in a varying degree.

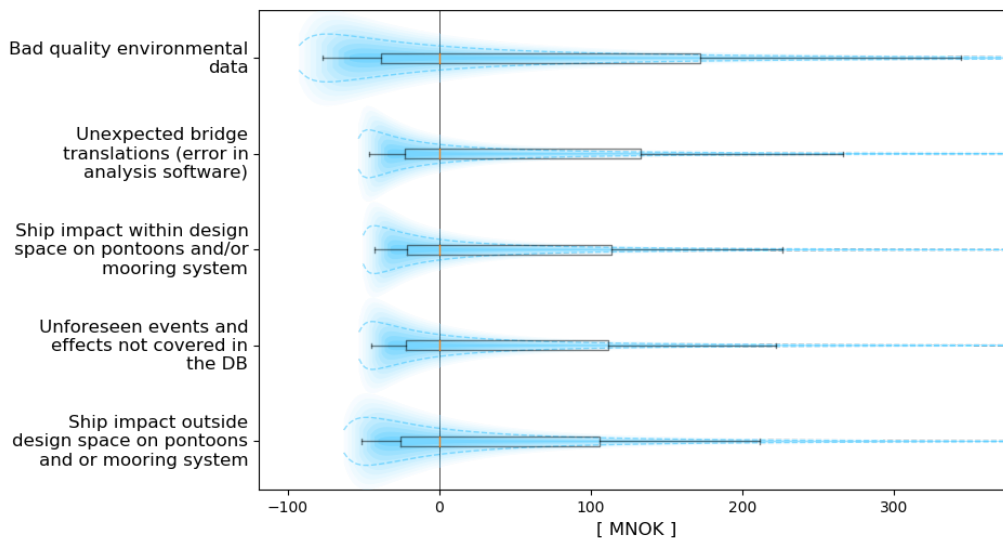


> Figure 9-3: Tornado-diagram of total consequence for K12.

9.4 K12 Robustness Evaluation

K12 has the lowest expected cost from robustness in total. It was expected that K11, having low redundancy, would receive a considerable downside on robustness. However, higher concept complicity in the form of more construction elements or load carrying systems seem to have a significant negative impact on the estimated probabilities of failure, resulting a marginal 10% lower expected cost for K12 than K11. The contribution from each of the consequences summarized in **Error! Reference source not found.** are evenly distributed, indicating that no single source is dominating the result, but ship impact inside the design space is introduced on the major uncertainties, while only contributing with about 5 % in the total cost from robustness. The large uncertainty indicate that further insight should be sought on both the probability and consequence of this topic.

In comparison to K11, the expected cost from robustness from environmental data is less for K13 as a result of high flexibility, though it was evaluated to be more challenging to analyse and design the concept. As a result, the total contribution from error in the analyse procedure is about 4% lower for K12 as the increased tuning flexibility significantly reduce the consequence of such errors for K12. The mooring system also increase the overall contribution from vessel collision as the probability of this incident with significant impact is deemed to increase.

Further development of the concept should focus on capability and verification of design and analysis procedures on long moored structures, as well as minimizing the consequence of high probability collisions with lesser vessels. As an example, adding redundancy by increasing the number of mooring lines to counter total collapse in one event will cause increase in the probability of failure and consequence of production faults, installation faults or implications of bad materials. In short, ensuring redundant load bearing capacity by adding structural parts should be done with care to avoid reducing the total robustness. An optimal solution could be identified by iterating over cost of construction, maintenance and expected robustness cost. Based on the current findings, it indicates that the load carrying system should only be needed in extreme situations (low probability), allowing the bridge to operate without having a large number of parts that require maintenance to function (high probability). Although not addressed in depth in this project, the maintenance procedures is a driving force in the probability of failure for the mooring system. K13 and K14 are highly dependent on a working mooring system and any fail or error has a large damage potential.

Further work is needed to identify the optimal path, whether to have two redundant load carrying systems or one simple one but with improved strength as used for other type of constructions as airplanes, where one typically only one pair of wings – without redundancy, but with a high focus on maintenance and control.

10 COST, SCHEDULE AND SUSTAINABILITY

The cost, sustainability and schedule studies are performed with the basis of workflow as described in chapter 8. Hence, the results represent a combination of qualitative knowledge cross project disciplines related to strategy and feasibility, estimates and assumptions, as well as using the latest results and variables from various sub-studies of the project.

10.1 Total cost

The most interesting finding of the cost study is the remarkable low difference in total cost between each concept. However, by examining concept specific activities step by step, significant differences emerge, as shown in below table:

Activity	K11	K12	K13	K14	Unit X
South landfall incl. prep. tower	275	262	262	262	MN OK
North landfall	211	146	57	146	MN OK
South road arrangement	488	476	437	437	MN OK
North tunnel	2 654	2 654	2 634	2 630	MN OK
Raw material, bridge elements	821	696	661	669	MN OK
Raw material, pontoons and columns	404	375	357	362	MN OK
Fabrication of bridge elements FE	2 767	2 408	2 274	2 321	MN OK
Fabrication of pontoons and columns FE	1 280	1 206	1 143	1 157	MN OK
Shipping of bridge elements to Hanøytangen	571	565	569	569	MN OK
Shipping of pontoons and columns to Hanøytangen	238	233	232	233	MN OK
Tower construction	287	286	287	286	MN OK
Cable fabrication	281	256	258	256	MN OK
Installation of cable-stayed bridge cables	102	93	93	93	MN OK
Installation of cable-stayed bridge elements	478	459	462	461	MN OK
Establish temporary assembly site Hanøytangen	653	654	654	653	MN OK
Assembly of super elements at Hanøytangen	997	968	920	981	MN OK
Towing and positioning at Eike landsfjorden, super elements	140	139	130	129	MN OK
Highbridge assembly Hanøytangen	314	316	307	306	MN OK
Towing and positioning at Eike landsfjorden, high bridge	23	23	24	24	MN OK
Towing and installation landfall North	60	59	88	59	MN OK
Global assembly at Eike landsfjorden	620	601	506	507	MN OK
Sea bed prep. and anchor installation	0	511	918	770	MN OK
Towing to Bjørnafjorden (complete bridge)	137	138	0	0	MN OK
Towing and positioning in Bjørnafjorden (sections)	0	0	96	76	MN OK
Mooring system hook-up (during installation)	0	0	302	239	MN OK
Bridge installation Bjørnafjorden (complete bridge)	43	39	0	0	MN OK
Mooring system hook-up (after installation)	0	176	0	0	MN OK
Towing to Bjørnafjorden (infills)	0	0	236	236	MN OK
Bridge complete installation and assembly (infills)	0	0	190	187	MN OK
Finalization	970	970	923	982	MN OK
Total cost	13 521	13 424	13 691	13 605	MN OK

> Figure 10-1: Main cost elements and activities for all concepts, compared

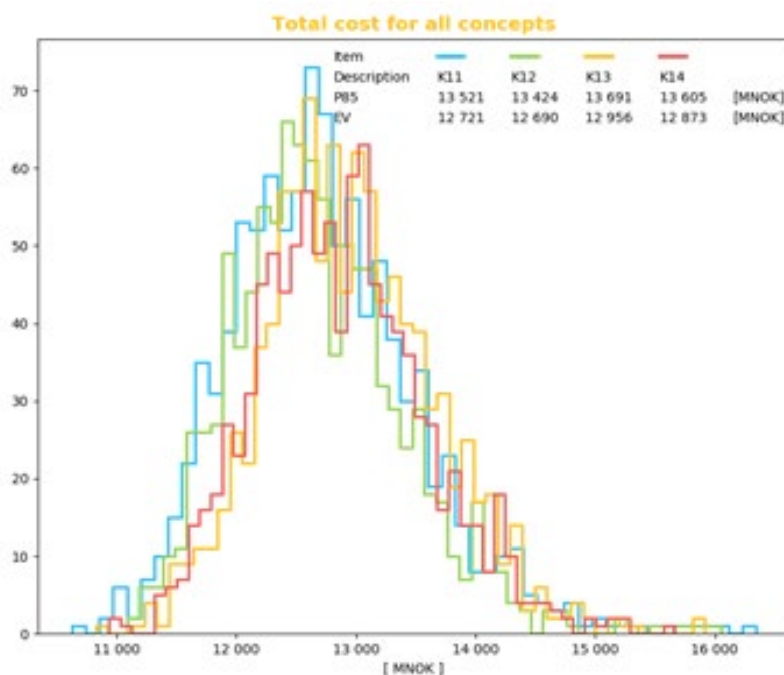
For K12 in specific:

- North landfall of K12 has 3 times the cost of K13 due to the significant differences in structural design of the bridge girder
- Raw material cost and fabrication cost of both bridge girder elements (pre-produced in Far East at lengths of 100m) and pontoon and columns (pre-joined for the low-

bridge section), are significantly higher for K11 compared to the other concepts. Variations in total bridge length will also influence these costs.

- There are no major differences in costs of building the cable-stayed bridge, however effects such as increased time for welding and joining operations, as well as increased strengths in cables, due to structural design of K11, are considered.
- Furthermore, there will be more joining operations in Eikelandsfjorden for K11 and K12, compared to K13 and K14. As assembly of super elements in Hanøytangen are on critical path for execution, K13 and K14 will get added cost of operation in Eikelandsfjorden (waiting for elements, etc.) compared to the actual cost of operation during assembly and joining processes. However due to the costly operations in Bjørnafjorden it is chosen as the best strategy both from a feasibility and cost perspective. Hence, Eikelandsfjorden will act as a storage area of elements, with temporary mooring systems as described in chapter 8.
- Sea bed preparations and installation of anchors are based on the actual chosen anchor types for each concept, including effects of large-scale operations, giving K13 advantage compared to K12. However, total costs are still significant for all concepts relying on a mooring system.
- Installation strategy in Bjørnafjorden are significantly different between K11 / K12 (whole bridge assembly) and K13 / K14 (sections hooked to mooring lines and later joined by infill sections). Not surprisingly towing operation costs for K13/K14 increase by 4 times to that of K11/K12, and total installation cost, including mooring system connections, are more than twice as costly for K13 compared to K12, and 12 times as costly as for K11.

Due to extra operations for both K13 and K14 as described above, the expected value of total cost is considerably higher, as shown in below comparison:



- > *Figure 10-2: Histogram showing the cost of each concept. Illustrating the difference in uncertainty and expected value difference between the concepts.*

10.2 Sustainability

Histograms for the computed CO₂-footprint of each concept is shown below. K12 has the lowest footprint, followed by K11. K13 and K14 has a large footprint, mainly due to increased marine operations. The footprint is modelled based on the major activities in the construction process and follow an identical structure as the cost analysis. Only the main CO₂

contributors are modelled, mainly material production and energy- and fuel consumption. It is expected that this account for 80-90% of the total emissions in the project.

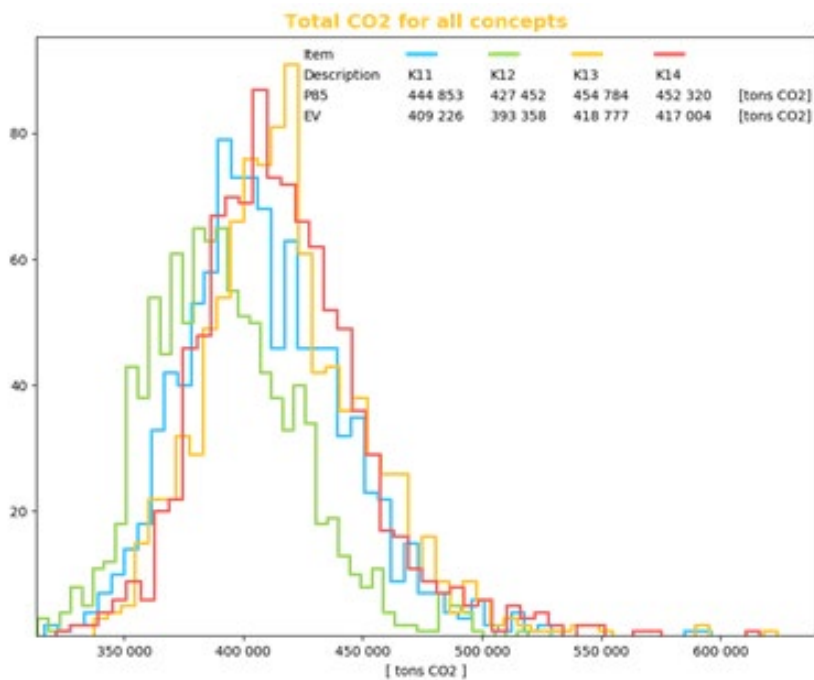


> Figure 10-3: Histogram showing the computed Co2-footprint for each of the concepts

10.3 Schedule

Below-shown schedule illustrates a simulated outcome based on activities, cost and volume assumptions as used in the cost- and sustainability model described above. Below schedule is based on P85 result for K12.



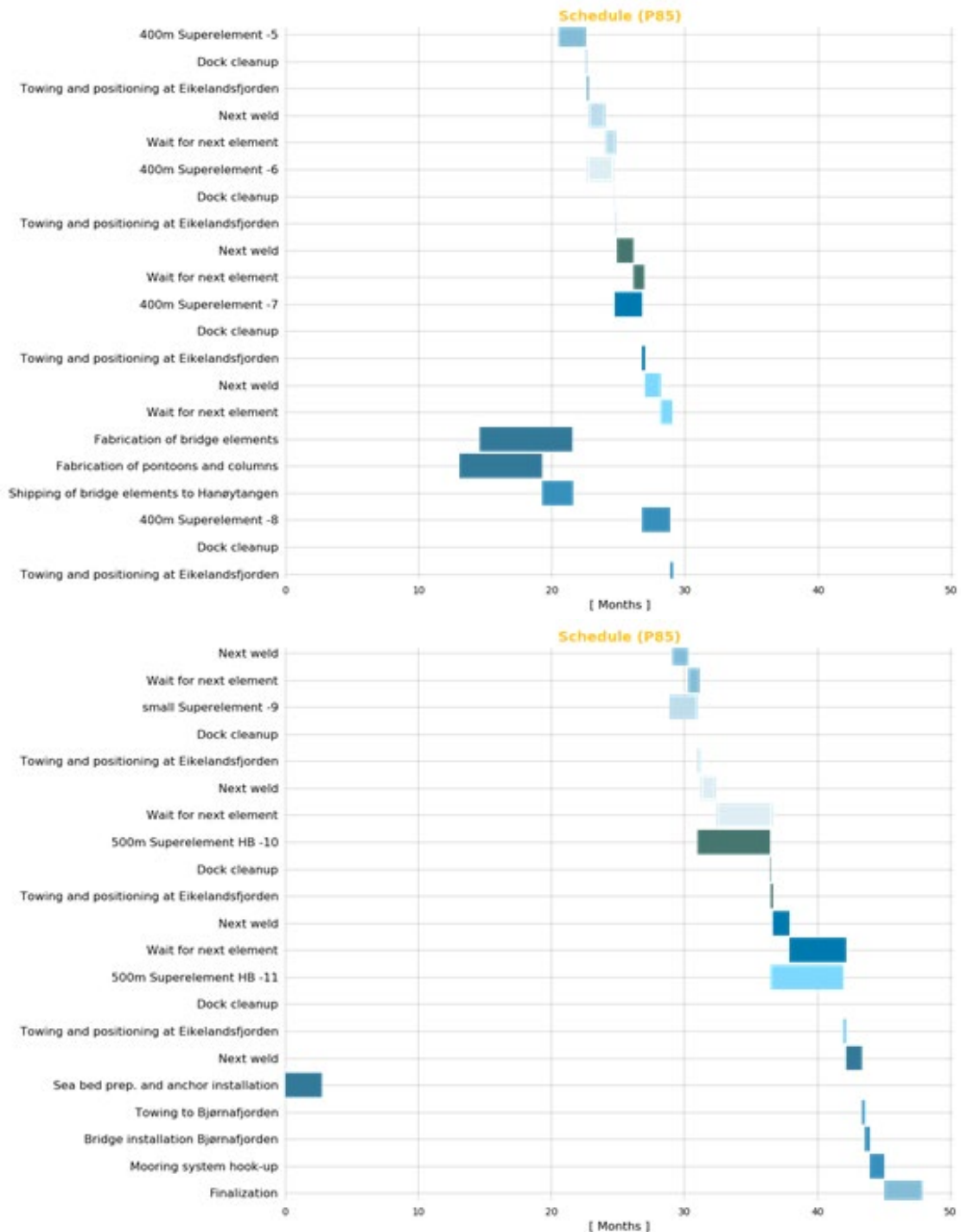


> Figure 10-4: Schedule simulation K12: P85.

As with the cost analysis, simulated schedule, and expected execution is found to be quite similar cross all concepts. Again, variation in duration of specific activities are present, based on similar logic as outlined, and as seen by comparing above schedule cross concepts. An element not considered in the schedule studies is seasonal effects. Both K13 and K14 will be highly dependent on execution on time to perform time-consuming activities in Bjørnafjorden.

Delay in previous workflow, with Hanøytangen assembly process being on critical part, may cause severe delay in the project, favoring K11 and also K12.

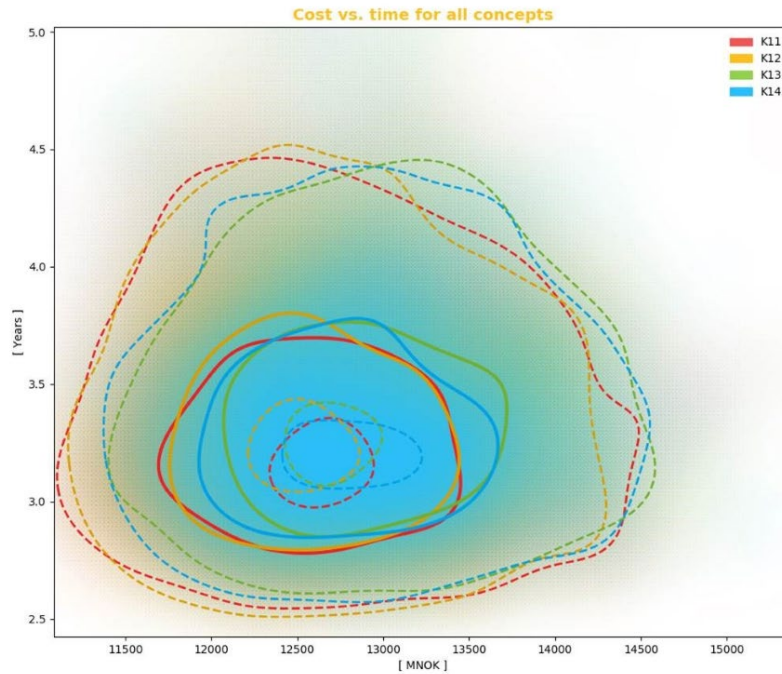


> *Figure 10-5: Contour plot, comparing concepts in total cost and schedule*

11 REFERENCES

- [1] Multiconsult, «Bjørnafjorden, straight floating bridge phase 3 Analysis and design (Base Case) Appendix J - Design of anchorages».
- [2] Håndbok N400 , «Bruprosjektering,» Statens vegvesen Vegdirektoratet, 2015.
- [3] SBJ-32-C5-OON-22-RE-003, «Analysis method,» Olav Olsen, Norconsult, 2019.
- [4] SBJ-32-C4-SVV-90-BA-001, «Design Basis Bjørnafjorden floating bridges,» Statens Vegvesen, 2018.
- [5] Olav Olsen, Olav Olsen interactive; Project Bjørnafjorden phase 5, Oslo.
- [6] Olav Olsen, Norconsult, SBJ-32-C5-OON-22-RE-005-A Influence of swell waves, 2019.
- [7] Simulia, «Abaqus/CAE 2017,» Dassault Systèmes, 2016.
- [8] Drawing no. K7-057, «E39 Bjørnafjorden K7 End-anchored Floating Bridge,» Norconsult, Dr. Techn. Olav Olsen, Aker Solutions, 2017.
- [9] Drawing no. K7-063, «E39 Bjørnafjorden K7 End-anchored Floating Bridge,» Norconsult, Dr. Techn. Olav Olsen, Aker Solutions, 2017.
- [10] K. M. Ofstad, «Finite element modelling of steel bridge structures exposed to ship collisions (Matster thesis),» NTNU, Trondheim, 2018.
- [11] A. S. Hagbart, O. S. Hopperstad, R. Törnqvist og J. Amdahl, «Analytical and numerical analysis of sheet metal instability using a stress based criterion,» *International Journal of Solids and Structures*, vol. 45, nr. 7-8, pp. 2042-2055, 2008.
- [12] Drawing no. K7-031, «E39 Bjørnafjorden K7 End-anchored Floating Bridge,» Norconsult, Dr. Techn. Olav Olsen, Aker Solutions, 2017.
- [13] Drawing no. SBJ-33-C5-OON-22-DR-006-A, «E39 Bjørnafjorden Reksteren-Os K12 - Side-anchored floating bridge,» Norconsult/Dr. Techn. Olav Olsen, 2019.
- [14] DNV GL, «SBJ-31-C3-DNV-62-RE-020-A-Fatigue design methodology for BJF floating bridges,» 2018.
- [15] DNV GL , «RP-C203 Fatigue design of offshore steel structures,» DNV GL, 2016.
- [16] NS-EN 1992-1-1:2004+A1:2014+NA:2018, «Eurocode 2: Design of concrete structures - Part 1-1: General rules and rules for buildings,» Standard Norge, 2004.
- [17] NS-EN 1993-1-1:2005+A1:2014+NA:2015, «Eurocode 3: Design of steel structures - Part 1-1: General rules and rules for buildings,» Standard Norge, 2005.
- [18] Statens vegvesen, Design Basis Bjørnafjorden Side- and end anchored floating bridge, 2017.
- [19] Statens vegvesen, Vegdirektoratet, Håndbok N400 Bruprosjektering, Prosjektering av bruer, ferjekaier og andre bærende konstruksjoner, 2015.
- [20] SBJ-32-C4-SVV-90-BA-001, «Design Basis Bjørnafjorden floating bridges,» Statens vegvesen, 2018.
- [21] DNVGL-RP-C208, «Determination of structural capacity by non-linear finite element analysis methods,» DNV GL, 2016.